

SYNTHESES AND REACTIONS OF
POLYMER-BOUND MOLYBDENUM COMPLEXES

and

HYDROGENOLYSES OF AN ALKYNYL COBALT CARBONYL CLUSTER

Thesis by

Jane Elizabeth Frommer

In Partial Fulfillment of the Requirements
for the Degree of
Doctor of Philosophy

California Institute of Technology
Pasadena, California

1981

(Submitted August 22, 1980)

© 1981

Jane Elizabeth Frommer

All Rights Reserved

Acknowledgement is due the members of the Bergman research team who accompanied me through the process. To Bob I give credit and thanks for seeing me through four years of graduate work. I am particularly grateful for the support of my parents and Stephen, who encouraged me to take it on, and had confidence throughout that I would make it.

ABSTRACT

$\text{Co}_3(\text{CO})_9\text{CCH}_2\text{C}(\text{CH}_3)_3$ (1) was prepared and its hydrogen-mediated decomposition was studied. 1 reacted with hydrogen in aromatic solvents (60°C, 2-7 atm H_2) to yield three products: 3,3-dimethylbutene (2), 2,2-dimethylbutane (3), and 4,4-dimethylpentanal (4). The final ratio of alkene to alkane to aldehyde was approximately 2.5 : 1.5 : 1.0. Kinetic data collected from both NMR- and vpc-monitored experiments indicated first order decomposition of starting material 1 and a hydrogen pressure dependence for the rate of appearance of total products. Nearly total inhibition of the hydrogenation was observed in the presence of carbon monoxide ($\text{CO}:\text{H}_2$, 3.7:3.7 atm, 60°C). However, at elevated temperatures (85°), under the same CO/H_2 atmosphere, aldehyde (4) production became the predominant reaction pathway at the expense of earlier-formed olefin 2. Incorporation of independently added olefins in the hydrogenation of 1 suggested the intermediacy of olefin in aldehyde and alkane production.

A polystyrene-attached n^5 -cyclopentadienyl(tricarbonyl)-hydridomolybdenum complex (P-6) was prepared and its reactions with several THF-soluble bases were investigated. Enolates of β -dicarbonyl compounds quantitatively deprotonated P-6, giving polymer-bound salts of the corresponding anion (P^- - $\text{Cp}(\text{CO})_3\text{Mo}^-$, P-7). Equilibration studies involving polymers P-6 and P-7 and their soluble monomeric analogues in THF demonstrated that little change in pK_a was induced by binding the molybdenum

hydride to the polymer. Even though the polymer-supported partners in these experiments were not soluble and therefore rendered the reactions heterogeneous, the systems adhered reasonably well to conventional equilibrium behavior, as exhibited by a simple equilibrium analysis which yielded effectively constant K_{eq} values. A polymer-bound carboxylic acid (P-1) and its conjugate base (P-2) also displayed essentially conventional equilibrium dynamics.

Table of Contents

I. Syntheses and Reactions of Polymer-Bound Molybdenum Complexes	
A. Introduction	2
B. Results	3
C. Discussion	16
D. Experimental	25
E. References and Notes	36
II. Hydrogenolyses of an Alkynyl Cobalt Carbonyl Cluster	
A. Introduction	43
B. Results	45
C. Discussion	55
D. Experimental	79
E. References and Notes	90
III. Propositions	
A. The Mechanism of Formation of $\text{Co}_3(\text{CO})_9\text{CR}$ Compounds.	94
B. Negative Ion Mass Spectroscopy of Transition Metal Hydrides.	105
C. Synthesis and Utility of a Polymeric Reducing Agent.	115
D. Alkyl to Cyclopentadienyl Migration in Transition Metal Complexes.	128
E. Ester Enolates to β -Keto Esters: a Ketene Intermediate.	144

Chapter 1

Syntheses and Reactions of
Polymer-Bound Molybdenum Complexes

Introduction

Molecules have been attached to polymers for many purposes,¹ including organic² and stereospecific³ synthesis, catalysis,⁴ separation and purification,⁵ and isolation of reactive species.⁶ In addition, interest in functionalized polymers has been furthered by their analogy to multifunctional biological molecules, e.g., polypeptides and enzymes.⁷ However, one cannot assume that the chemistry of a bound species will be identical to that of its homogeneous, monomeric counterpart. In regarding the polymer that surrounds the affixed reagent as a primary solvation sphere, one must take into account the properties of the polymer backbone which might influence the reaction to be studied. These include the polymer's compatibility with the solvent system, i.e., solvation of the polymer backbone (hydrophobicity, hydrophilicity), polymer morphology (secondary and tertiary structures "directing" effective dilution of bound species), and electronic stabilization or destabilization of the affixed functionality's incipient transition states or intermediates (i.e., whether the backbone "supports" ionic charge or delocalizes radicals).

Previous treatment of the polymer's influence on the chemistry of affixed molecules has dealt primarily with kinetic effects. These include frequency of site-site interactions (intrapolymeric encounters),^{6b,8} affixed reagents' mobility,⁹ prolongation of supported reactive intermediate lifetimes,⁶ and diffusion of soluble reagents within the polymer.¹⁰ Few attempts have been made to characterize the role of these polymer-bound species in thermodynamic equilibria. To this end, we chose to study the acid-base equilibria of several polymer-bound acids.

Polyprotic molecules have long been of interest in biochemistry. In particular there has been much discussion over the determination of the pKa

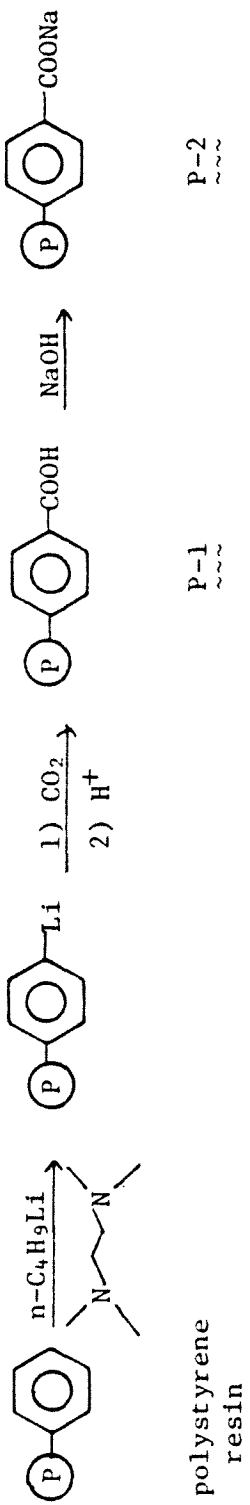
of a particular acidic site as a function of surrounding acidic and basic sites in varying degrees of ionization. Traditionally, such methods as titration¹¹ and ultraviolet spectroscopy¹² have been used to observe ionization equilibria in polyprotic molecules; recently, such sophisticated techniques as ¹⁵N nmr have probed buried active enzymatic sites for information leading to an acidic site's ionization state.¹³ The approach which we employed involved spectrophotometric monitoring of soluble species in equilibrium with polymer-bound acids. An additional impetus to this study was the fact that although many organotransition metal complexes have been attached to polymers, few such systems containing charged metal centers (especially anions) are available.

Synthesis of Starting Materials

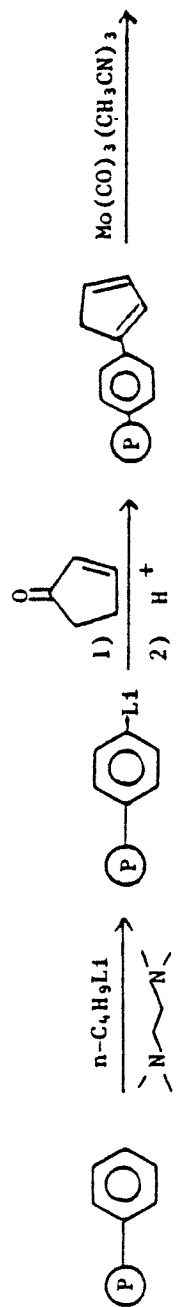
Polymer-bound sodium benzoate (P-2) was synthesized as outlined in Scheme 1.^{14,15} Polymer supports were 3% crosslinked, macroporous, styrene-divinylbenzene copolymers. The degree of carboxylate functionalization was determined to be 2.3 mM of acid per gram of polymer by titration of polybenzoic acid resin (P-1) in dioxane or THF with aqueous sodium hydroxide solutions. Final organic/aqueous ratios of approximately 2:1 in titration solutions were necessary to achieve reproducible results. Too high an aqueous component led to low figures for loading, presumably due to insufficient swelling of the polymer and therefore lack of exposure of all acidic sites.¹⁶ Infrared carbonyl absorbances for resins P-1 and P-2 are given in Table I.

The polymer-bound CpMo(CO)₃ anion P-7 was prepared according to Scheme 2. Resinocyclopentadiene (P-3) was synthesized by direct lithiation of polystyrene (macroporous, 3% crosslinked with divinylbenzene) followed by reaction with

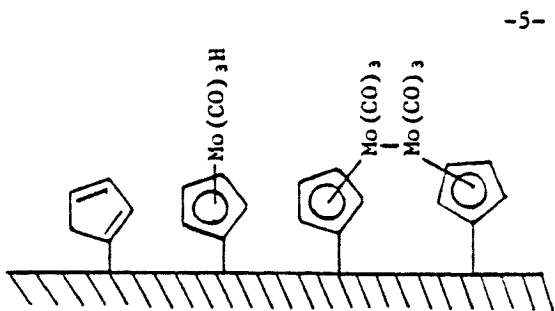
Scheme 1



Scheme 2

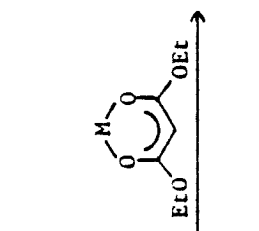


P-3

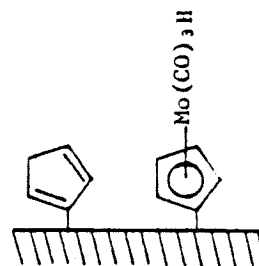


P-4

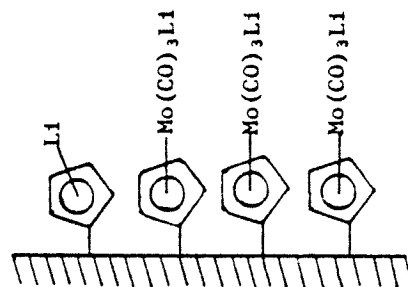
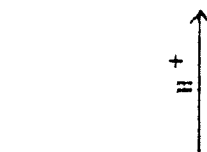
-5-



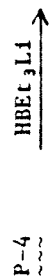
$M = \text{Na}, \text{P-7Na}$
 $M = \text{Li}, \text{P-7Li}$



P-6

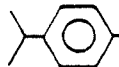

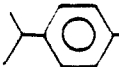
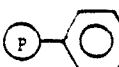
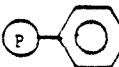
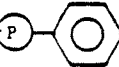
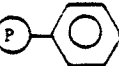
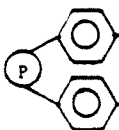
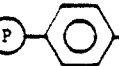


P-5



P-4

Table 1. Infrared Carbonyl Absorbances

<u>Soluble Compound</u>	<u>Polymer-bound analogue</u>
<u>cm⁻¹</u>	<u>cm⁻¹</u>
 - 1722 (s), 1610 (w), (THF) <u>1</u>	 - 1722 (s), 1685 (s), (KBr) <u>P-1</u>
 - 1587 (s), 1545 (s), 1400 (s), (KBr) <u>2</u>	 - 1600 (s), 1555 (s,br), 1395 (s), (KBr) <u>P-2</u>
CpMo(CO) ₃ H - 2015 (m), 1932 (s), (THF) 2006 (m), 1883 (s,br), (KBr) <u>6</u>	 - 2010 (s), 1930 (s,br)(KBr) <u>P-6</u>
CpMo(CO) ₃ Na - 1903 (s), 1798 (s), 1745 (s)(THF) <u>7-Na</u>	 - 1900 (s), 1840(s), 1730 (w) (KBr) <u>P-7-Na</u>
CpMo(CO) ₃ Li - 1910 (s), 1810 (s), 1785 (m), 1718 (s), (THF) <u>7-Li</u>	 - 1905 (s), 1803(sh), 1775 (s), 1710 (s,br), (KBr) <u>P-7-Li</u>
[CpMo(CO) ₃] ₂ - 1958 (s), 1910 (s), (THF) <u>4</u>	 - 1954 (s,br), 1904 (s,br) (KBr) <u>P-4</u>
CpMo(CO) ₃ CH ₃ - 2014 (m), 1924 (s) (THF) <u>8</u>	 - 2012 (s), 1935 (s,br)(KBr) <u>P-8</u>

cyclopentenone. This method afforded slightly lower loading than published methods^{6b} which entailed a bromination step previous to lithiation, but our resulting polymer (P-3) was free of residual bromine.¹⁷

The conditions of the metallation of cyclopentadienyl polymer P-3 resulted in some dimerization of metal centers on the polymer, as evidenced by both the characteristic red color and infrared absorbances of the molybdenum dimer moiety of resin P-4 (Table 1). This result contrasted with that of Gubitosa and Brintzinger,¹³ who found that 18% crosslinked polystyrene prevented dimerization of metal centers, presumably due to site-site isolation. Our results were compatible in view of the decreased rigidity of the polymer support on decreased crosslinking, resulting in an increase in the probability of interaction between active sites.

Lithium triethylborohydride converted both the molybdenum hydride and molybdenum dimer groups in resin P-4 to the molybdenum anion of resin P-5.¹⁹ In doing so, the borohydride reagent proved sufficiently basic to deprotonate residual, unfunctionalized resinocyclopentadiene.²⁰ Two further synthetic steps were required to generate resin P-7, polymer-bound molybdenum anion free of polymer-bound cyclopentadienyl anion (in order that the bound cyclopentadienyl anion not interfere in later equilibrium experiments). Protonation of all anionic sites on polymer P-5 afforded polymer-bound molybdenum hydride (P-6). The supported metal hydride was then selectively deprotonated with an alkali metal salt of diethylmalonate, yielding resin P-7 (under these conditions, the residual polymer-bound cyclopentadiene remained neutral²¹). The molybdenum anion's presence on resin P-7, indicated by IR spectroscopy, was confirmed by treatment of a sample of P-7 with methyl iodide: an IR spectrum of the resulting polymer-bound complex P-8 showed strong, sharp bands characteristic of an $\text{RCpMo}(\text{CO})_3\text{CH}_3$ moiety (Table 1).

Functionalized resins were analyzed by a combination of methods compatible with the resin's insolubility. Infrared absorbances of the bound metal carbonyls correlated well with those of their homogeneous models (Table 1). IR spectra were recorded either on KBr pellets or on suspensions of the insoluble resin in reaction solvents. The latter method avoided the workup and drying steps in KBr pellet preparation and allowed *in situ* observation of the progress of reactions.²²

Elemental analysis served as a more qualitative than quantitative measure of loading due to unacceptable irreproducibility in duplicate analyses, a problem shared by many researchers in this field.^{5c,23} Cyclopentadiene loading on resin P-3 was estimated by lithium analysis of a sample of resin P-3 which had been previously treated with methyllithium.^{6b} In the case of resin P-7, alkali metal analysis as well as molybdenum analysis was used in estimating the degree of polymer functionalization (cf. experimental section). Typically, 0.6mM of molybdenum was incorporated in 1g of polymer; this corresponds to substitution of approximately one-eighth of the styrene monomers of the polymer backbone.

Titration of functionalized polymers provided information about the number of active sites on a polymer within a certain pKa range. Resin P-3 was assayed for cyclopentadiene loading by titration with a solution of sodium triphenylmethide, the red color of the titrant serving as the end point indicator. The titration of bound molybdenum hydride P-6 with sodium diethylmalonate was monitored by IR for the appearance of the carbonyl absorbances of the corresponding conjugate acid. All polymer titrations had to be carried out very slowly over long periods of time (typically, 12 h) because of the slow diffusion of soluble reactants into the polymer's interstices.

Finally, careful weighing of the polymer before and after each synthetic step provided information on the degree of functionalization that

had been achieved in each step. These data were in good agreement with results from the previously mentioned methods of analysis.

Equilibration Experiments

Reactions of polymer-bound acids with soluble bases, and those of polymer-bound bases with soluble acids, were carried out in THF solutions of varying concentrations of the soluble component. Typically, 100 mg of resin were equilibrated with 5 or 10 ml of a 0.05 to 0.15 M solution of the soluble reagent. For example, resin P-6, containing a known loading of molybdenum hydride, was combined with a specified molarity of $\text{CpMo}(\text{CO})_3^- \text{Na}^+$ in a 5 ml volumetric flask. This mixture was then allowed to stir for six hours to assure complete equilibration of soluble components with all polymeric sites; longer reaction times led to decomposition of the species in solution. Infrared carbonyl absorbances were used to measure the ratio of concentrations of dissolved species: in the above example, of soluble molybdenum hydride formed to remaining soluble molybdenum anion. Extinction coefficients for the carbonyl bands of each soluble molybdenum compound in THF were predetermined from Beers Law plots (cf. experimental section). In the same manner, polymer-bound molybdenum anion (P-7) was equilibrated with homogeneous molybdenum hydride: the appearance in solution of molybdenum anion was coupled with an equal decrease in soluble molybdenum hydride concentration.

Equilibrium experiments were similarly carried out with polymeric benzoic acid (P-1) and with monomeric p-isopropylbenzoic acid. These reactions, however, produced quantitatively unreliable data due to the unsupported benzoate salt's limited solubility in organic solvents. Neither substitution of Na^+ by the more hydrophobic tetraalkylammonium cation, nor addition of crown ether,

improved its solubility. Studies on the acidity of the polymeric benzoic acid(P-1) were successfully carried out with $\text{CpMo}(\text{CO})_3^-\text{Na}^+$ (7-Na) as a soluble base. Reactions between polycarboxylic resin(P-1) and THF solutions of molybdenum anion were performed both as a function of added soluble molybdenum anion, and additionally as a function of the amount of added polymer in equilibrating solutions.

This same method for monitoring equilibria was applied to reactions between the supported molybdenum compounds and a series of infrared active organic carbon acids and their conjugate bases, in reactions designed to monitor the proton transfer activity of the functionalized polymer (*vide infra*).

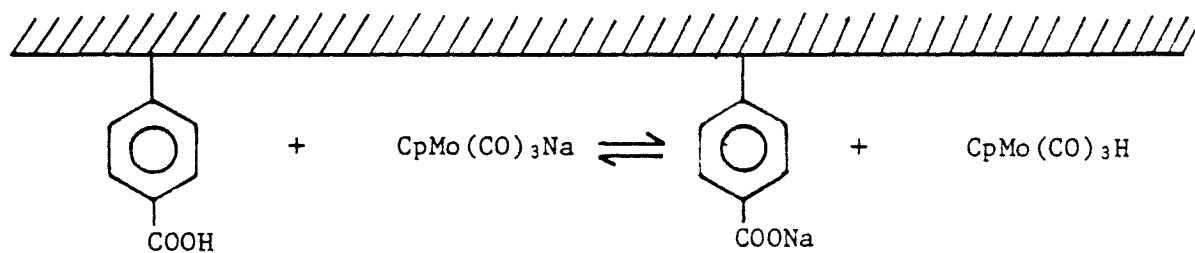
Equilibrium studies

1. Equilibration of polycarboxylate polymers $\text{P}-\text{COOH}$ (P-1) and $\text{P}-\text{COONa}$ (P-2)

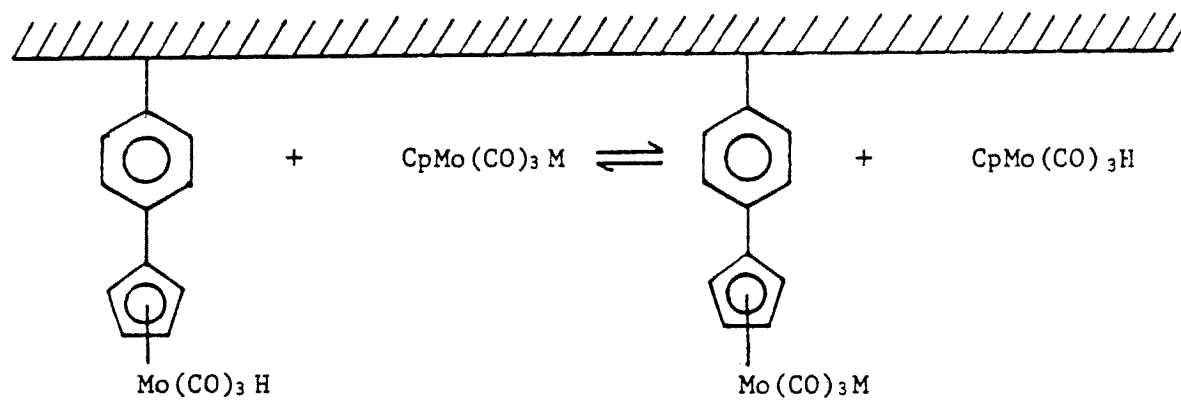
Polystyrenecarboxylic acid(P-1) and soluble molybdenum salt 7 were equilibrated in THF (as indicated in the previous section, solubility problems prevented us from quantitatively examining the equilibration of P-1 with p-isopropylbenzoate(2)). The equilibrium was also approached from the reverse direction, i.e., from equilibration of polystyrenesodium carboxylate(P-2) and soluble molybdenum hydride 6. To emphasize that these experiments involve a polyfunctional acid and a soluble base (or, as in the latter case, a polyfunctional base and a soluble acid), we write the equilibrium as shown in equation (1). Table 2 summarizes the exact quantities of starting materials used in each case, and the quantities of soluble molybdenum hydride and anion observed by IR after the system had reached equilibrium.

The polymer-bound acid $\text{P}-\text{CO}_2\text{H}$ and soluble hydride $\text{CpMo}(\text{CO})_3\text{H}$ appear to have similar acidities. This may be seen, for example, in the first three experiments of Table 2 in which increasing amounts of polymeric acid were added to a constant amount of molybdenum anion. With

Equation (1)



Equation (2)



Equation (3)

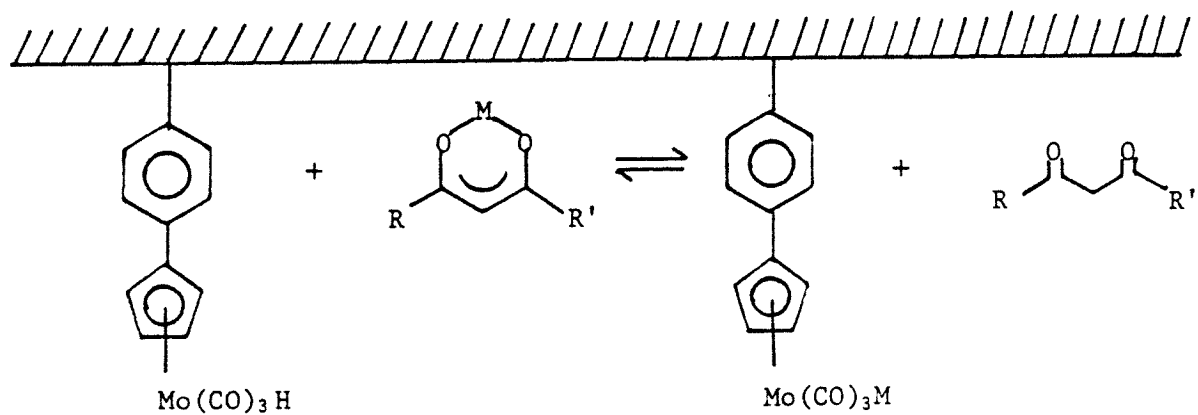


Table 2. Equilibration of P-COOH with $\text{CpMo}(\text{CO})_3\text{Na}$ and P-COONa with $\text{CpMo}(\text{CO})_3\text{H}$

Expt	Resin	Amt. of Resin (mg)	Starting Materials ^a			Soluble Components at Equilibrium		
			meq ^b CO_2H or CO_2^- on resin	$\text{CpMo}(\text{CO})_3^- \text{Na}^+$ (mmoles)	$\text{CpMo}(\text{CO})_3\text{H}$ (mmoles)	$\text{CpMo}(\text{CO})_3^- \text{Na}^+$ (mmoles)	$\text{CpMo}(\text{CO})_3\text{H}$ (mmoles)	
1	$\text{P-CO}_2\text{H}$ P-1	32	0.074	0.080	--	0.047	0.033	
2 ^c	"	46	0.106	0.080	--	0.035	0.040	
3 ^c	"	61	0.141	0.080	--	0.031	0.048	
4	"	30	0.070	0.076	--	0.045	0.031	
5 ^d	"	30	0.070	0.115	--	0.081	0.034	
6	"	54	0.125	0.121	--	0.072	0.049	
7 ^d	"	54	0.125	0.262	--	0.199	0.063	
8	"		0.134	0.164	--	0.092	0.072	
9	$\text{P-CO}_2^- \text{Na}^+$ P-2	35	0.076	--	0.076	0.037	0.039	
10	"	37	0.081	--	0.074	0.038	0.036	

^aIn each case, 10 ml THF was used as solvent. ^bDetermined by titration of polymer (in acidic form) by OH^- (see experimental section). ^cPerformed by adding sequential amounts of $\text{P-CO}_2\text{H}$ to the equilibrated solution of the previous experiment. ^dPerformed by adding sequential amounts of $\text{CpMo}(\text{CO})_3^- \text{Na}^+$ to the equilibrated solution of the previous experiment.

roughly equal amounts of starting acid and base, the soluble anion is less than half protonated. Addition of more acid does not produce a concomitant amount of soluble hydride; doubling the amount of acid in solution produces significantly less than double the initial amount of hydride observed after the first addition. Similarly, adding sequential amounts of soluble anion to a stationary amount of polymeric acid produces soluble hydride, but not in quantities equal to the amount of anion added (experiments 4 through 10). This is just the sort of observation expected in a weak acid, weak base titration.

2. Equilibrations of metalated polymers $\text{P-CpMo(CO)}_3\text{H}$ (P-6) and $\text{P-CpMo(CO)}_3^- \text{M}^+$ (P-7)

Similar experiments were carried out on the polymer-bound molybdenum hydride (and anion) with soluble molybdenum anion (and its conjugate acid), equation (2). Again, to rule out kinetic effects, each equilibrium was approached from both sides. As can be seen from Tables 3 and 4, polymeric acid $\text{P-CpMo(CO)}_3\text{H}$ (P-6) and its soluble analog 6 have similar acidities: this is shown by the less-than-quantitative proton transfer between the soluble species of equation (2) (a display of weak acid-weak base behavior as was observed in the case of P-COOH and P-COONa). The nearly identical behavior of the sodium and lithium salts indicates that this behavior is due to properties inherent in the neutral acids and anions, rather than being controlled by ion-pairing energetics. In support of this conclusion, addition of crown ether to preequilibrated solutions of polymers and soluble reagents produced no dramatic change in the concentrations of the reactants. In order to establish that the polymeric acid $\text{P-CpMo(CO)}_3\text{H}$ (P-6) could be deprotonated quantitatively with anions whose base strengths were somewhat stronger than that of CpMo(CO)_3^- (7) we also subjected P-6 to treatment with enolate anions of diethylmalonate, ethylacetoacetate, 2-carboethoxycyclopentanone, and 2-carboethoxycyclohexanone, equation (3). These were selected not only because they had pK_a 's in the appropriate range, but also because the concentrations of each β -dicarbonyl and its conjugate base could be

Table 3. Equilibration of P^- -CpMo(CO) $_3$ H with CpMo(CO) $_3^-$ Na $^+$ and CpMo(CO) $_3^-$ Li $^+$.

Expt	Resin	Starting Materials ^a			Soluble Components at Equilibrium			
		Amt. of Resin (mg)	meq CpMo(CO) $_3$ H bound to resin	CpMo(CO) $_3^-$ Na $^+$ (mmoles)	CpMo(CO) $_3^-$ Li $^+$ (mmoles)	CpMo(CO) $_3^-$ Na $^+$ (mmoles)	CpMo(CO) $_3^-$ Li $^+$ (mmoles)	CpMo(CO) $_3$ H (mmoles)
1	P^- -CpMo(CO) $_3$ H P-6	89	.058	.019	--	.008	--	.011
2 ^c	"	89	.058	.030	--	.015	--	.015
3 ^c	"	89	.058	.042	--	.024	--	.018
4 ^c	"	89	.058	.063	--	.040	--	.023
5	"	101	.066	--	.018	--	.007	.011
6 ^d	"	101	.066	--	.033	--	.017	.016
7 ^d	"	101	.066	--	.047	--	.026	.021
8 ^d	"	101	.066	--	.061	--	.039	.022
9 ^d	"	101	.066	--	.087	--	.066	.021 ^e

^a In each case, 5 ml THF was used as solvent. ^b Determined by elemental analysis of molybdenum on the resin. ^c Performed by adding sequential amounts of CpMo(CO) $_3^-$ Na $^+$ to the equilibrated solution of the previous experiment. ^d Performed by adding sequential amounts of CpMo(CO) $_3^-$ Li $^+$ to the equilibrated solution of the previous experiment. ^e Decrease in CpMo(CO) $_3$ H concentration from previous experiment is probably due to decomposition of the hydride in solution.

Table 4. Equilibration of $(P) - CpMo(CO)_3^- Na^+$ and $(P) - CpMo(CO)_3^- Li^+$ with $CpMo(CO)_3 H$

Expt	Resin	Starting Materials ^a				Soluble Components at Equilibrium					
		Amt. of Resin (mg)	Meq ^b $CpMo(CO)_3^- Na^+$ on resin	Meq ^c $CpMo(CO)_3^- Li^+$ on resin	Meq ^c $CpMo(CO)_3 H$ on resin	$CpMo(CO)_3^- Na^+$ (mmoles)	$CpMo(CO)_3^- Li^+$ (mmoles)	$CpMo(CO)_3 H$ (mmoles)	$CpMo(CO)_3^- Na^+$ (mmoles)	$CpMo(CO)_3^- Li^+$ (mmoles)	$CpMo(CO)_3 H$ (mmoles)
1	$(P) - CpMo(CO)_3^- Na^+$ P-7-Na	94	.060	--	--	.02405	.01585	--	--	--	.00820
2 ^d	"	94	.060	--	--	.03477	.01970	--	--	--	.01507
3 ^d	"	94	.060	--	--	.04556	.02300	--	--	--	.02256
4 ^d	"	94	.060	--	--	.06152	.02662	--	--	--	.03490
5 ^d	"	94	.060	--	--	.06682	.02886	--	--	--	.03796
6	$(P) - CpMo(CO)_3^- Li^+$ P-7-Li	100	--	.0495	.0495	.02228	--	.01719	--	--	.00509
7 ^d	"	100	--	.0495	.0495	.03545	--	.02300	--	--	.01245
8 ^d	"	100	--	.0495	.0495	.05237	--	.02923	--	--	.02314
9 ^d	"	100	--	.0495	.0495	.07225	--	.03559	--	--	.03666

^aIn each case, 5 ml THF was used as solvent. ^bDetermined from elemental analysis of sodium on the resin, P-7-Na. ^cDetermined from elemental analysis of lithium on the resin, P-7-Li. ^dPerformed by adding sequential amounts of $CpMo(CO)_3 H$ to equilibrated solution of previous experiment.

clearly monitored by observing the carbonyl region of the infrared spectrum. In each of these cases, the equilibrium lay completely on the side of protonated enolate and deprotonated polymeric hydride.

Discussion

The first question we can now address on the basis of our results is: does the pK_a (acidity) of $CpMo(CO)_3H$ change appreciably upon binding to a swellable polymer? Although there are some important uncertainties in the quantitative analysis of our results, the qualitative result is clear: the fact that partial proton transfer is achieved on exposure of $CpMo(CO)_3H$ (6) to the polymer-bound analog of its conjugate base $\textcircled{P}-CpMo(CO)_3^-$ (P-7) requires that their effective acidities be very similar²⁴.

That solutions of polymer-bound weak acids P-1 and P-6 and soluble weak bases behave as buffers is most conveniently demonstrated by plotting the data given in Tables 2, 3, and 4 to show how the amount of newly generated soluble species (anion 7 or hydride 6) depends upon the ratio (rather than the absolute amounts) of starting acid and base. Figure 1, for example, combines the data of Table 2 in one chart. As the ratio of initially "reacted" molybdenum anion to polymeric acid increases, the amounts of molybdenum anion and hydride observed in solution change rather weakly, until the amount of anion is high enough to have deprotonated most of the accessible acidic sites on the polymer. In a similar manner, figures 2 and 3 present graphically data from Tables 3 and 4.

One difficulty with quantifying this result, that polymer-attached and soluble acids of similar structure have similar acidities, arises from the problem of measuring (and even defining) acidities in relatively nonpolar solvents such as THF. Ideally, we would like to have carried out our studies in aqueous or other highly polar media (e.g., DMSO), in which good pK_a data are available for a wide range of soluble organic acids.²⁵ The use of these solvents was precluded by the

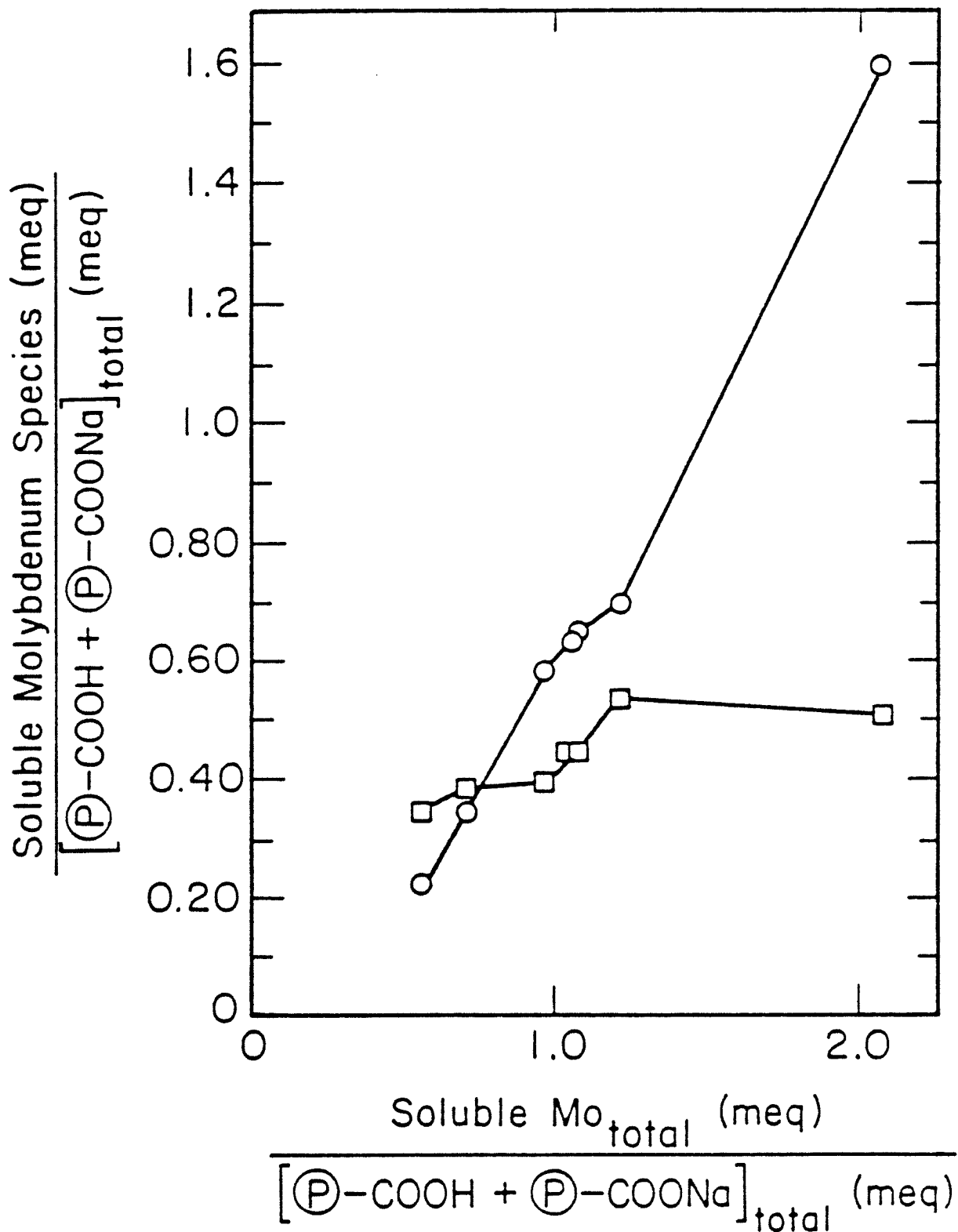


Figure 1. Dependence of the concentrations of soluble molybdenum species at equilibrium on the molar ratio of $\text{CpMo}(\text{CO})_3\text{Na}$ added to P-COOH ; cf. equation (1).

$(\square) = \text{CpMo}(\text{CO})_3\text{H}$, $(\circ) = \text{CpMoCO}_3\text{Na}$.

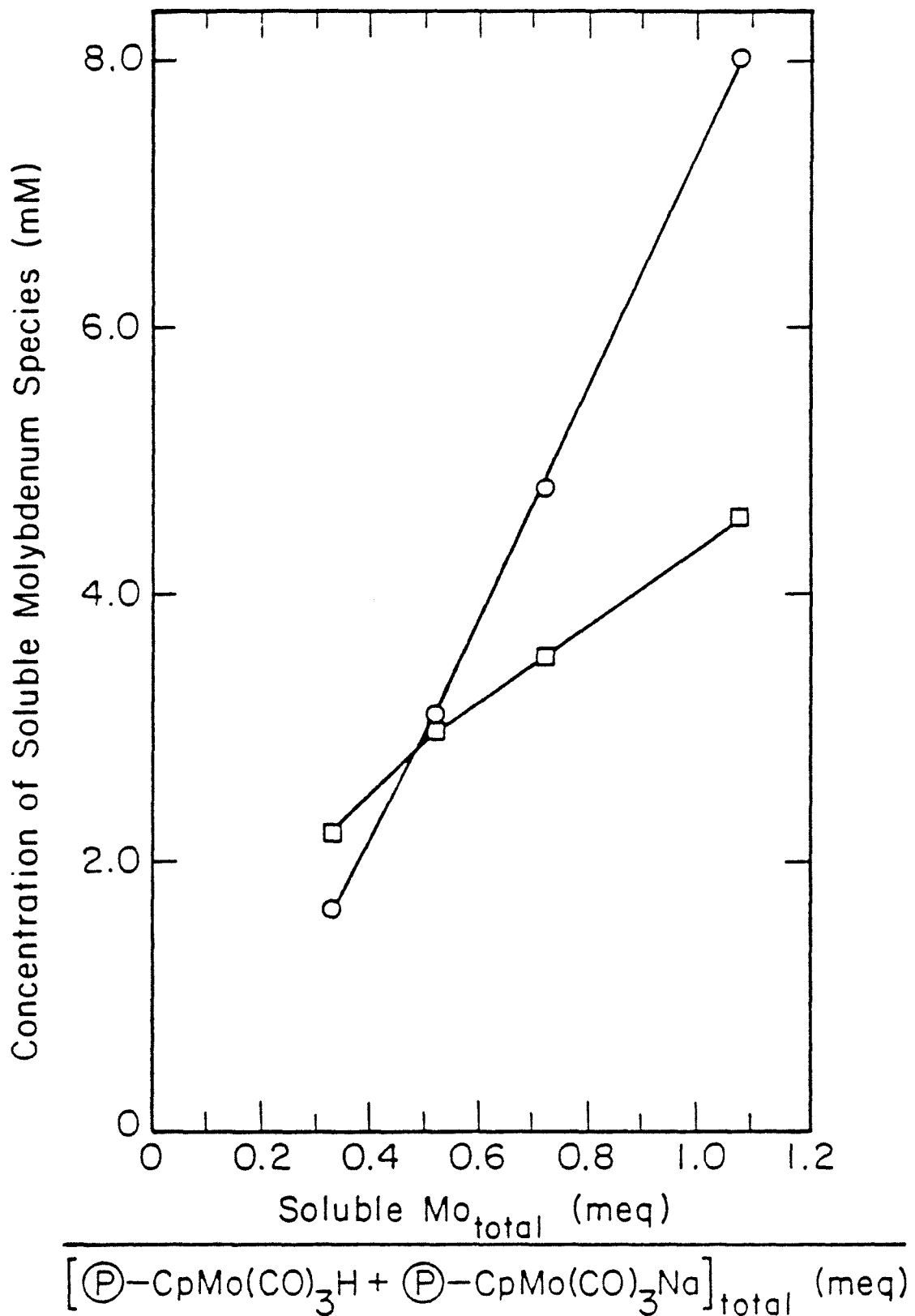


Figure 2. Dependence of the concentrations of soluble molybdenum species at equilibrium on the molar ratio of $\text{CpMo(CO)}_3\text{Na}$ added to $\text{Ⓟ-CpMo(CO)}_3\text{H}$; cf. equation (2). $(\square) = \text{CpMo(CO)}_3\text{H}$, $(\circ) = \text{CpMo(CO)}_3\text{Na}$.

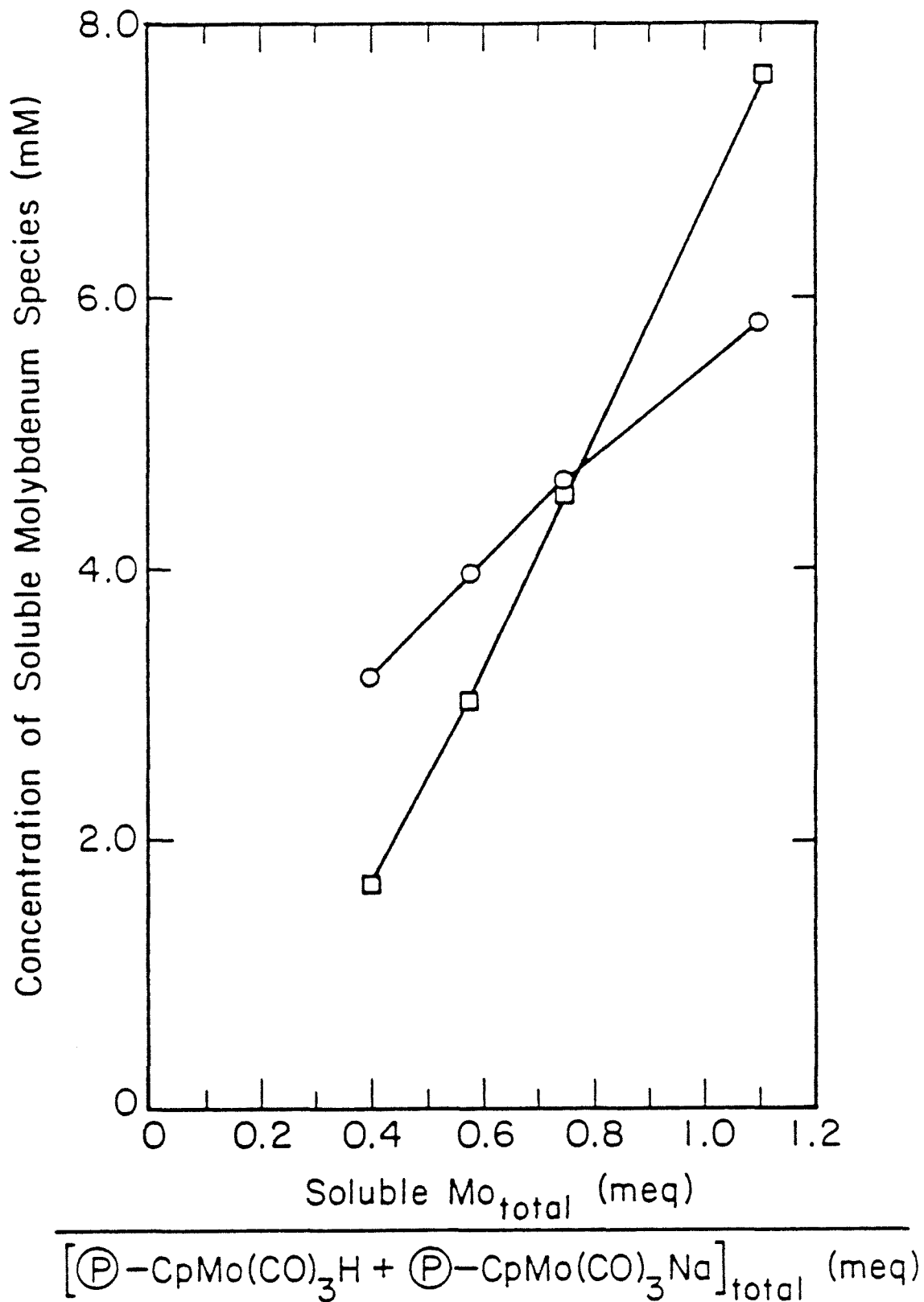


Figure 3. Dependence of the concentrations of soluble molybdenum species at equilibrium on the molar ratio of $\text{CpMo}(\text{CO})_3\text{H}$ added to $\text{Ⓟ}-\text{CpMo}(\text{CO})_3\text{Na}$; cf. equation (2). $[\square] = \text{CpMo}(\text{CO})_3\text{H}$, $(\circ) = \text{CpMo}(\text{CO})_3\text{Na}$.

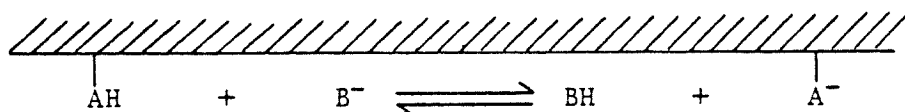
fact that our molybdenum hydride is insoluble in water and unstable in highly polar solvents such as DMSO, acetonitrile and HMPA. We chose THF as the best alternative because it swells the polymer and dissolves our molybdenum compounds reasonably well.²⁶

We now wish to concern ourselves with a second, and somewhat more complicated, question arising from our results: are equilibria between swellable polymers and dissolved species analyzable in a simple manner; i.e., is it possible to write equilibrium expressions in which the swelled polymeric acids and anions behave as though they were dissolved species?

It seemed to us the most straightforward way to investigate this problem would be to write equilibrium expressions for the proton transfer reactions examined here, define equilibrium "constants" in the usual way, and then see if these K's do in fact remain constant as the total amounts of starting acid and base are varied.

By definition, the equilibrium constant for reaction between a polymer-bound acid and its polymer-bound conjugate anion, in the presence of a soluble acid and its soluble conjugate base (equation (4)) is given by equation (5), where the symbols in the first ratio represent activities. For dilute soluble systems, we would normally replace these activities by concentrations, and the K_{eq} so defined would remain constant over a wide range of initial concentrations of acid and base.²⁷ In our polymer systems, we define the concentrations of soluble species in the normal way, using conventional symbolism for these values. We define the "concentrations" of polymer-bound species as the ratio of the number of milliequivalents of polymer-attached acid or base in a given experiment to the number of ml of solvent used. Since these are not dissolved species, we use the modified brackets shown in equation (5) to represent these quantities.

Equation (4)



Equation (5)

$$K_{\text{eq}} = \frac{a_{\text{BH}} a_{\text{P}^- \text{A}^-}}{a_{\text{B}^-} a_{\text{P}^- \text{AH}}} \approx \frac{[\text{BH}] \{\text{P}^- \text{A}^-\}}{[\text{B}^-] \{\text{P}^- \text{AH}\}}$$

We first examined the supported molybdenum hydride/soluble molybdenum anion system to determine whether it adhered to this equilibrium model. The data given in Table 3 were used to calculate a value of K for several different ratios of added soluble $\text{CpMo}(\text{CO})_3\text{Na}$ to polymer-bound $\text{CpMo}(\text{CO})_3\text{H}$ (see experimental section for the method of K_{eq} calculation). A plot of these K 's vs. the ratio of soluble to bound molybdenum shows that they are in fact constant; i.e., the system adheres quite nicely to the equilibrium model. Constructing a similar plot using the data obtained with the lithium salt of the soluble anion also gives a constant K , with an average value very close to that obtained for the sodium salt (figure 4).

This equilibrium was next approached from the opposite side. Data taken from experiments in which soluble hydride 6 was added to supported anion P-7Na (Table 4) were again used to construct a plot of K vs. the ratio of soluble Mo to supported Mo (figure 4). Again a constant K was obtained, although the absolute value did not quite match that obtained from the experiments which started with soluble base and supported hydride. The equilibrium was also investigated using the supported lithium salt P-7Li. In this case, although still in agreement within an order of magnitude, the absolute value of K differed markedly from that observed in the first three plots. We believe this is due to the fact that the polymer used to obtain the Li^+ data was prepared by a synthetic route different from that used in the first three runs. The uncertainty in our measurement of the total amount of active molybdenum bound to the resin (*vide supra*) probably accounts for this difference in calculated values of K_{eq} .

Effective equilibrium constants were obtained for the reactions between $\text{P}^{\ominus}\text{-COOH}$ and $\text{CpMo}(\text{CO})_3\text{Na}$ (and its reverse reaction, $\text{P}^{\ominus}\text{-COONa}$ and $\text{CpMo}(\text{CO})_3\text{H}$) from the data of Table 2. The calculated equilibrium constants are once again essentially constant at varying ratios of starting materials, and, within experimental error, the same K_{eq} is obtained starting from both sides of the equilibrium.

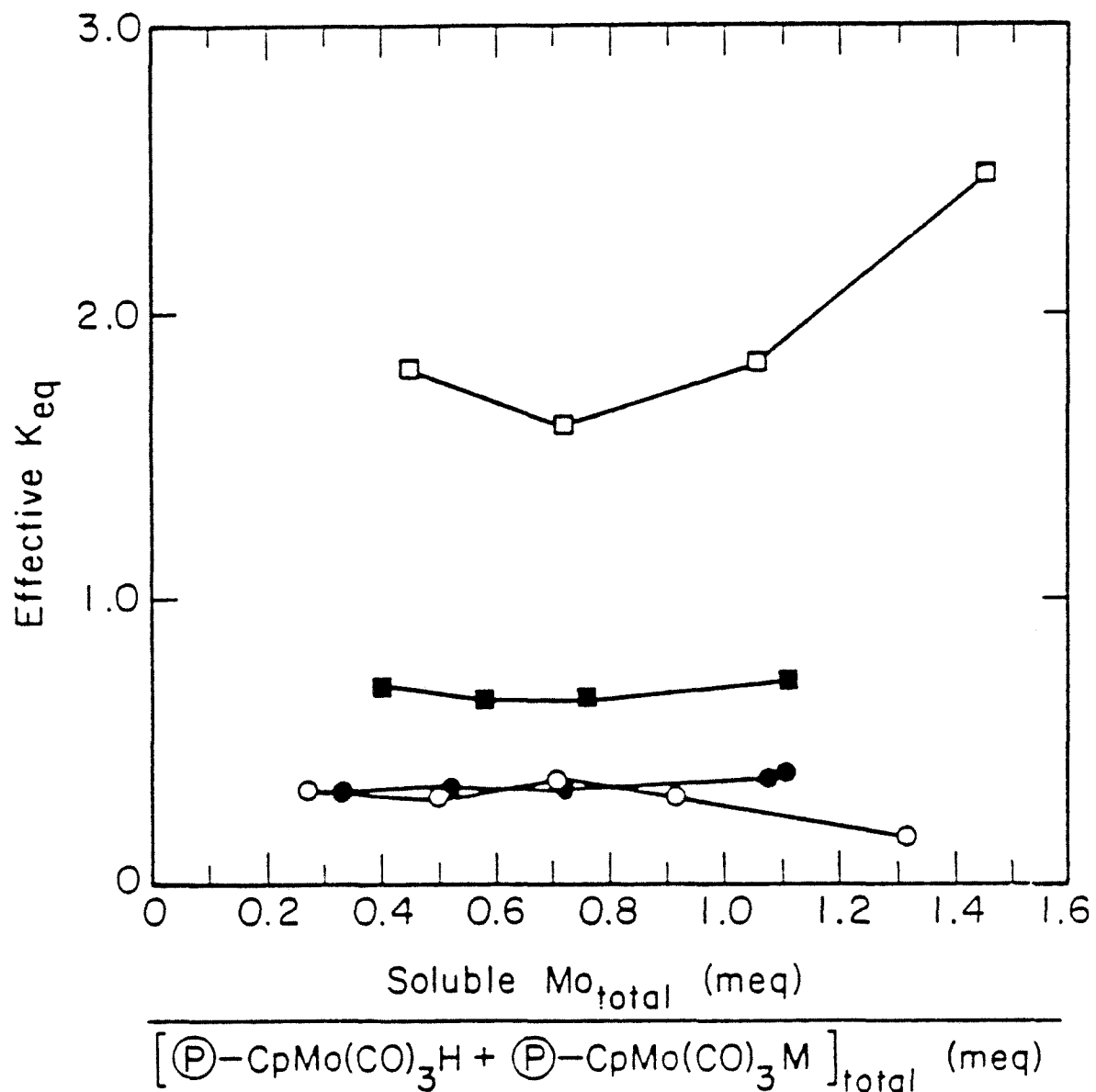


Figure 4. Equilibrium constants plotted as a function of the molar ratios of soluble to polymer-bound components of equilibrium mixtures. The equilibrium mixtures result from combination of: (a) $\text{P-Cp-Mo(CO)}_3\text{H}$ and $\text{CpMo(CO)}_3\text{Li}$ (\circ); (b) $\text{P-Cp-Mo(CO)}_3\text{H}$ and $\text{CpMo(CO)}_3\text{Na}$ (\bullet); (c) $\text{P-Cp-Mo(CO)}_3\text{Li}$ and $\text{CpMo(CO)}_3\text{H}$ (\square); (d) $\text{P-Cp-Mo(CO)}_3\text{Na}$ and $\text{CpMo(CO)}_3\text{H}$ (\blacksquare), (equation (2)).

In conclusion, we have been able to demonstrate that proton transfer equilibria between soluble and polymer-bound acids and bases can be effectively investigated, especially if the soluble components are quantitatively analyzable by IR spectroscopy. The reactions of the supported molecules studied behave analogously to reactions between soluble species, and seem to obey conventional equilibrium theory. Finally, although we do not feel absolute pK_a 's of these species in THF are very meaningful, it is clear that the acidities of soluble $CpMo(CO)_3H$ and its polymer-bound analog are very nearly identical, and that this conclusion also applies to the organic acid $p-C_3H_7C_6H_4COOH$ and its polymer-bound analog.

Experimental Section

General

The 3% cross-linked macroreticular polystyrene divinylbenzene copolymer was purified from industrial contaminants^{5c} by stirring in the following solvents under the specified conditions: CH₂Cl₂, reagent grade, 25°, 2.5h; THF, reagent grade, 50°, 2h; H₂O, distilled, 70°, 2h; HCl (aq.), 1M, 70°, 2h; H₂O, distilled, 50°, overnight; KOH (aq.), 1M, 50°, 1h; H₂O, distilled, 3 x 5 min; MeOH, reagent grade, 50°, 2h; benzene, reagent grade, 55°, 2h; benzene, purified, 55°, 2h; CH₂Cl₂, purified, 55°, 2h; Et₂O, anhydrous, 55°, 1h. The beads were then dried overnight in vacuo.

The use of magnetic stirrers led to pulverization of the polymer beads. This was not considered disadvantageous since it was observed that diffusion rates of soluble reagents into internal polymer sites increased on reduced particle size. In addition, the IR bands of mulls of powdered resins were better resolved than those of mulls made from intact beads.

N-butyllithium (2.2M in hexane), methyllithium (1.45M in diethyl ether) and lithium triethylborohydride (1M in THF) were used as received. Tetramethylethylenediamine (TMEDA) was distilled from CaH₂ and degassed before use. 2-Cyclopentenone was distilled at reduced pressure immediately prior to its use. Mo(CO)₆ and [MoCp(CO)₃]₂ were used as received. NaH and LiH were rinsed free from mineral oil with hexane and stored in an inert atmosphere. P-toluenesulfonic acid monohydrate was dehydrated by azeotropic distillation with benzene. Diethyl malonate, ethyl acetoacetate, 2-carboethoxycyclohexanone, and 2-carboethoxycyclopentanone were each fractionally distilled from molecular sieves (4Å) at reduced pressure, and degassed prior to use.

Tetrahydrofuran (THF), benzene, cyclohexane, diethyl ether, and 1,4 di-

oxane were purified by distillation from sodium benzophenone ketyl at reduced pressure and thoroughly degassed. Acetonitrile was distilled from P_2O_5 and thoroughly degassed.

Unless indicated otherwise, all reactions and routine manipulations were carried out at 20°C under a nitrogen atmosphere in a dry box. Reactions requiring heating or cooling were performed on conventional vacuum lines using Schlenk techniques.

Infrared spectra were recorded on a Perkin-Elmer 283 spectrophotometer, using the absorbance mode for quantitative analysis. Proton nuclear magnetic resonance spectra were recorded on a Varian EM-390 spectrometer.

Elemental analyses were performed by the University of California (Berkeley) Microchemical Analytical Laboratories. Metal analyses were performed by atomic absorption spectrometry on resin samples which had been digested in sulfuric acid and hydrogen peroxide.

Polymer-bound phenyllithium^{14a}

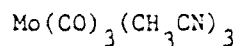
Polystyrene resin (5g, 47.6 meq in styrene monomer) was stirred in cyclohexane (30 ml) under argon at 50° for 1 h in a 300 ml Schlenk flask. To this stirring slurry, TMEDA (11.2 ml, 74.2 mM) was added via syringe over 15 min, followed by a similar addition of n-BuLi (30 ml, 72.6 mM) over 5 min. The beads rapidly changed from white to tan. The mixture was stirred at 65° for 7 h during which time the cyclohexane solution changed from yellow to dark orange. The lithiated polymer was filtered under reduced pressure and washed with cyclohexane (6 x 30 ml) and THF (3 x 30 ml) until the washings were clear. The remaining salmon-colored beads were charged with THF (30 ml) for the following reaction with cyclopentanone.

Polymer-bound cyclopentadiene (P-3)^{6b}

To the stirring THF slurry of lithiated polystyrene from the previous

reaction, cooled in an ice bath, was added cyclopentenone (9 ml, 108 mM) via syringe over 4 min. The beads turned from pink to yellow then to white over the course of the addition. After stirring under argon for 12 h, the cyclopentadienyl polymer was filtered under positive argon pressure and washed with the following solvents: THF (2 x 30 ml); THF:H₂O(1:1, 2 x 30 ml); H₂O (30 ml) (beads changed from light yellow to white); MeOH (2 x 30 ml); benzene (3 x 30 ml). The resulting polymer was dried in vacuo at 40°. A weight gain of 1.18g was recorded corresponding to a 38% substitution of styrene monomers by cyclopentadiene, or 2.95 meq of cyclopentadiene per gram of cyclopentadienyl polymer. Elemental analysis for lithium on a sample of cyclopentadienyl resin (P-3) which had been previously treated with methyllithium^{6b} agreed well with the cyclopentadienyl substitution percentages derived from weight gain calculations. The resinolithium cyclopentadienide was prepared by adding to a slurry of polymer-bound cyclopentadiene (P-3) in THF a diethyl ether solution of methyllithium (five-fold excess), whereupon bubbling was observed (presumably methane). After 4 h the resulting light pink polymer was washed with diethyl ether and THF, and dried in vacuo.

The degree of cyclopentadiene substitution on the polystyryl resin derived from the above two methods agreed with a third analysis performed by titration of resin P-3. A standardized THF solution of sodium triphenylmethide, prepared by reaction of NaNH₂ with triphenylmethane, was added slowly from a buret to a stirring THF slurry of P-3 over 12 h. The red color of sodium triphenylmethide served as an endpoint indicator. The titration required the lengthy term to assure equilibration with all internal polymeric sites.



The procedure described in the literature²⁸ was followed. The reaction was monitored by IR for disappearance of $\text{Mo}(\text{CO})_6$ (1980 cm^{-1} (THF)) over 2 days, after which time the solvent (CH_3CN) was removed at reduced pressure, leaving a light yellow, powdery residue.

Reaction of polymer-bound cyclopentadiene (P-3) with $\text{Mo}(\text{CO})_3(\text{CH}_3\text{CN})_3$

In a representative synthesis of resin P-4, a slurry of polymer-bound cyclopentadiene (P-3) (1.15 g, ~3.4 meq. in Cp) in THF (40 ml) was combined with an excess of $\text{Mo}(\text{CO})_3(\text{MeCN})_3$ (3 g, 9.9 mM) and the mixture was stirred at 70° under argon, 12 h. The resulting beads, red after extensive washing in THF and drying in vacuo, exhibited infrared bands at 2025 (m), 1948 (s,br) and 1902 (s) cm^{-1} (KBr). Such a pattern of bands corresponds to a mixture of monomers of $\text{MoCp}(\text{CO})_3\text{H}$ (2006 (m), 1883 (s,br) cm^{-1} (KBr)) and $(\text{MoCp}(\text{CO})_3)_2$ (1900 (s), 1950 (s) cm^{-1} (KBr)). The red color of the resulting beads also implicates the formation of dimeric ($[\text{RCp}(\text{CO})_3\text{Mo}]_2$) groups on the polymer. Elemental analysis of this molybdenum resin P-4 showed approximately 0.8 meq of molybdenum per gram of polymer (7.77% Mo). This corresponds to approximately 31% of the cyclopentadienyl ligands on the resin being bound to molybdenum.

Reaction of molybdenum resin P-4 with $\text{HB}(\text{C}_2\text{H}_5)_3\text{Li}$

Resin P-4 (0.75 g, ~0.6 meq Mo), containing a mixture of bound $\text{CpMo}(\text{CO})_3\text{H}$ and bound $[\text{CpMo}(\text{CO})_3]_2$, was swelled in THF (10 ml), 1 h. Immediately on addition of $\text{HB}(\text{C}_2\text{H}_5)_3\text{Li}$ (3.0 ml of a 1M THF solution, 3 mM), a change in the resin's color from red to brown was accompanied by vigorous gas evolution. The resin was stirred 5 h, filtered, washed with THF, and dried in vacuo. The

resulting beige polymer P-5 exhibited IR absorptions at 1898 (s), 1773 (s) and 1703 (s) cm^{-1} (KBr), characteristic of $\text{RCpMo}(\text{CO})_3^- \text{Li}^+$.

$\text{P-CpMo}(\text{CO})_3\text{H}$ (P-6)

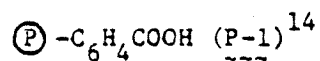
In a representative acidification of P-5, P-5 (3.21 g, ~2.6 mM Mo) was swelled in THF (40 ml) over 1 h. P-toluenesulfonic acid (0.50 g, 2.75 mM) in THF (20 ml) was added over several hours from an addition funnel to the stirring polymer slurry. After an additional 6 h of stirring, an aliquot of the reaction solvent was tested with an indicator for residual acidity to assure that an excess of protonating reagent had been used. On confirmation of acidity, the slurry was extensively washed with clean THF until the rinses, in contact with the resin for at least an hour, contained no further acid. The resulting beige resin P-6 was then dried in vacuo. Infrared absorbances for P-6 are given in Table I. Elemental analysis was performed on its sodium derivative P-7Na (cf. next section).

$\text{P-CpMo}(\text{CO})_3^- \text{M}^+$ (P-7)

In a representative synthesis of polymer-bound molybdenum anion (P-7), polymer-bound molybdenum hydride (2.86 g, ~1.86 mM Mo) was swelled in THF (20 ml), 1 h. Monosodium diethylmalonate (vide infra) (6.59 mM in 35 ml THF) was added from an addition funnel to the stirring resin over several hours. After an additional 6 h of stirring, the reaction solvent was checked by IR for residual sodium diethylmalonate to assure that an excess of the deprotonating reagent had been used. The resin was then extensively washed with clean THF until rinses, in contact with the resin for at least an hour, concentrated on a rotary evaporator and checked by IR, contained no detectable

diethylmalonate or its sodium salt. The resulting light beige resin P-7Na was dried in vacuo. IR absorbances for P-7Na are given in Table 1. Elemental analysis of P-7Na gave a molybdenum content of 0.74 mM Mo per gram of polymer, slightly higher than that for sodium of 0.64 mM Na per gram of polymer (Mo, 7.08%; Na, 1.47%). The lithium salt of polymer-bound molybdenum anion P-7Li was prepared in an analogous manner using monolithium diethylmalonate as a base. Elemental analysis of resin P-7Li yields 0.67 mM Mo and 0.49 mM Li per gram of polymer (Mo, 6.43%; Li, 0.34%). IR absorbances of resin P-7Li are given in Table 1.

Polymer-bound Organic Carboxylates



Polymer-bound phenyllithium (3g) was prepared as described above, charged with THF (75 ml), cooled to -78°C , and evacuated. Carbon dioxide was introduced to the THF solution of resinophenyllithium in the following manner. A 300 ml flask of dry ice, connected to a vacuum manifold, was subjected to several freeze-pump-thaw cycles to remove oxygen. The flask was then allowed to warm to room temperature: gaseous CO_2 boil-off was passed through a column of activated molecular sieves (4 \AA) and bubbled into the THF resin slurry (now at ambient temperature) via a gas dispersion stick. The color of the resin quickly changed from pink to white. The positive pressure in the manifold was monitored with a mercury bubbler, an increase in pressure (i.e. a decrease in CO_2 uptake by the resin) indicating completion of the reaction. After 15 min the CO_2 uptake was negligible; however, the bubbling was continued an

additional 2 h to assure exposure of all internal polymeric sites to the CO_2 . In the air, the resin was worked up according to the method of Fyles and Leznoff^{14b} and the resulting resin P-1 was dried *in vacuo*. The degree of carboxylic functionalization was determined by titration (next section). The infrared carbonyl absorptions of carboxylic acid resin P-1 are given in Table I.

$\text{P-C}_6\text{H}_4\text{COONa}$ (P-2)

Polymeric sodium benzoate was prepared by titration of $\text{P-C}_6\text{H}_4\text{COOH}$ (P-1) with sodium hydroxide. Direct titration of the polymeric carboxylic acid with the alkaline titrant was tedious because of slow diffusion rates of reactants into the polymer. For this reason the following back titration method was employed (in this case, no precautions were taken to exclude air). The aqueous NaOH titrant (0.09M) was standardized against primary standard potassium acid phthalate. The aqueous HCl titrant (0.11 M) was standardized against primary standard sodium carbonate. Phenolphthalein and bromophenol blue were used as indicators in titrations for acid and base, respectively. In a typical titration, 100 mg of polycarboxylic resin P-1 was placed in a flask equipped with a magnetic stir bar, and allowed to swell in THF or 1,4-dioxane (10 ml) for ~ 1 h. An amount of alkaline titrant corresponding to a slight excess relative to the estimated number of acidic polymeric sites was then added all at once. The slurry was allowed to equilibrate with stirring overnight. The total solution was then back titrated with the acid titrant, using standard buret techniques, until an endpoint was reached. The loading of carboxylic acid sites on the polymer P-1, calculated from the net amount of base "consumed" by the resin, was found to be $2.32 \pm .06$ meq H^+ per gram of P-COOH (P-1). Unreasonably low results for carboxylate functionalization were obtained when the resin P-1 was not preswelled in the organic solvent. This is presumably due to the inaccessibility

of internal polymer sites which rely on solvation by a relatively non-polar solvent for exposure to external reagents.¹⁶ The volume of organic solvent had to be at least that of the total aqueous titrant introduced during the titration. Infrared absorptions for $\text{P-C}_6\text{H}_4\text{COONa}$ (P-2) are given in Table 1.

Alkali metal salts of β -dicarbonyl compounds

Diethylmalonate, ethylacetoacetate, 2-carboethoxycyclopentanone and 2-carboethoxycyclohexanone were converted to their monosodium salts in the following manner. A THF solution (~ 0.3 M) of the β -dicarbonyl was added from an addition funnel to a stirred slurry of a slight excess of NaH in THF (of approximately equal volume) over 1 h. Rapid gas evolution was observed. The resulting solution, checked by IR for complete conversion to the monosodium salt, was decanted from residual NaH and treated as follows. When the β -dicarbonyl sodium salts were to be used in excess as a synthetic reagent (e.g., in the conversion of P-6 to P-7) the salts were used *in situ* in their THF solutions. However, when the β -dicarbonyl salts were to be used to carefully monitor proton transfer activity of polymeric hydride P-6, they were first purified by crystallization. After the removal of THF at reduced pressure the following anhydrous crystallizing solvents were employed for each salt: sodium diethylmalonate, hot methylene chloride; sodium ethylaceto-

acetate, hot diethyl ether; sodium 2-carboethoxycyclopentanone, ethanol; sodium 2-carboethoxycyclohexanone, ethanol. Infrared carbonyl absorbances in THF for each β -dicarbonyl and its conjugate base were as follows: diethylmalonate: 1750, 1735 cm^{-1} , sodium salt: 1670, 1550 cm^{-1} , lithium salt: 1660, 1530 cm^{-1} ; ethylacetoacetate: 1745, 1720 cm^{-1} , sodium salt: 1660, 1510 cm^{-1} ; 2-carboethoxycyclopentanone: 1760, 1735 cm^{-1} , sodium salt: 1665, 1515 cm^{-1} ; 2-carboethoxycyclohexanone: 1745, 1717 cm^{-1} , sodium salt: 1660, 1483 cm^{-1} . The lithium salt of diethylmalonate was prepared as above, except that LiH was substituted for NaH.

Monomeric molybdenum compounds

$\text{CpMo}(\text{CO})_3\text{H}$ (6), $\text{CpMo}(\text{CO})_3^-\text{Na}^+$ (7-Na) and $\text{CpMo}(\text{CO})_3\text{CH}_3$ (8) were synthesized according to literature methods.²⁹ $\text{CpMo}(\text{CO})_3^-\text{Na}^+$ was also synthesized by substituting NaBH_4 for sodium amalgam in the literature procedure. Infrared spectral data are given in Table 1.

$\text{CpMo}(\text{CO})_3^-\text{Li}^+$ (7-Li)¹⁹

To a stirring solution of $[\text{CpMo}(\text{CO})_3]_2$ (2.0 g, 4.08 mM) in THF (10 ml) was added $\text{HB}(\text{C}_2\text{H}_5)_3\text{Li}$ (15 ml of a 1.0 M THF solution, 15 mM) from an addition funnel over 10 min. The solution changed from red to brown over the course of the addition; an infrared spectrum immediately following the addition indicated that the reduction was complete. Solvent was removed under reduced pressure and the lithium salt was crystallized from diethylether/benzene. Yield 1.98 g (75%). Infrared data are given in Table 2. The NMR spectrum of 7-Li indicates that one molecule of THF is incorporated into the crystal of $\text{CpMo}(\text{CO})_3^-\text{Li}^+$ (^1H NMR (acetone- d_6) δ 4.93 (s, C_5H_5 , 5H), δ 3.60 (s, THF, 4H), δ 1.79 (s, THF, 4H) ppm).

Beer's Law Determination of Extinction Coefficients

Standard procedures for deriving Beer's Law plots were followed. Plots of ϵ vs. concentration covered the concentration range in which equilibration experiments were to be run: .01 to .11 M for organic carbonyl compounds and .001 to .015 for transition metal carbonyl compounds. All extinction coefficient determinations (and subsequent equilibration reactions) were carried out in THF, typically in a 5 or 10 ml volumetric flask equipped with a magnetic stir bar. Infrared spectra were recorded in absorbance units. An electronic expansion feature on the IR spectrophotometer was employed for solutions of low concentrations. Each spectrum was recorded five times, yielding an averaged peak height for each band from the five scans at each concentration. Extinction coefficients for the carbonyl bands of the following compounds were determined: [compound, CO wavenumber in cm^{-1} (extinction coefficient, ϵ)] $\text{CpMo}(\text{CO})_3\text{H}$, 2015 (3.20×10^3), 1932 (5.55×10^3); $\text{CpMo}(\text{CO})_3^- \text{Na}^+$, 1903 (4.18×10^3), 1798 (4.50×10^3), 1745 (3.13×10^3); $\text{CpMo}(\text{CO})_3^- \text{Li}^+$, 1910 (2.50×10^3), 1810 (3.10×10^3), 1785 (1.0×10^3), 1718 (2.45×10^3); diethylmalonate, 1750 (5.96×10^2), 1735 (7.01×10^2); sodium diethylmalonate, 1673 (1.67×10^3), 1550 (1.11×10^3).

Equilibration Reactions

Equilibria between polymer-bound and soluble species were set up and monitored as described earlier. Reactions between bound acids and soluble species of similar pK_a were monitored in the same manner (by IR) as reactions between bound acids and substrates of greatly differing acidity (e.g., the reactions between $\text{P-CpMo}(\text{CO})_3\text{H}$ (P-6) and the β -dicarbonyl sodium salts). The former followed weak acid-weak base behavior and the latter behaved essentially as an acid exchange resin.

"Effective K_{eq} " calculations

The numbers for equation (5) were supplied in the following manner. The concentrations of soluble species, $[B^-]$ and $[BH]$, were calculated directly from IR absorbances using Beer's Law and the above-determined extinction coefficients. The effective concentration of $\textcircled{P}-A^-$, $\{\textcircled{P}-A^-\}$, was assumed to be equal to that of BH , in accordance with equation (4). $\{\textcircled{P}-AH\}$ was then determined from the difference between $\{\textcircled{P}-AH\}_{initial}$ and $\{\textcircled{P}-A^-\}$. For example, K_{eq} for experiment 1 of Table 3 would be calculated as follows:

$$K_{eq} = \frac{[BH] \{\textcircled{D}-A^-\}}{[B^-] \{\textcircled{P}-AH\}} = \frac{(.011) (.011)}{(.008) (.058-.011)} = 0.32$$

References and Notes

1. Recent reviews of functionalized polymers:
 - a. G. Manecke and P. Reuter, J. Polymer Sci., Polymer Symposium 62, 227 (1978).
 - b. Israeli J. Chem. 17, #4 (1978). An issue devoted to polymeric reagents.
 - c. J. Molec. Catal. 3, numbers 1-3 (1977). A compilation of articles in the field of functionalized solid supports.
 - d. W. Heitz, "Polymeric Reagents, Polymer Design, Scope, and Limitations," Adv. in Polymer Science 23, 1, (1977).
 - e. Y. Chauvin, D. Commereuc and F. Dawans, "Polymer-Supported Catalysts," Progress in Polymer Science, Vol. V, 95 (1977).
 - f. F.R. Hartley and P.N. Vezey, "Supported Transition Metal Complexes as Catalysts," Adv. in Organometallic Chemistry, 15, 189 (1977).
 - g. C.C. Leznoff, Acc. Chem. Res., 11, 327 (1978).
 - h. D.C. Neckers, Chemtech 8, 108 (1978).
 - i. R.H. Grubbs, Chemtech 7, 512 (1977).
2.
 - a. J.M.J. Frechet, L.J. Nuyens and E. Seymour, J. Am. Chem. Soc. 101, 432 (1979).
 - b. R.H. Schwartz and J. San Filippo, J. Org. Chem. 44, 2705 (1979).
 - c. C.R. Harrison and P. Hodge, J. Chem. Soc. Perkin I 1976, 2252, 605.
 - d. N.M. Weinshenker and C.M. Shen, Tetrahedron Lett. 1972, 3281, 3285.
3.
 - a. F. Dawans and D. Morel, J. Molec. Catal., 3, 403 (1978).
 - b. G. Wulff, W. Vesper, R. Grobe-Einsler and A. Sarhan, Makromolec. Chem. 178, 2799 (1977).
 - c. S.J. Fritschel, J.J. Ackerman, T. Keyser and J.K. Stille, J. Org. Chem. 44, 3152 (1979).

4.
 - a. G.A. Olah, R. Malhotra and S.C. Narang, J. Org. Chem. 43, 4628 (1978).
 - b. M. Terasawa, K. Kaneda, T. Imanaka and S. Teranishi, J. Catal. 51, 406 (1978).
 - c. C.U. Pittman and Q. Ng, J. Organomet. Chem. 153, 85 (1978).
 - d. M.S. Jarrall, B.C. Gates and E.D. Nicholson, J. Amer. Chem. Soc. 100 5727 (1978).
 - e. P. Buschmeyer and S. Warwel, Angewandte Chem. Int'l. Ed. 17, 131 (1978).

5.
 - a. H.W. Gibson and F.C. Bailey, J.C.S. Chem. Comm., 1977, 815.
 - b. G. Cainelli, G. Cardillo, M. Orena and S. Sandri, J. Amer. Chem. Soc. 98, 6737 (1976).
 - c. H.M. Relles and R.W. Schluez, J. Am. Chem. Soc. 96, 6469 (1974).
 - d. R. Michels, M. Kato and W. Heitz, Makromolec. Chem. 177, 2311 (1976).
 - e. G.A. Crosby, N.M. Weinschenker and H-S. Uh, J. Am. Chem. Soc. 97, 2232 (1975).

6.
 - a. S. Mazur and P. Jayalekshmy, J. Amer. Chem. Soc. 101, 677 (1979).
 - b. W.D. Bonds et al, J. Am. Chem. Soc. 97, 2128 (1975).
 - c. C.U. Pittman, S.E. Jacobson and H. Hiramoto, J. Am. Chem. Soc. 97, 4774 (1975).
 - d. P. Perkins and K.P.C. Vollhardt, J. Am. Chem. Soc. 101, 3985 (1979).

7.
 - a. G. Wulff and I. Schulze, Israel J. Chem., 17, 291 (1978).
 - b. T. Shimidzu, "Cooperative Actions in the Nucleophile-Containing Polymers," Adv. Polymer Science 23, 56 (1977).
 - c. A. Pollack, R.L. Baughn, O. Adalsteinsson and G.M. Whitesides, J. Am. Chem. Soc. 100, 302 (1978).
 - d. K. Mosbach, Sci. Am. 26, 225 (1971).

8. a. R. Grubbs, C.P. Lau, R. Cukier and C. Brubaker, Jr., J. Am. Chem. Soc. 99, 4518 (1977).
b. J. Rebek and J. Trend, J. Am. Chem. Soc. 101, 737 (1979).
9. a. J.P. Collman, L.S. Hegedus, M.P. Cooke, J.R. Norton, G. Dolcetti and D.N. Marquardt, J. Am. Chem. Soc. 94, 1790 (1972).
b. J.D. Aplin and L.D. Hall, J. Am. Chem. Soc. 99, 4162 (1977).
c. S.L. Regen and D.P. Lee, J. Am. Chem. Soc. 96, 295 (1974).
d. S.L. Regen, J. Am. Chem. Soc. 99, 3838 (1977).
e. H. Molinari and F. Montanari, J.C.S. Chem. Comm., 639 (1977).
10. a. R.H. Grubbs and L.C. Kroll, J. Am. Chem. Soc. 93, 3062 (1971).
b. G.O. Evans, C.U. Pittman, R. McMillan, R.T. Beach and R. Jones, J. Organomet. Chem. 67, 295 (1974).
c. C.U. Pittman and R. Hanes, "Frontiers in Organometallic Chemistry," Ann. N.Y. Acad. Sci. 239, 76 (1974).
d. J.A. Greig and D.C. Sherrington, Polymer 19, 163 (1978).
11. C. Tanford and J.D. Hauenstein, J. Am. Chem. Soc. 78, 5278 (1956).
12. E. Katchalski and M. Sela, J. Am. Chem. Soc. 75, 5278 (1956).
13. W.W. Bachovchin and J.D. Roberts, J. Am. Chem. Soc. 100, 8041 (1978).
14. a. M.J. Farrall and J.M.J. Frechet, J. Org. Chem. 41, 3877 (1976).
b. T.M. Fyles and C.C. Leznoff, Can. J. Chem. 54, 935 (1976).

15. The figures are drawn with para-substitution for clarity only. Previous investigations have indicated that lithium substitution in resinophenyl-lithium is meta and para. C.D. Broaddus, J. Org. Chem. 35, 10 (1970); D.C. Evans, L. Phillips, J.A. Barrie and M.H. George, Polymer Letters Ed. 12, 199 (1974).
16. For other examples of the effects of incomplete polymer swelling see, for example, D.C. Neckers, D.A. Kooistra and G.W. Green, J. Amer. Chem. Soc. 94, 3984 (1972); R.H. Grubbs, L.C. Kroll and E.M. Sweet, J. Macromolec. Sci., Chem. 7, 1047 (1973); J.M.J. Frechet and K.E. Hague, Macromolecules 8, 130 (1975); M.D. Sanner, R.G. Austin, M.S. Wrighton, W.D. Honnick, C.U. Pittman, Jr., Inorg. Chem. 18, 928 (1979).
17. In our hands, resinocyclopentadiene made via the bromination-lithiation route yielded a resin of which ~55% of the styrene monomers were substituted with cyclopentadiene, whereas the direct lithiation route (Scheme 2) resulted in ~38% substitution of styrene monomers with cyclopentadiene.
18. G. Gubitosa and H. Brintzinger, J. Organomet. Chem. 140, 187 (1977).
19. For homogeneous precedent to this reaction, see J.A. Gladysz, G.M. Williams, W. Tam and D.L. Johnson, J. Organomet. Chem. 140, C1 (1977).
20. This was established by treating resinocyclopentadiene P-3 with HBET_3Li . After extensive rinses with clean solvent to insure complete removal of the borohydride, the resulting resin was exposed to a THF solution of diethylmalonate. Appearance of lithium diethylmalonate carbonyl absorbances in the ir spectrum of the solution above the polymer indicated to us that lithium cyclopentadienide had been formed on the polymer by

reaction of HBEt_3Li with resinocyclopentadienide. As a standard, the above procedure was repeated on unfunctionalized polystyrene. Those results indicated that no deprotonation of the polymer backbone was occurring.

21. No carbonyl absorbances for diethylmalonate were observed in the ir spectrum of a THF solution of sodium diethylmalonate which had been in contact with resinocyclopentadiene P-3.
22. This method posed some difficulties in that commercial IR cells had to be specially adapted to handle the slurried samples, and subtraction of solvent absorptions required a variable pathlength reference cell.
23. R.J. Card and D.C. Neckers, J. Am. Chem. Soc. 99, 7734 (1977).
24. a. A referee has indicated some concern about the fact that no direct information is available about the distribution of functionalities on the polymers discussed here. If we had observed that polymer-attachment caused a dramatic change in the pK_a of the molybdenum hydride, site-aggregation effects would have to be considered as a possible explanation. However, the fact that little change in pK_a is produced upon polymer attachment makes it seem quite unlikely that site-site interaction, if it occurs, has a detectable effect on the acidity of the attached functional groups. Additional support for this point of view is provided by earlier work from Collman's group demonstrating that materials prepared by functionalization of preformed polymers are chemically very similar to those formed by polymerization of analogously functionalized monomers. Cf. (b) J.P. Collman, L.S. Hegedus, M.P. Cooke, J.R. Norton, G. Dolcetti and D.N. Marquardt, J. Am. Chem. Soc. 94, 1789 (1972).

25. a. F.G. Bordwell et al, J. Am. Chem. Soc. 97, 7006 (1975); b. H.W. Walker, C.T. Kresge, P.C. Ford, R.G. Pearson, J. Am. Chem. Soc. 101, 7428 (1979); c. R.P. Bell, "The Proton in Chemistry," Cornell University Press, Ithaca, N.Y., 1959; d. H.C. Brown, D.H. McDaniel, O. Hafliger in "Determination of Organic Structures by Physical Methods," Vol. 1, E.A Braude and F.C. Nachod, Eds., Academic Press, N.Y., 1955, p. 588.
26. We agree wholeheartedly with a referee's suggestion that an absolute value of the pK_a of $CpMo(CO)_3H$ in a solvent such as methanol (in which other hydride pK_a 's have recently been measured, cf. ref. 25b above) would be very useful in general. However, it would be somewhat risky to extrapolate such a value to THF, an aprotic solvent of substantially lower dielectric constant than methanol.
27. Rys and Steinegger, drawing on an analogy between the insoluble polymeric matrix and a solid surface, have applied Langmuir Isotherm theory to an analysis of the acidic activity of a polysulfonated resin. P. Rys and W.J. Steinegger, J. Am. Chem. Soc. 101, 4801 (1979).
28. S.A. Keppie and M.F. Lappert, J. Organomet. Chem. 19, P5 (1969).
29. P.L. Watson and R.G. Bergman, J. Am. Chem. Soc. 101, 2055 (1979) and ref. 4 therein.

Chapter 2

Hydrogenolyses of an Alkynyl
Cobalt Carbonyl Cluster

INTRODUCTION

Interest in Fischer-Tropsch hydrocarbon synthesis is manifested in a wide range of research interests, from studies on single crystal metal surfaces to gasoline production from coal^{1,2}. Our entry into the field of metal cluster chemistry was impelled by an interest in a particular proposed stage of Fischer-Tropsch catalysis: the mode by which alkyl products leave the metal surface. Proposing a cobalt trimer as a metal 'surface' model, $\text{Co}_3(\text{CO})_9\text{CCH}_2\text{C}(\text{CH}_3)_3$ was synthesized to represent the penultimate site of the alkyl product in the homologation process.

Molecules of the form $\text{Co}_3(\text{CO})_9\text{CR}$ have been covered in numerous literature reports³ to which the reader is referred for background information. Briefly, Seyferth and coworkers⁴ have studied the thermolyses and other reactions of $\text{Co}_3(\text{CO})_9\text{CX}$, $\text{X} = \text{H}$, R , SiR_3 , COR , CHOHR , halides, etc. The photochemically-induced decompositions of $\text{Co}_3(\text{CO})_9\text{CH}$ and $\text{Co}_3(\text{CO})_9\text{CH}_3$ under hydrogen to yield CH_4 and $\text{C}_2\text{H}_6/\text{C}_2\text{H}_4$, respectively, have been investigated by Geoffroy and Epstein⁵. That $\text{Co}_3(\text{CO})_9\text{CPh}$ can serve as a hydroformylation catalyst is the subject of an article by Ryan, Pittman and O'Connor⁶. Despite all that has been done with the tricobalt cluster, still little is known about the actual machinery of its reactions.

We chose this particular alkyl derivative of the $\text{Co}_3(\text{CO})_9$ cluster, $\text{Co}_3(\text{CO})_9\text{CCH}_2\text{C}(\text{CH}_3)_3$ (1), with the hope that reactions

of its carbynyl carbon with the accessible terminal methyl sites of the tert-butyl group under thermal hydrogenation conditions would model a carbyne's reactivity patterns in Fischer-Tropsch catalysis. Hydrogenations of cobalt alkyl 1 under carefully controlled conditions have provided information on: 1) product distribution; 2) kinetics of cluster decomposition; 3) inhibiting factors; and 4) possible reaction pathways.

RESULTS

A. Preparation of Materials

In the synthesis of $\text{Co}_3(\text{CO})_9\text{CCH}_2\text{C}(\text{CH}_3)_3$ (1), the following modifications were made on the literature procedure^{7,8} for the preparation of compounds of the form $\text{Co}_3(\text{CO})_9\text{CR}$ (Scheme 1). Reaction of $\text{Co}_2(\text{CO})_8$ with tert-butylacetylene to form $\text{Co}_2(\text{CO})_6(\text{HCCC}(\text{CH}_3)_3)$ was complete immediately on dissolution of the cobalt carbonyl in the acetylene (reaction solvent), as opposed to the reported⁷ 'overnight' reaction time. Subsequent conversion of the cobalt dimer to trimer 1 did require the strong acid (H_2SO_4) and refluxing methanol temperature⁹ (see Table 1 for IR absorbances of metal carbonyl species). Crucial for total reaction of starting material was dilution with a sufficient amount of methanol to avoid the formation of a lower oily layer (mostly product) which seemed to trap unreacted cobalt hexacarbonyl, thereby removing it from the acidic reagent in the alcohol layer. The most abundant crystal crops of product 1 were obtained by simply refrigerating the final acidic methanol solution overnight (as opposed to a lengthy literature work-up). Syntheses of compounds of the form $\text{Co}_3(\text{CO})_9\text{CR}$ have been reported with fairly low yields - typically 29 to 49%^{7,10}. In our hands, yields of ~40% of 1 were realized. The liquors remaining from crystallizations of 1, when concentrated, did not appear to contain the majority (~60%) of the cobalt introduced to the reaction. It is the author's belief that the low product yields

Scheme I

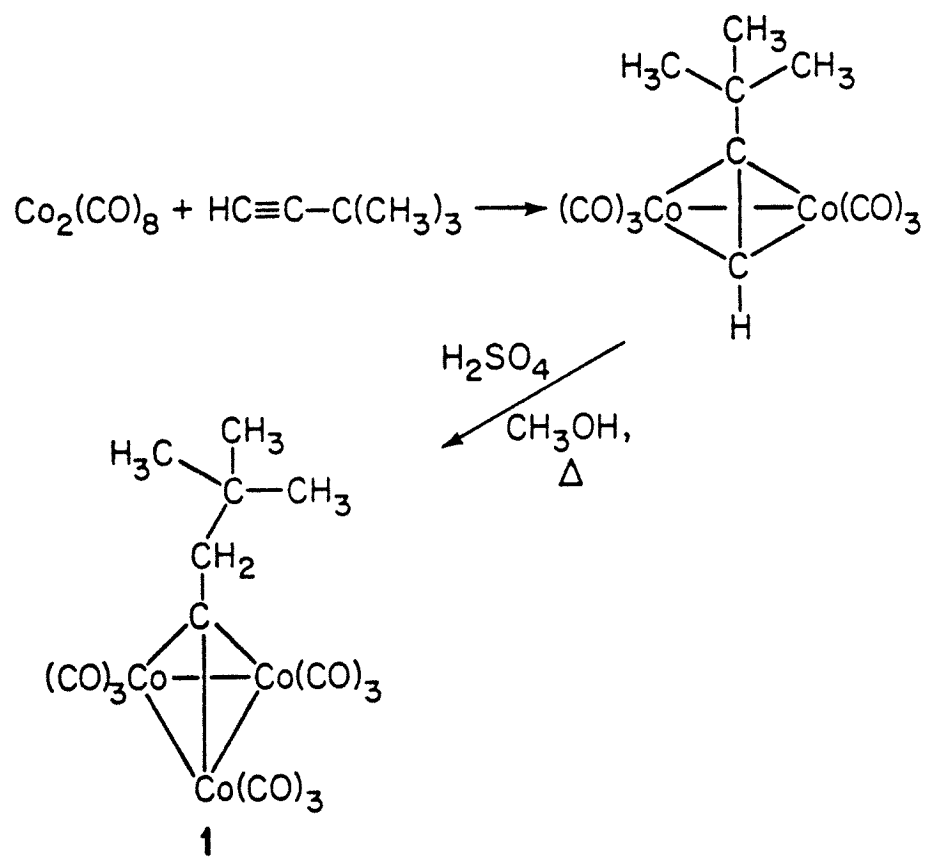


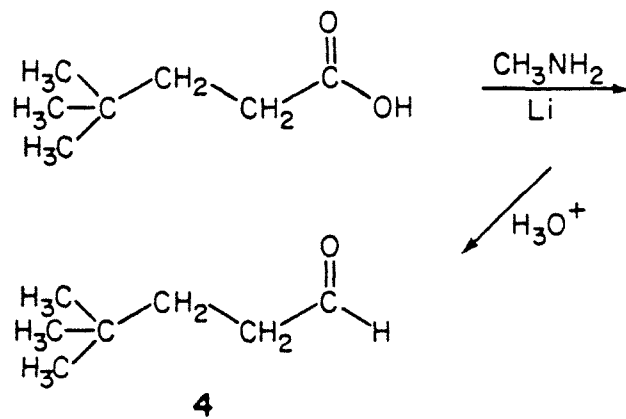
Table 1. Metal Carbonyl Infrared Absorbances

<u>Compound</u>	<u>ν_{CO} (cm⁻¹)</u>
Co ₂ (CO) ₈ (mesitylene)	2006 (s), 2038 (s), 2016 (s), 1853 (m)
Co ₂ (CO) ₆ (HC≡CCMe ₃) (hexane)	2089 (m), 2060 (w), 2049 (vs), 2026 (vs), 2016 (2), 2006 (mw)
Co ₃ (CO) ₉ CCH ₂ CMe ₃ (mesitylene)	2098 (w), 2048 (vs), 2032 (s), 2012 (w)
Co ₄ (CO) ₁₂ (mesitylene)	2062 (s), 2050 (s), 2863 (m)
Co(CO) ₄ ⁻ Na ⁺ (THF)	1890 (s), 1856 (m)
Co(CO) ₄ ⁻ Li ⁺ (THF)	1889 (s)
Co(CO) ₄ ⁻ PPN ⁺ (THF)	1890 (s), 2855 (sh)

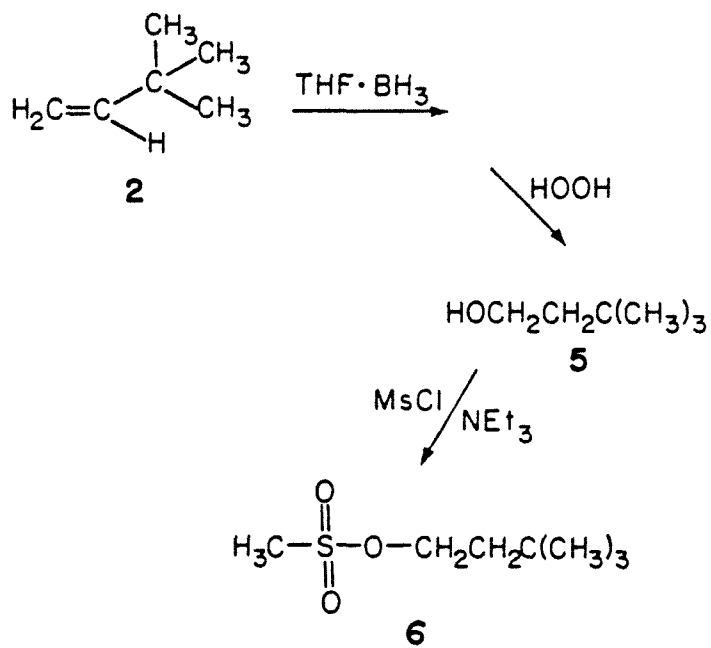
and the overall 'disappearance' of metal in this reaction sequence are due to the generation of a volatile cobalt carbonyl component during trimer formation. Further discussion of this hypothesis is the subject of a thesis proposal.

An authentic sample of the experimentally derived aldehyde, $\text{CHO}(\text{CH}_2)_2\text{C}(\text{CH}_3)_3$ (**4**), was synthesized by reduction of the corresponding acid, $\text{COOH}(\text{CH}_2)_2\text{C}(\text{CH}_3)_3$, with lithium in neat methylamine (Scheme 2). An elaboration on the parsimonious literature procedure for this reduction is included in the Experimental Section. Aldehyde **4** (not listed in Beilstein) was characterized by IR, NMR, MS, and GC. Its NMR spectrum displays the expected downfield triplet of the aldehyde hydrogen at 9.35 ppm, a strong singlet at 0.67 ppm for the *tert*-butyl group, and two *aa'**bb'* multiplets at 1.21 and 1.83 ppm for the two methylene groups. Its solution IR spectrum contains the two traits most characteristic of aldehydes¹¹: a C-H stretch of the CHO group at 2715 cm^{-1} (weak) and a C=O band at 1728 cm^{-1} (strong). Broadening and shifting of the IR bands occurred with thin-film samples, presumably owing to the hygroscopicity (and therefore hydrogen bonding) of the viscous, neat sample¹¹. The mass spectrum of aldehyde **4** (at 10, 15, 20, 30, or 70 eV) displayed typical aldehyde behavior under the ionizing conditions: lack of a parent ion and strong ion intensities attributable to fragmentation of alkyl groups and elimination of water. (It is of interest to note that aldehyde **4** does not contain the gamma-

Scheme 2



Scheme 3



hydrogens necessary to perform the McLafferty rearrangement often observed in the mass spectra of organic carbonyl compounds, i.e., a six-membered transition state in which a gamma-hydrogen is bonded to the carbonyl oxygen and which breaks down to acetaldehyde and olefin¹².)

Attempts to synthesize $\text{Co}(\text{CO})_4(\text{CH}_2)_2\text{C}(\text{CH}_3)_3$ independently (as a model compound for a proposed hydrogenation intermediate, *vide infra*) led to the synthesis¹³ of several candidates for agents to alkylate $\text{Co}(\text{CO})_4^-$. Hydroboration of 3,3-dimethylbutene (2) generated alcohol 5 which on treatment with methanesulfonyl chloride yielded mesylate 6 (Scheme 3). No reaction was observed on treatment of sodium tetracarbonyl cobaltate in THF with mesylate 6 (as monitored by IR for disappearance of the $\text{Co}(\text{CO})_4^-$ carbonyl bands). Changing the counterion from sodium to lithium or $(\text{Ph}_3\text{P})\text{N}^+$ (PPN) did not increase the cobalt anion's reactivity toward the mesylate. Attempts to alkylate the above three salts of $\text{Co}(\text{CO})_4^-$ with the alkyl chloride, $(\text{CH}_3)_3\text{C}(\text{CH}_2)_2\text{Cl}$, were also unsuccessful. A third candidate, $(\text{CH}_3)_3\text{C}(\text{CH}_2)_2\text{I}$, was synthesized by treating mesylate 6 with sodium iodide in refluxing 2-butanone. This alkyl iodide was also an ineffective alkylating agent under the previous reaction conditions (room temperature, THF, anaerobic atmosphere) or at 70° in benzene. If time permits, two more attempts will be made to generate $\text{Co}(\text{CO})_4(\text{CH}_2)_2\text{C}(\text{CH}_3)_3$. The first will involve synthesis of and attempted alkylation with the trifluoromethanesulfonyl alkyl. The second employs a crown ether to 'activate' the cobalt anion

for nucleophilic displacement on the alkylating agent. The resulting tetracarbonyl cobalt alkyl is not expected to be stable ¹⁴ and therefore might have to be generated *in situ* under hydrogenation conditions. Monitoring the reaction of $\text{Co}(\text{CO})_4(\text{CH}_2)_2\text{C}(\text{CH}_3)_3$ with hydrogen for appearance of products 2 (*tert*-butylethylene), 3 (neohexane), and 4 (4,4-dimethylpentanal) might provide information on the mechanism of hydrogenation of 1.

B. Hydrogenation Reaction Conditions

Hydrogenations were carried out either in sealed NMR tubes or in a high-pressure gas manifold (*vide infra* and Figure 1). In the former case, the sample was prepared by placing a solution of cobalt complex 1 (0.023-0.069 M) in an NMR tube on a vacuum line ($<10^{-4}$ mm) which was equipped with a mercury manometer for measuring gas pressure (up to 1 atm). After transferring in an internal standard (tetramethylsilane) under vacuum, a metered pressure of hydrogen was exposed to the cooled (-196°C), evacuated tube and the tube was sealed off (with a torch). This method for introducing hydrogen to the NMR solution allowed for incorporation of up to ~ 2.3 atm H_2 in the NMR tube (at room temperature, or 2.55 atm H_2 at the reaction temperature, 56°C). Experiments were monitored either by removing the tube periodically from a heated constant-temperature bath (56°C) and recording the NMR spectrum (90 MHz instrument) or by leaving the tube in a 56°C NMR probe and recording its spectrum at regular

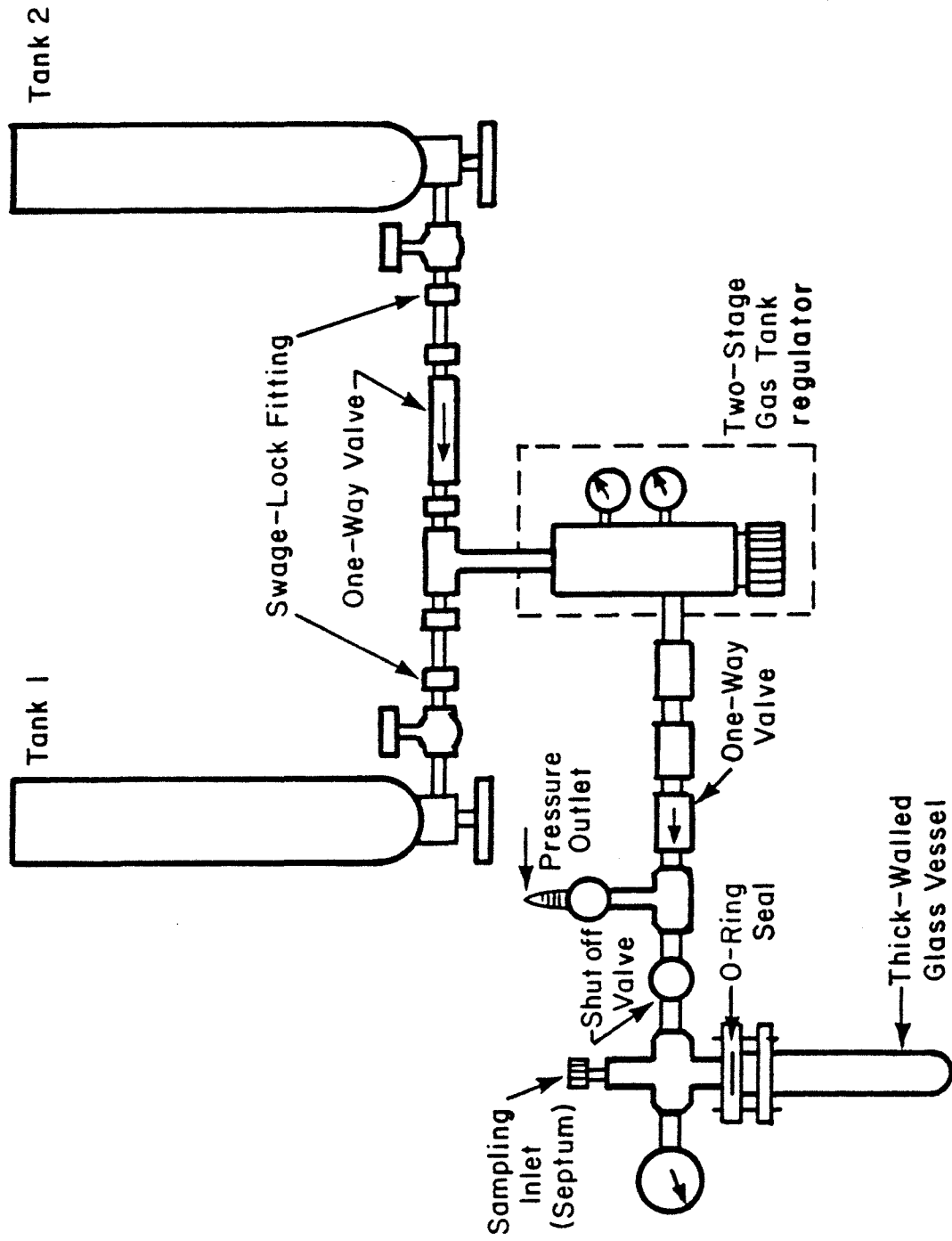


Figure 1. Stainless steel manifold for high pressure hydrogenations (gas tanks lie perpendicular to the plane of the page).

intervals (180 MHz Fourier Transform instrument). NMR data provided information on disappearance of the starting material cobalt complex 1 and appearance of the three organic products, best monitored in the tert-butyl region (the four species have distinctly different chemical shifts for their tert-butyl groups).

Alternatively, hydrogenation reactions were monitored by gas chromatography for appearance of organic products. In these experiments, a high-pressure manifold (stainless steel) with the following capacities was employed (Figure 1): 1) a septum inlet for direct sampling of the reaction mixture (while still under pressure); 2) a gauge to monitor gas pressure during the reaction; 3) access to the gas source (lecture bottle) and a bleeder valve to maintain constant gas pressure throughout the reaction (some loss of pressure was observed on sampling through the septum via syringe); and 4) access to a second tank of gas (for reactions carried out under CO and H₂).

For reactions carried out on the high-pressure manifold, mesitylene solutions of $\text{Co}_3(\text{CO})_9\text{CCH}_2\text{C}(\text{CH}_3)_3$ (1) and an internal standard (benzene) were prepared in a glove box. They were then 'degassed' on the reaction manifold in several hydrogen pressurization cycles prior to pressurizing the reaction vessel to the given reaction pressure. The reaction mixture was heated in an oil bath and stirred with a magnetic stir bar. Samples were removed through the septum with a syringe (equipped with a long needle), transferred to a microliter syringe, and injected

into the gas chromatograph. Details of the chromatography and integration conditions are given in the Experimental Section.

The above-described high-pressure manifold was also used to monitor decomposition of 1 in a CO/H₂ atmosphere. The manifold was equipped with a T-joint (see Figure 1) to accommodate a second gas source (the T-joint was placed between the gas tanks and the two-stage regulator in order to be able to use the one regulator to allot both gasses); a one-way valve was inserted between the two tanks to prevent mixing of gasses in the tanks. The apparatus was assembled and the reaction was monitored in the same manner as for the previously described hydrogenations. The order in which the two gasses were introduced to the reaction solution (on repressurizing, if needed, after aliquoting) did not seem to influence the reaction according to the consistency in GC analyses for appearance of products.




For the hydrogenation in the presence of added olefin (2), a mesitylene solution of 1, 2, and an internal standard (benzene) was prepared and hydrogenated as described previously. Early samples collected at time intervals (@ 10 min) shorter than g.c. trace times (~40 min) were stored at -20° C in septum-capped, nitrogen-filled vials until being analyzed by g.c. Negligible increase in experimental error was observed in the analyses of these samples - a possible problem if volatile components were being lost on handling and storing (the boiling points of tert-butyl ethylene (2) neohexane (3) are 41° and 50° C, respectively).

C. Reaction Results and Discussions

Hydrogenations of **1** in hydrocarbon solvents (cyclohexane, pentane) yielded nearly quantitatively two products: tert-butylethylene (**2**) and neohexane (**3**), in a ratio of ~4.5 to 1.0 (experiments 1 and 2 of Table 2, and Scheme 4). The identities of the two organic products were established in previous studies of the hydrogenation of **1** in these laboratories¹⁵. Hydrogenations of **1** under similar conditions in aromatic solvents (benzene, toluene, mesitylene) resulted in formation of a third product in addition to the previously observed olefin and alkane (Scheme 4). This third product, 4,4-dimethylpentanal (**4**), appeared as the minor product in the final product ratio of olefin: alkane: aldehyde, ~2.5: 1.5: 1.0.

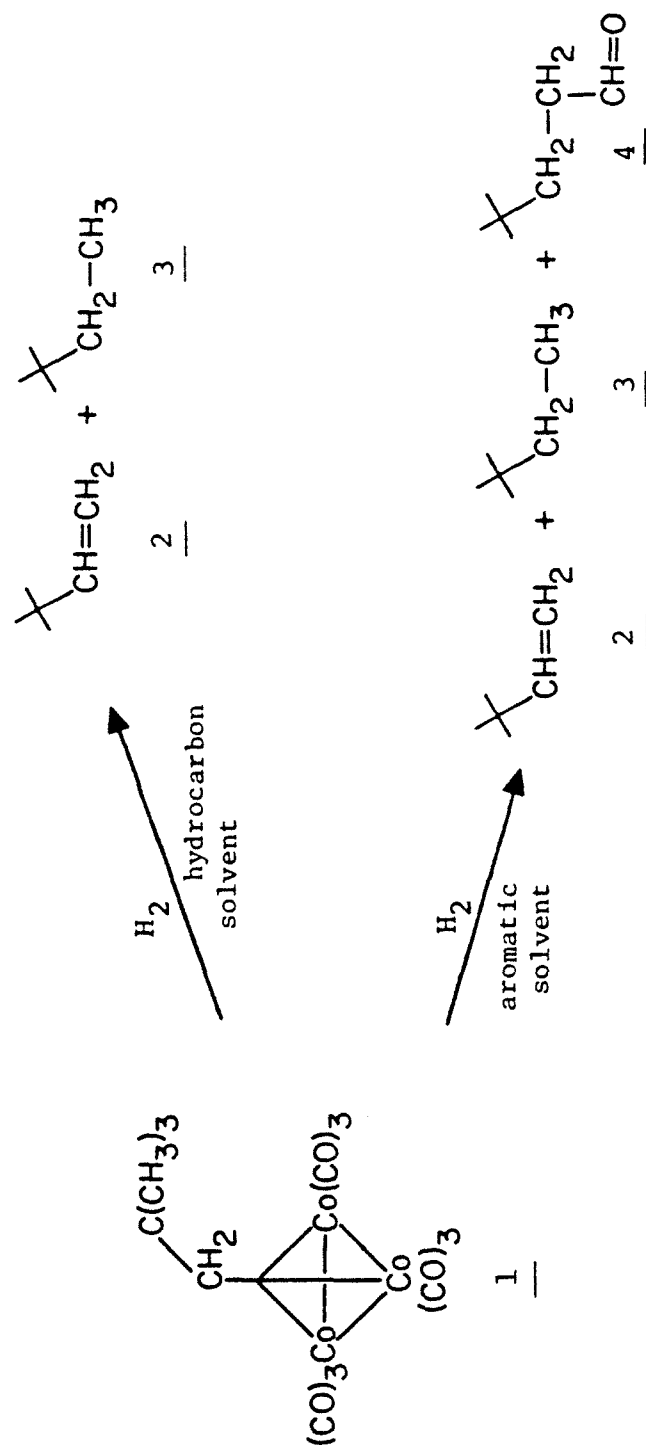
This third product was identified after isolation by preparative gas chromatography by comparison with an authentic sample. Although at first surprising, the appearance of aldehyde from hydrogenation of **1** in the absence of CO gas has related precedent in other cobalt carbonyl systems. It has been reported¹⁶ that $\text{Co}_4(\text{CO})_{12}$ (a suspected product of our hydrogenations, *vide infra*) causes stoichiometric hydroformylation of propene under hydrogen pressure, and that this hydroformylation does not proceed until less polar solvents are replaced by ethanol as the reaction solvent. Moreover, other researchers have reported enhancement in hydroformylation rates on addition of more polar solvents¹⁷. Finally, a report by Ryan, Pittman, and O'Connor⁶ that $\text{Co}_3(\text{CO})_9\text{CC}_6\text{H}_5$ catalyzes

Table 2. Hydrogenation Reactions

exp	Starting Materials	Method ^d	Solvent	[I]	pH ₂ (atm) (at rxn T)	T (°C)	Time (h)	2 (Z) ^e	3 (Z) ^e	4 (Z) ^e
1	<u>1</u> , H ₂	A	d ¹² cyclohexane	.082	1.80	56	14	.046M (74Z)	.028M (26Z)	0
2	<u>1</u> , H ₂	C	pentane	.087	1.13	65	22	b	b	0
3	<u>1</u> , H ₂	A	d ⁶ benzene	.023	2.55	56	25	.014 (70)	.004 (20)	.002 (10)
4	<u>1</u> , H ₂	B	mesitylene	.140	2.5	60	12.5	.056 (51)	.033 (30)	.021 (19)
5	<u>1</u> , H ₂	B	mesitylene	.140	5.1	60	8.5	.063 (50)	.040 (32)	.023 (18)
6	<u>1</u> , H ₂	B	mesitylene	.140	6.8	60	8.5	.060 (51)	.037 (31)	.021 (18)
7	<u>1</u> , H ₂ , CO(3.7atm)	B	mesitylene	.140	3.7	60	19.5	.003 (100)	0	0
8	exp 7's final rxn mixture (incl H ₂ +CO)	B	mesitylene	.137	3.7	85	45	.001 (1)	.010 (12)	.076 (87)
9	<u>1</u> , H ₂ , +  (.08M)	B	mesitylene	.140	6.8	60	8	c	.037 (c)	.030 (c)
10	<u>1</u> , H ₂ , +  (3.2atm)	A	d ⁶ benzene	.052	1.36	75	16.5	.037 (72) ^d	.007 (14) ^d	.007 (14) ^d
11	<u>1</u> +  (3.8atm)	A	d ⁶ benzene	.050	0	75	16.5	0	0	0
12	<u>1</u> + argon	A	d ⁶ benzene	.069	0	56	11	0	0	0

a. Methods: A = NMR-monitored, B = g.c.-monitored from high pressure manifold, C = sealed reaction flask.
 b. Quantitative data unavailable due to interference from solvent in NMR and g.c. analyses. Yields appear similar to those of exp 1 (by g.c.).
 c. Not meaningful due to initial addition of olefin 2.
 d. Percentage of sum of products 2 + 3 + 4.
 e. Percentage of sum of products.

Scheme 4



hydroformylation forewarns of the possibility of hydroformylation activity of our tricobalt nonacarbonyl complex or its derivatives. Paths by which the aldehyde might arise will be discussed later.

All of the following experiments, including the effects of H₂ pressure, CO, and added olefin, were carried out in aromatic solvents to observe the formation of all three products.

1. NMR-Monitored Hydrogenation

The disappearance of starting material (1) and the appearance of products were monitored simultaneously by NMR during the hydrogenation of 1 (exp 3 of Table 2). Figure 2 shows the time dependence of the appearance of *tert*-butylethylene (2), neohexane (3), and 4,4-dimethylpentaldehyde (4) (relative to an internal standard, TMS). The olefin is the first product to appear, followed somewhat later by the alkane and aldehyde. A plot of starting material reacted coincides quite closely to one for appearance of total products, demonstrating nearly complete mass balance (Figure 3). Applying first order kinetic analyses¹⁸ to the data of Figure 3 yields two straight lines: one for disappearance of starting material ($k = 1.45 \times 10^{-5} \text{sec}^{-1} \text{atm}^{-1}$) and one for appearance of total products ($k = 0.78 \times 10^{-5} \text{sec}^{-1} \text{atm}^{-1}$). That the rate of appearance of total products agrees fairly well with that of starting material decay confirms our observation by NMR that no appreciable build-up of intermediate is occurring. It should be kept in mind that this rate constant

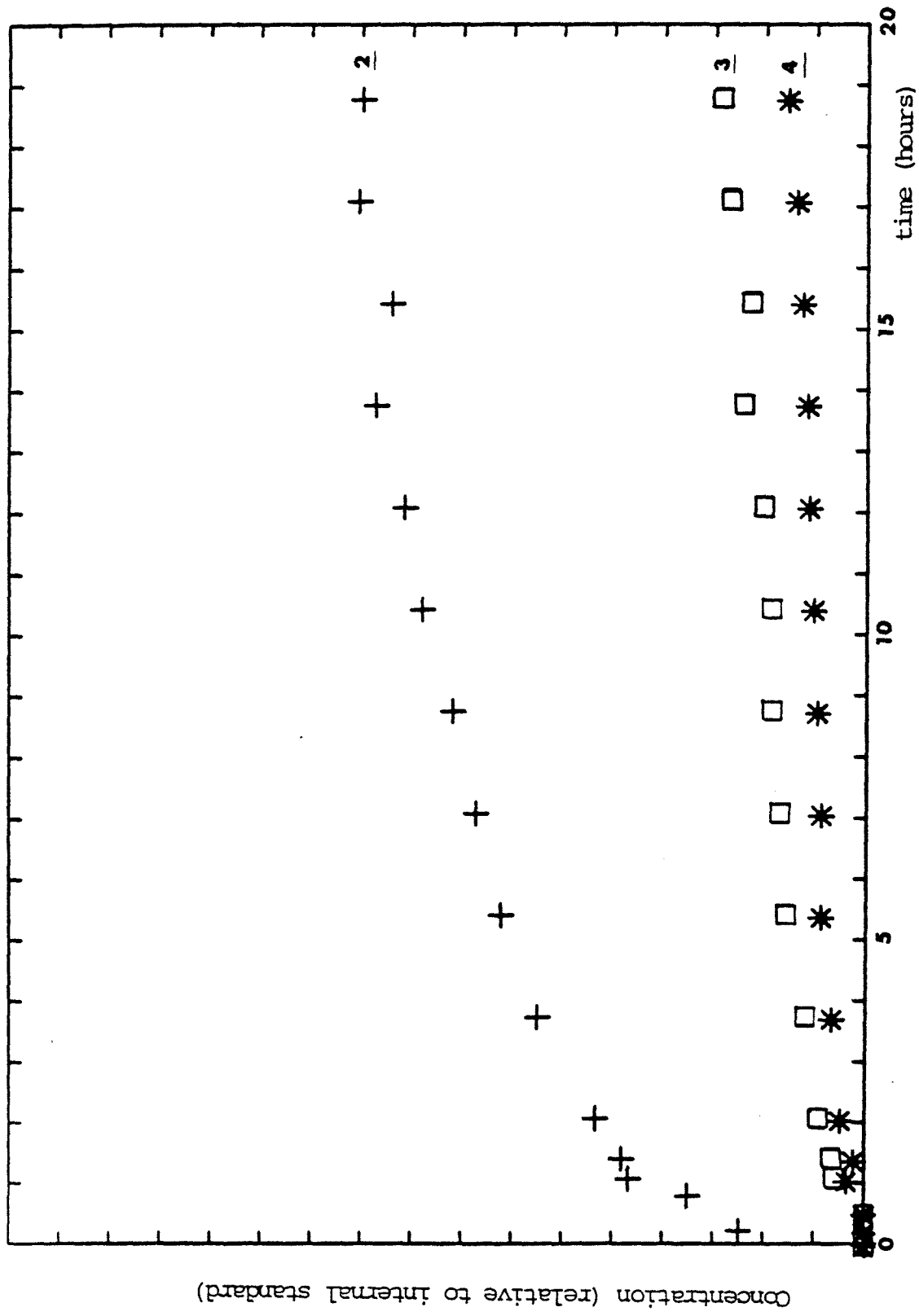


Figure 2. Appearance of products vs time, experiment 3.

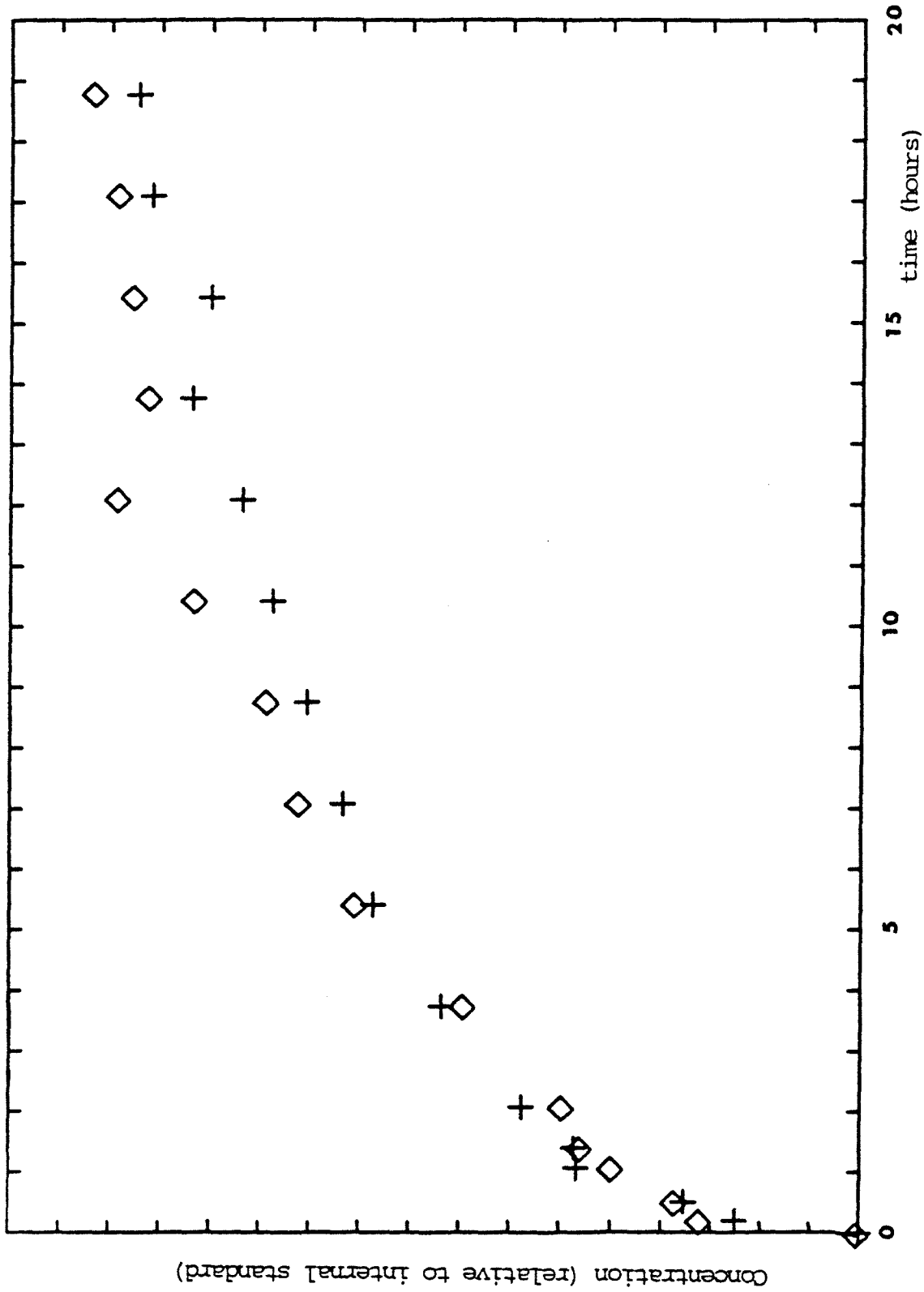


Figure 3. Disappearance of starting material (1) and appearance of total products, exp 3:
 $\diamond = [1]_0 - [1]_t$, $+$ = [total products] $_t$.

for total product appearance is descriptive rather than quantitative since it masks several individual rate constant components for the three products' formations.

Significantly, the ratio of products does not remain constant during the reaction (Figure 4). At an early time, olefin makes up the majority of the product mixture (~83%), whereas at the completion of the reaction it comprises only ~68%. Similarly, alkane and aldehyde comprise ~11 and 6% (respectively) of the total products at $t=0.5$ h, and grow to ~20 and 11%, respectively, at the reaction's end. This phenomenon will be documented again in later reactions. Since the product ratio data indicate that the three products are not formed from one common path, it is difficult to compute their rates of formation from the available data. Conclusions from the NMR-monitored experiment are therefore limited to the following observations: 1) disappearance of starting material 1 follows first order kinetics; 2) conversion of starting material to products occurs nearly quantitatively with no appreciable build-up of detectable cobalt-containing intermediates; 3) the percentage of each product in the product mixture changes over the course of the reaction, perhaps signaling an interconversion between products.

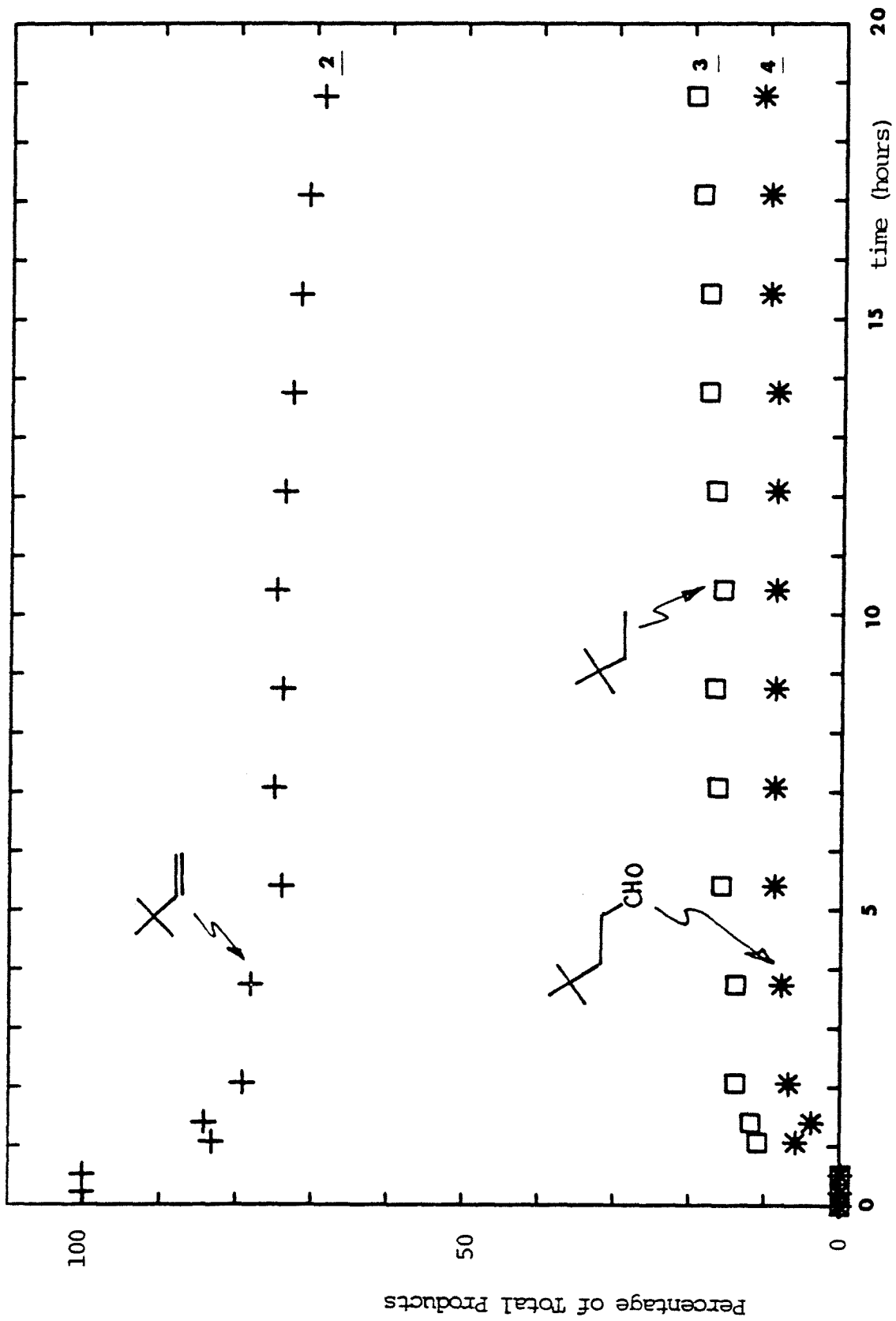


Figure 4. Appearance of products, plotted as a percentage of total products, exp. 3.

2. Hydrogen Pressure Dependence

In order to determine the order that hydrogen assumes in the hydrogenation of 1, the reaction was carried out under three different hydrogen pressures: 2.5, 5.1, and 6.8 atm (exps 4-6 of Table 2). Data on the disappearance of starting material 1 were not provided by the monitoring technique used (g.c.); however, disappearance of 1 and appearance of metal carbonyl products were followed qualitatively by IR.

The rate of appearance of total products¹⁹ at the three hydrogen pressures is plotted against increasing hydrogen pressure in Figure 5. The 'effective' rate constants, $6.28 \times 10^{-5} \text{sec}^{-1}$, $1.09 \times 10^{-4} \text{sec}^{-1}$, and $1.34 \times 10^{-4} \text{sec}^{-1}$ for 2.5, 5.1, and 6.8 atm (respectively), demonstrate a linear dependence on hydrogen pressure in the pressure range studied. For the hydrogenation of 1, the following rate expression can be written:

$$-d[1]/dt = k_1(pH_2)^m[1]^n$$

Under the pseudo-first order conditions of the three hydrogenations (i.e., an excess of H_2),

$$k_{\text{obs}} = k_1(pH_2)^m$$

and

$$\log k_{\text{obs}} = m \log(pH_2) + \log k_1$$

On plotting the data from the three hydrogenations in the form of this last equation, k_1 and m are obtained: $k_1 = 3.11 \times 10^{-5} \text{sec}^{-1}$ and $m = 0.77$ (k_1 is pictured in Figure 5). It can be seen from

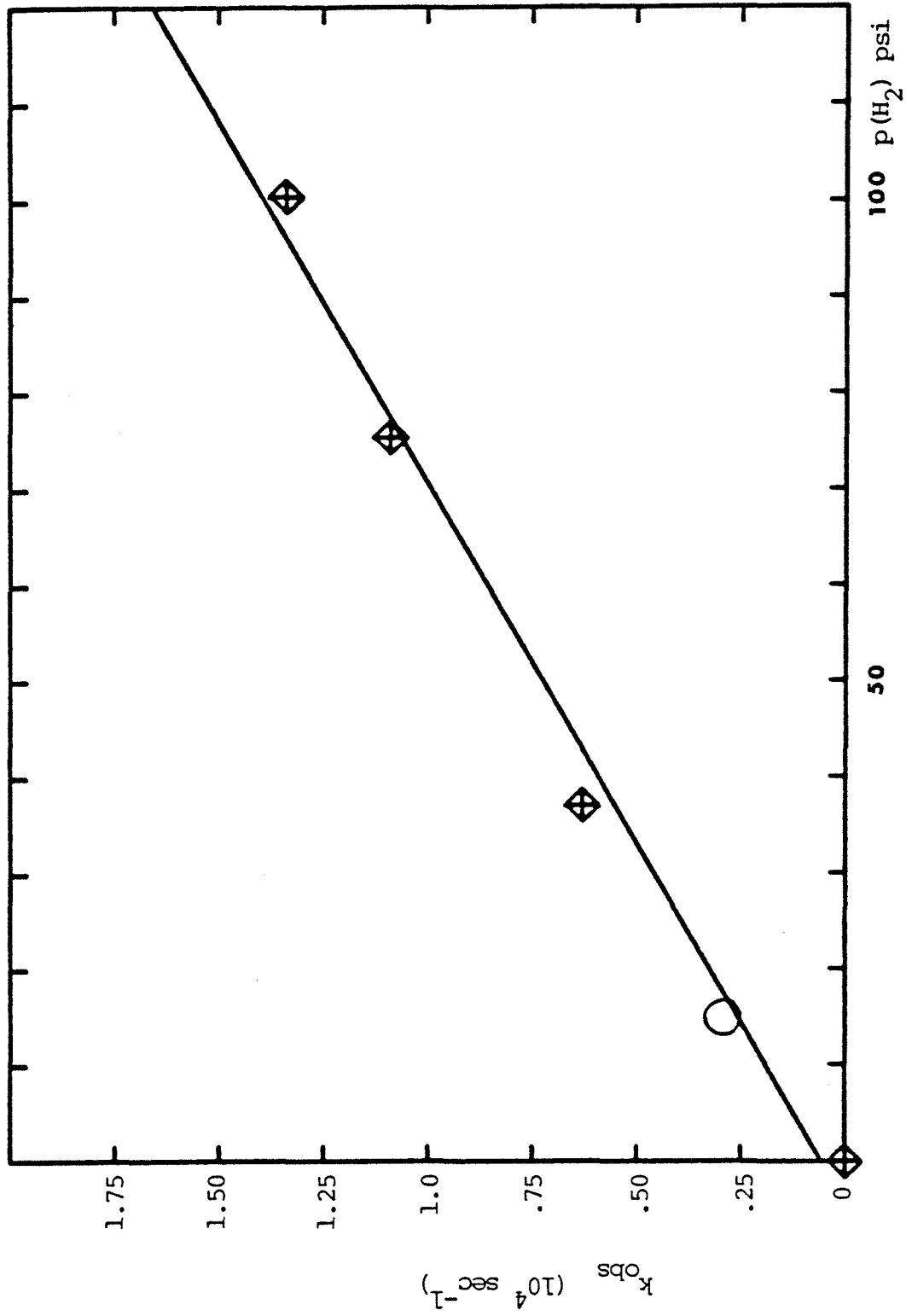


Figure 5. Rate of total product appearance vs hydrogen pressure, \diamond = exps 4-6,

\circ = calculated (see text). 1 atm = 14.7 psi.

the good agreement between the calculated k_1 and the line of Figure 5 (derived from experimental k 's) that the calculated value for k_1 is consistent with the overall kinetic trend. Given only these three hydrogenation pressures as data points, discussion on the value of m (i.e., an order of 0.77 for (p_{H_2})) is restricted. According to literature sources, the limit for hydrogen saturation in benzene lies above 250 psi (17 atm)^{21d}, thereby indicating that our three hydrogen pressures are probably not providing near-saturation levels of hydrogen in solution²⁷. The line observed in Figure 5 might indeed not be in the pseudo-first order region of excessive hydrogen concentration; instead, its slope might be reflecting a hydrogen-deficient reaction. At higher pressures one might observe an eventual leveling off in k_{obs} which could be attributed to either an arrival at the upper limit for hydrogen solubility or a departure from the limiting effect of hydrogen concentration in the rate expression.

The data derived from the hydrogenations at three different pressures have been plotted to show the effect of hydrogen pressure on the formation of each of the products, Figure 6. It can be seen that the effect of hastening product formation to completion is considerably more dramatic on increasing the hydrogen pressure from 2.5 to 5.1 atm than from 5.1 to 6.8 atm. For example, hydrogenation at 2.5 atm requires ~10h for final product concentrations to level off, whereas at 6.8 atm this stage is reached within ~6h. This effect was mirrored previously in Figure 5 which pointed out the consistent dependence of k_{obs}

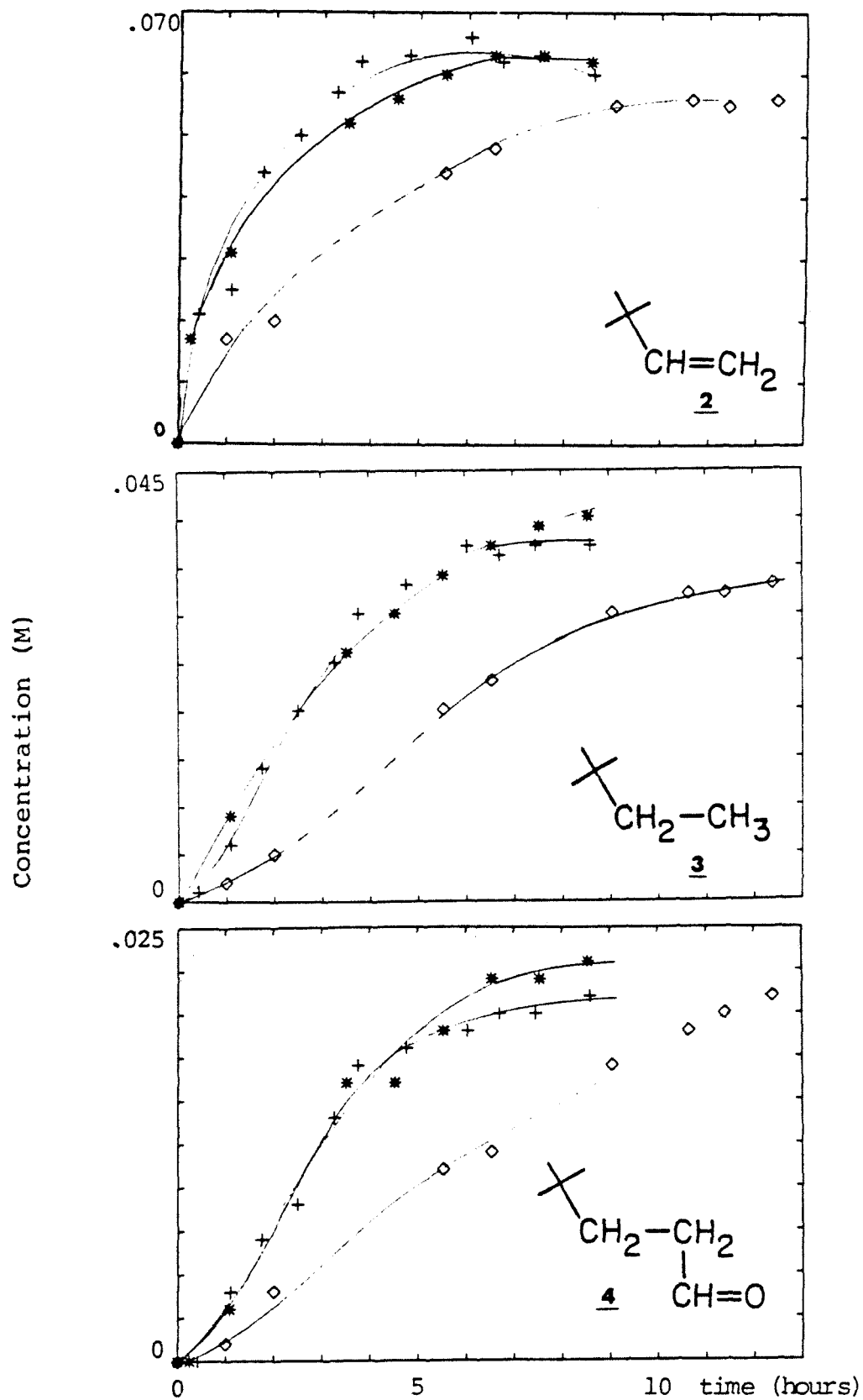


Figure 6. Appearance of each product at three hydrogen pressures, expts 4-6. $\diamond = 2.5$ atm H_2 , $*$ = 5.1 atm H_2 , $+$ = 6.8 atm H_2 .

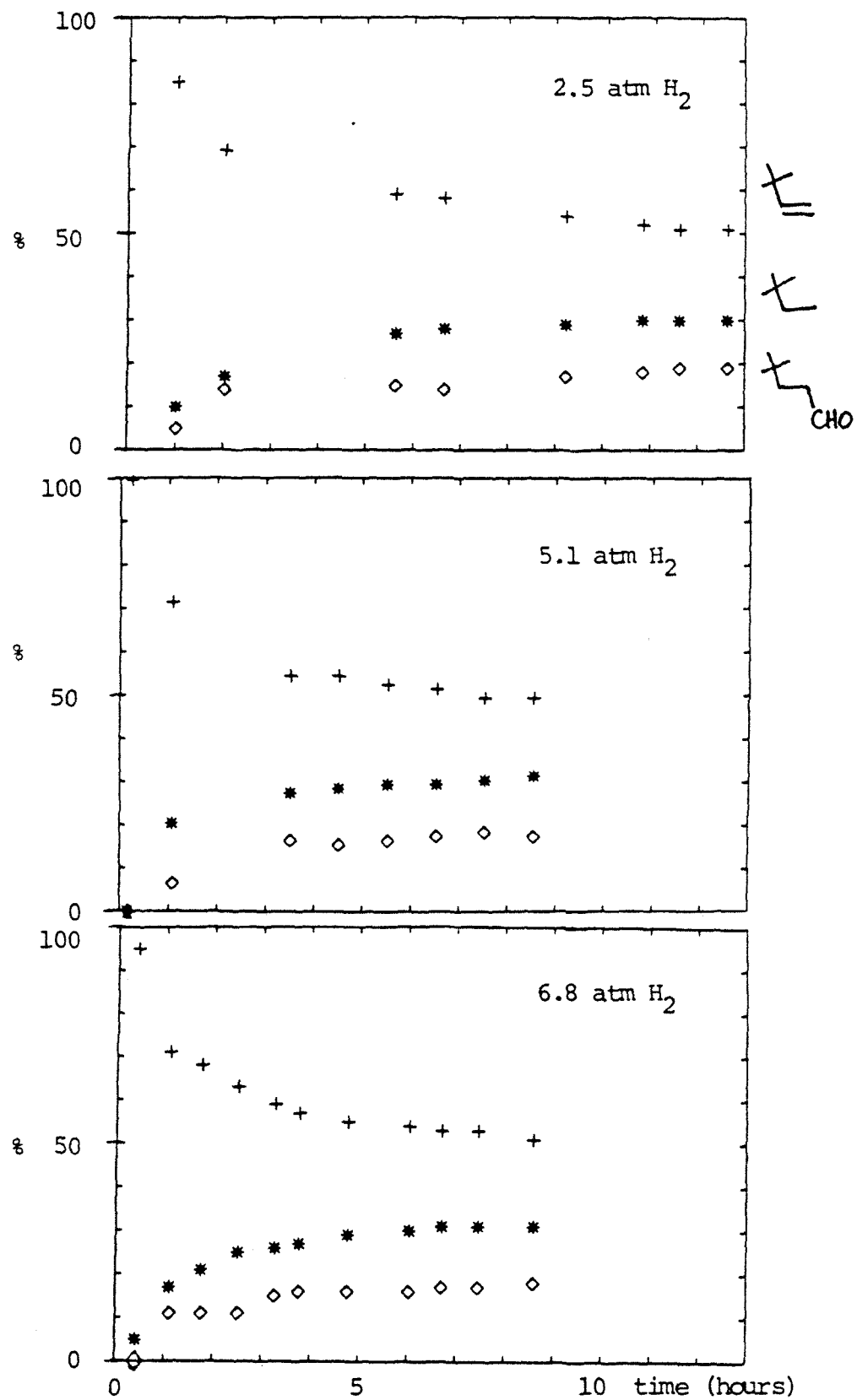


Figure 7. Percentage of each product in total product mixtures at three hydrogen pressures, exps 4-6. + = olefin 2, * = alkane 3, \diamond = aldehyde 4.

on hydrogen pressure for total product formation. Figure 7 contains plots of product ratios during the course of hydrogenation. As was seen earlier in the NMR-monitored experiment (Figure 4) the percentage of each product in the hydrogenation mixture progressively changes with time, a trend implicating formation from non-common intermediates, or even interconversion of products. The fact that *tert*-butylethylene continues to grow in throughout the reaction detracts somewhat from the theory that it is the source of aldehyde and alkane (later experiments were designed to dwell on this point). However, postulating the transitory presence of some hydrogenation/hydroformylation reagent which acts at a rate smaller than olefin formation might account for the observed simultaneous growth of the three products (*vide infra*). The nonobservance of reaction intermediates makes this a difficult proposition to verify.

Infrared spectra of metal carbonyl products (ν_{CO} (mesitylene): 2062 (s), 2049 (vs), 2032 (m), 2024 (m), 2005 (w), 1864 (m), 1825 (w) cm^{-1}) seem to contain, among the large number of CO bands, absorbances attributable to $\text{Co}_4(\text{CO})_{12}$ (ν_{CO} (mesitylene): 2062 (s), 2050 (s), 1863 (m) cm^{-1}). The remainder of the bands have not been identified.

3. The Effect of CO on Hydrogenation of 1

Photochemical studies of the hydrogenation of $\text{Co}_3(\text{CO})_9\text{CCH}_3^5$ have demonstrated inhibition of complex decomposition in the presence of carbon monoxide. The conclusion drawn was that dissociation of CO from the parent compound initiated the photochemically-induced hydrogenation (to ethane and ethylene, 2:1). The lability of carbonyl ligands of some $\text{Co}_3(\text{CO})_9\text{CR}$ complexes has been shown in reactions designed to monitor CO exchange²². It was therefore of interest to know the effect of CO on hydrogenations of 1 (exp 7, Table 2).

After 19.5h, a solution of 1 in mesitylene under H_2 (3.7 atm) and CO (3.7 atm) displayed almost no hydrogenation reactivity. IR indicated that the solution contained essentially the initial amount of 1 and by g.c. only a trace amount of tert-butylethylene (2). From these results we concluded that CO inhibits the thermal decomposition of 1 under hydrogen²³. The reversal of an initial preequilibrium involving loss of CO from 1 probably accounts for this CO inhibition, although a series of reversible equilibria prior to a CO-inhibited step cannot be ruled out.

Raising the temperature of the final solution of the previous experiment by 25° (while maintaining all other conditions the same) gave dramatic results (exp 8, Table 2). After 3.5h at 85°C , tert-butylethylene (2) had grown in (corresponding to ~5% conversion of starting material) accompanied by appearance of 4,4-dimethylpentanal (4) (~2%)

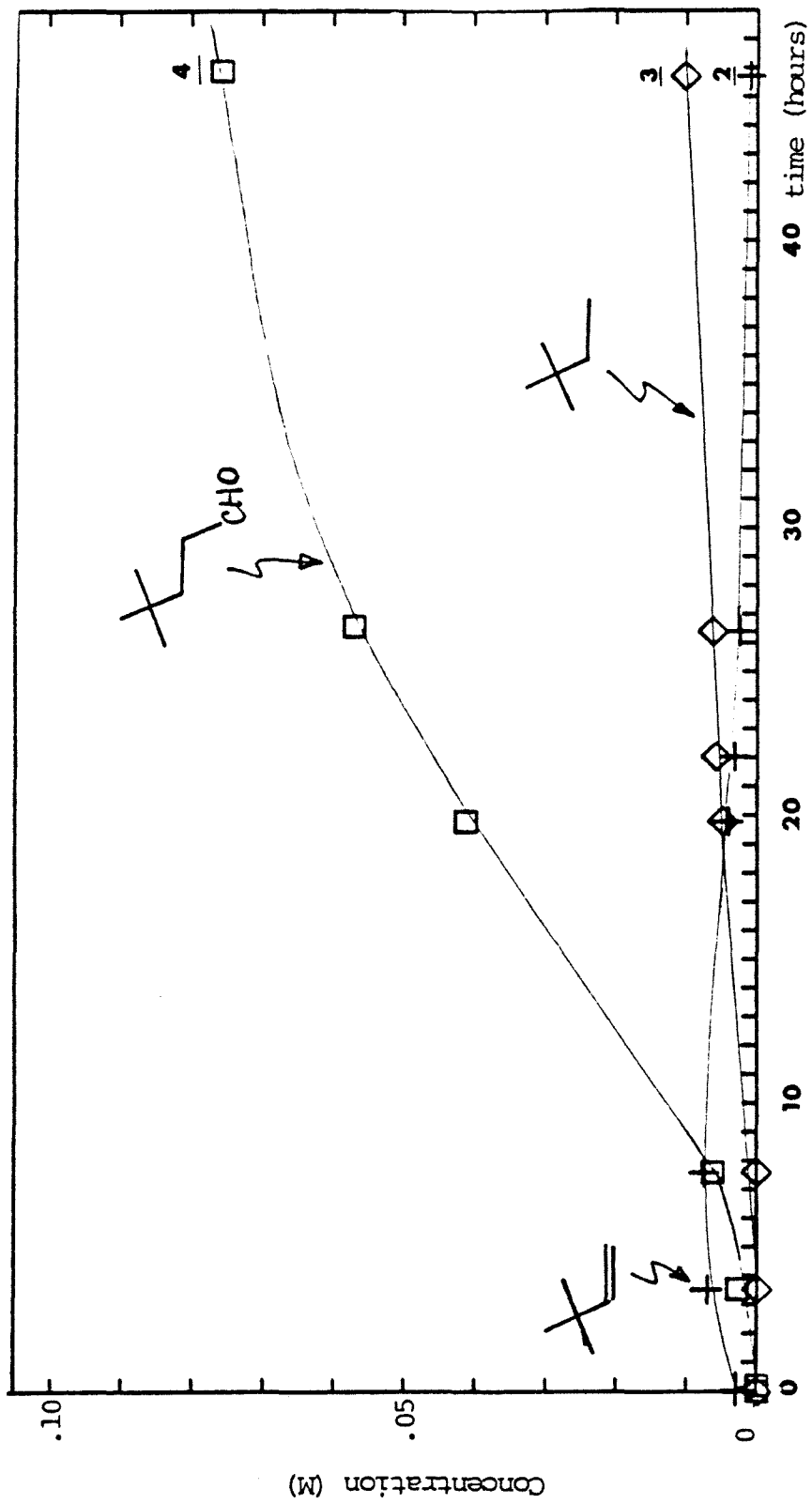
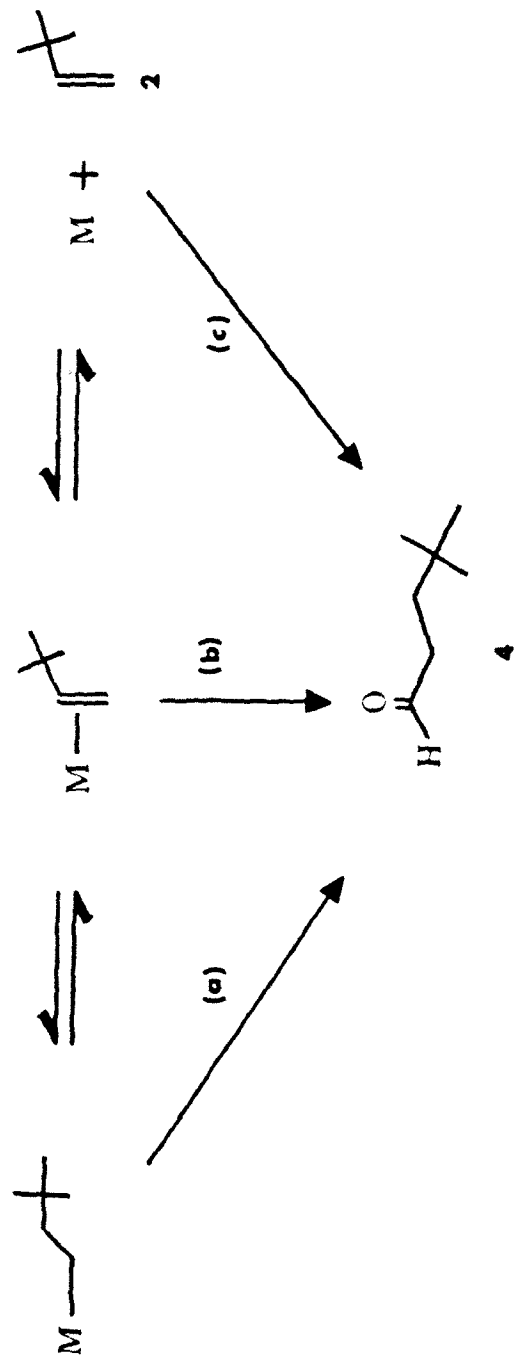


Figure 8. Appearance of products from hydrogenation in the presence of CO (85°C), exp 8.

(Figure 8). After 7.5h, aldehyde 4 concentration had doubled (over the 4.5h concentration) whereas olefin concentration showed no net change. No neo-hexane (3) was detected. At 20h a trend had begun in which olefin concentration dropped off to trace amounts over the next 26h and aldehyde grew in, accounting for ~87% of the final product mixture. Neo-hexane was finally detected at 20h and steadily grew to comprise ~12% of the final product mixture. Although the reaction was discontinued after 46h, a considerable amount of starting material 1 remained. This was evident by IR of the metal carbonyl region as well as by the fact that total product concentration comprised only ~60% of the original starting material (1) concentration. Production of aldehyde 4 would probably have progressed further (its trace in Figure 8 had not yet levelled off) had the reaction been allowed to continue. It is the author's feeling that more accurate data on aldehyde formation from 1 under H_2 and CO would be obtained by repeating the reaction at higher temperatures and gas pressures over shorter reaction times.

Examination of Figure 8 reveals that the numerical value for final aldehyde concentration is never reached by olefin. This raises the possibility that complexed olefin, once formed in the presence of the active hydroformylation reagent, does not freely dissociate into solution before (presumably) being converted into aldehyde (Scheme 5, path (b)). In fact, the final step of olefin production might be shut down entirely in favor of conversion of the olefin precursor to aldehyde (path (a) or (b)). If this is

Scheme 5

the case, the final step in releasing olefin to the solution (path (c)) would most likely have to be reversible to account for the disappearance of first-formed olefin in experiment 8.

Comparison of an IR spectrum of the resulting metal carbonyls with one for cobalt carbonyl products from normal hydrogenation conditions (i.e., no added CO) shows that in addition to containing the $\text{Co}_4(\text{CO})_{12}$ usually observed in hydrogenation product mixtures, broad bands at 2065, 2033 and 2017 cm^{-1} might correspond to $\text{Co}_2(\text{CO})_8$ (ν_{CO} (mesitylene): 2066 (s), 2038 (s), 2016 (s), 1853 (m) cm^{-1}). Starting material, $\text{Co}_3(\text{CO})_9\text{CCH}_2\text{C}(\text{CH}_3)_3$, complicates the product spectrum with CO bands at 2098 (w), 2048 (s), 2032 (s), and 2012 (w) cm^{-1} .

4. The Effect of Added Olefin 2 on the Hydrogenation of 1

An ideally designed experiment to test for the conversion of product *tert*-butylethylene (2) to products neohexane (3) and 4,4-dimethylpentanal (4) would involve addition of labelled *tert*-butylethylene to the hydrogenation of unlabelled 1. Detection of labelled products 3 and 4, either by ^{13}C , ^2H , or ^3H NMR, or by radiotracer B-scintillation detection of ^3H or ^{14}C , would surely implicate the intermediacy of first-formed product 2 in 3 and 4's geneses. Given certain time constraints, a modified version of the above-described experiment was undertaken which in its own way verified the validity of such a labelling experiment²⁴.

tert-Butylethylene was added to a standard mesitylene solution of 1 at approximately one-half the concentration of 1 (exp 9, Table 2). This solution of 1 plus olefin was then subjected to hydrogenation conditions identical to those of exp 6: 6.8 atm H_2 , 60°C. The most marked difference in exp 9 from exp 6 was the nearly immediate appearance and rapid growth of products 3 (alkane) and 4 (aldehyde) (Figure 9). *tert*-Butylethylene concentration steadily increased over the initially added amount during the first 2h of reaction. At reaction's end, the concentration of alkane 3 equaled that of exp 6 (Table 2) whereas the final concentration of aldehyde 4 increased by 50% over that of exp 6. (A comment on the negative slopes of several of the traces of Figure 9 from 4h onward is required. For lack of a better explanation, the author attributes this to escape of the reaction's more volatile components. *tert*-Butylethylene, the

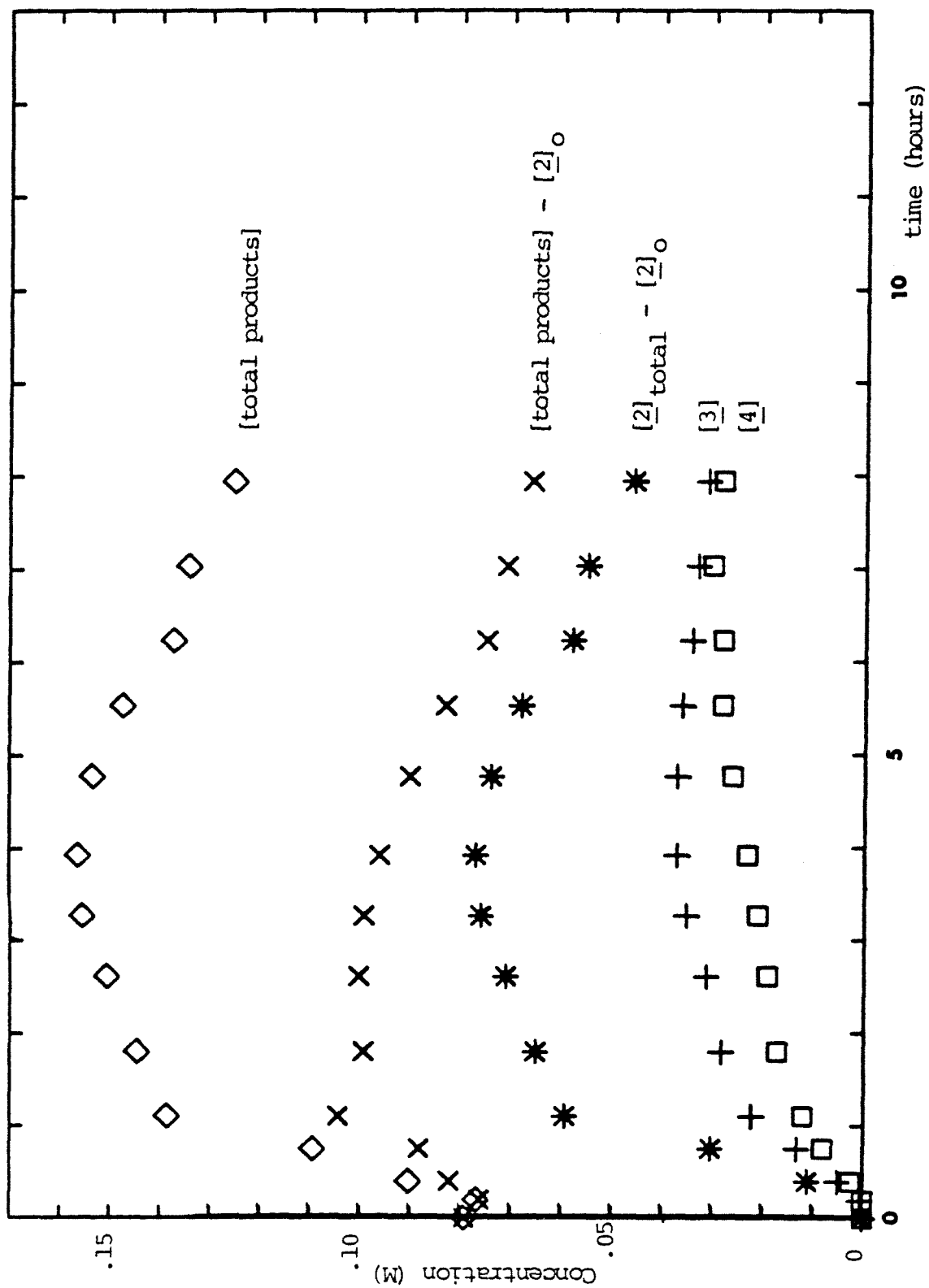


Figure 9. Appearance of products of hydrogenation in presence of added olefin 2, exp 9.

lowest boiling (bp 41°C STP), appears to be the major contributing factor to the negative slopes of the other two decreasing traces labelled [total products] and {[total products] - [added olefin]}. (During the reaction, loss of pressure **did** occur on sampling; repressurizing with H₂ to 6.8 atm would not replace any other lost gasses.) The dramatic loss of olefin after 4h is probably not due to its conversion to the other products since a decline is also noted after 4h for {[total products] - [added olefin]} - a figure which essentially serves the purpose of accounting for reacted starting material. An indicator of overall mass balance, the trace labelled [total products], also reflects a spurious depletion of reaction components. Simply repeating the reaction with tighter (leak-proof) sampling devices should confirm or negate this conclusion.)²⁵

From the results of exp 9, several aspects of the mechanisms of product formation can be briefly speculated. Preliminary indication that olefin 2 is involved in alkane (3) and aldehyde (4) production might be substantiated by a kinetics study in which the formations of products 3 and 4 are recorded as a function of initial added olefin concentration. Likewise, the presence of a yet-undetected cobalt carbonyl hydroformylation catalyst might be established by experiments in which added olefin concentration remains constant and the amount of cobalt introduced to the reaction (in the form of 1) is varied, again monitoring the appearances of alkane 3 and aldehyde 4. This

second study does not differentiate between the active hydroformylation catalyst's being 1 or some later-formed cobalt by-product; however, the latter is suspected to be the reagent responsible for aldehyde formation since at the start of rxn 9, in the presence of excess olefin and when all the cobalt is tied up as 1, production of 3 and 4 is not immediate. The existence at reaction's end of large amounts of olefin attests to the unavailability of a reagent to convert it all to alkane and aldehyde (despite the availability of hydrogen²⁶) - this observation, together with the results from exp 8 (predominant aldehyde production from hydrogenation under CO), further suggests that the cobalt hydroformylation catalyst requires external CO to survive beyond several turnovers.

Unfortunately, a straightforward kinetic model into which all the data of exps 3-9 can be plugged is not immediately obvious with the data at hand. At present, computation of the rates of appearance of aldehyde and alkane is precluded in the absence of both a detectable intermediate (other than olefin) and a recognized steady state situation. Ascertaining the laws governing olefin concentration promises to be complicated due to its seemingly simultaneous production from 1 and consumption to form aldehyde and alkane (at a rate likely to be limited by undetectable species). Probably the most valid approach to analyzing the kinetics of product formation from hydrogenation of 1 is via computer modeling.

CONCLUSIONS

Preliminary investigations into the reactions of $\text{Co}_3(\text{CO})_9\text{CCH}_2\text{C}(\text{CH}_3)_3$ (1) with hydrogen have provided information of the mode of organic product formation from alkyl cobalt carbonyl clusters. Hydrogenation of 1 in hydrocarbon solvents yielded two organic products, olefin 2 and alkane 3. Use of aromatic solvents resulted in formation of a third product identified as aldehyde 4. Hydrogen-mediated decomposition of 1, found to follow first order kinetics ($k = 1.45 \times 10^{-5} \text{sec}^{-1} \text{atm}^{-1}$), proceeded with nearly quantitative formation of organic products. CO (external source) inhibited the decomposition of 1 under normal hydrogenation conditions; however, at elevated temperatures, hydrogenation of 1 under CO yielded aldehyde 4 as the major product. This production of 4 from 1 seemed to be in part at the expense of earlier-formed olefin 2. Olefin added to hydrogenations of 1 appeared to get incorporated into the reaction manifold.

In tracing the fate of the carbonyl carbon of 1, we have observed via the three organic products from hydrogenation of 1 three modes of reaction for the carbyne: 1) addition of two hydrogen atoms to become the terminal, vinylic CH_2 group of olefin 2; 2) total saturation with hydrogen to become the methyl terminus of alkane 3; and 3) addition of the elements of H_2 and CO to become the **alpha**-methylene unit of aldehyde 4.

EXPERIMENTAL

General

For preparation of 1, $\text{Co}_2(\text{CO})_8$ was used as received. Sublimed $\text{Co}_2(\text{CO})_8$ ($<10^{-4}$ mm, 43° bath, 0° cold finger) was used in the preparations of tetracarbonyl cobaltate. *tert*-Butylacetylene, dried over 4A molecular sieves, was transferred under vacuum from a -25° flask to a -196° receiver and stored at -20° under nitrogen. 4,4-Dimethylpentanoic acid and 3,3-dimethylbutene were dried over 4A sieves. Sodium iodide was dried under vacuum with heating. Triethylamine was distilled from CaH_2 and stored over NaOH. 3,3-Dimethylchlorobutane was transferred under vacuum from 4A sieves. Monomethylamine was transferred under vacuum immediately prior to use. Used as received were mesyl chloride, 2,2-dimethylbutane, hydrogen peroxide (30% aq), LiBHET_3 (1.0M in THF), $\text{BH}_3 \cdot \text{THF}$ (1.0M in THF), H_2 (cylinder), and CO (cylinder).

Methanol was dried over 3A sieves, methylene chloride and 2-butanone were dried over 4A sieves. Mesitylene, toluene, and benzene were each purified by a vpc-monitored fractional distillation from 4A sieves. Tetrahydrofuran (THF) was transferred under vacuum from sodium benzophenone ketyl.

Except where noted, reaction mixtures were prepared in a Vacuum Atmospheres nitrogen atmosphere glove box and reactions performed outside of the glove box used conventional Schlenk techniques. Reactions requiring high gas pressures (higher than

1 atm at -196°) were performed in a stainless steel manifold (previously described in Results Section, Figure 1) assembled in these labs.

Routine ^1H NMR spectra were recorded on a Varian EM-390 (90 MHz) spectrometer. The kinetics-monitored hydrogenation of 1 (exp 3 of Table 2) was carried out in a 56°C probe of a 180.09 MHz Fourier Transform NMR instrument equipped with a Bruker superconducting magnet, Nicolet Technology Corp. model 1180 data system, and electronics assembled by Mr. Rudi Nunlist (U.C.Berkeley). For this reaction, the digitally interfaced pulse programmer was programmed to collect spectra every 20min over a 24h time period. The spectra thus collected were stored on a disk and later processed for integration on the instrument's computer terminal. NMR chemical shifts are reported in units of ppm downfield from tetramethylsilane (0.0 ppm).

Infrared spectra were recorded on a Perkin Elmer 283 spectrophotometer using NaCl solution cells (0.1mm path length) or NaCl salt plates for neat liquid samples.

Analytical vpc analyses were performed on a Perkin Elmer Sigma 3 GLC interfaced with a SpectraPhysics Autolab System 1 computing integrator. A $14' \times \frac{1}{8}"$ 8% OV-101/Chromosorb G-AWDMCS column (programmed from 30° for 9min to 185° at $6^{\circ}/\text{min}$) and 60° block (injector port and flame ionization detector) were used to monitor hydrogenations of 1. Preparative gas-liquid chromatography was conducted on a Varian Aerograph Model 90-P instrument using a $15' \times \frac{3}{8}"$ OV-17/Chromosorb P-AWDMCS column (175°

injector, 150° column, 155° detector). A helium flow of 60ml/min and -78°C glass collectors were used to collect the desired eluants.

Mass spectroscopic and GCMS analyses were performed by the UCB Chemistry Department Mass Spectroscopy Laboratory on AEI-MS12 and Finnigan 4000 spectrometers, respectively. Both systems are interfaced with Finnigan/INCOS data systems. MS data are reported in units of m/e and as percentages of relative ion current. Where appropriate, major fragments are also reported.

Plots were recorded by a Houston Instruments HIPLLOT™ digital x,y-plotter from data entered into a Northstar Horizon computer interfaced with a Hazeltine 1420 terminal. Line slopes were computed with a BASIC Least Squares linear regression program on the Northstar system.

Preparation of $\text{Co}_3(\text{CO})_9\text{CCH}_2\text{C}(\text{CH}_3)_3$ (1)²⁸

In a 250ml Schlenk flask, $\text{Co}_2(\text{CO})_8$ (20.0g, 58mmol) was dissolved in $\text{HCCC}(\text{CH}_3)_3$ (20.0ml, 163mmol) at room temperature (the reaction also proceeds at 0°C). Rapid bubbling and cooling (presumably due to solvent evaporation on CO gas evolution and/or endothermicity) was noted. The solution was allowed to stir 1h at which time its IR spectrum indicated no residual octacarbonyl. The solvent (residual t-butylacetylene) was removed under vacuum leaving a mobile orange oil, $\text{Co}_2(\text{CO})_6(\text{HCCC}(\text{CH}_3)_3)$: ^1H NMR (C_6D_6): δ 5.46 (s, 1H), 1.05 (s, 9H)ppm; IR (benzene) ν_{CO} 2089 (m), 2060 (w), 2049 (vs), 2026 (vs), 2016 (s), 2006 (mw) cm^{-1} . (tert-

Butylacetylene displays NMR signals at (C_6D_6) δ 1.88 (s, 1H) and 1.13 (s, 9H) ppm.) The oil, diluted with CH_3OH (70ml), was treated with H_2SO_4 (10ml conc in 10 ml MeOH) and the resulting solution was heated at reflux. After 12h, a lower, oily layer (containing more product 1 than the upper methanol layer by IR analysis) was removed via cannula into a fresh solution of H_2SO_4 (10ml, conc) in MeOH (100ml). Continued heating at reflux of both methanol solutions led to complete disappearance of starting material within 10h. The resulting acidic methanol solutions of product 1 were refrigerated at $-20^\circ C$ overnight to yield deep red-black needles which were washed with copious amounts of distilled water (until well after the washes tested neutral) and dried under vacuum. A total first crop of 7.7g was realized (40% yield, based on a stoichiometry of 1 $Co_2(CO)_8 \rightarrow 2/3 Co_3(CO)_9CCH_2C(CH_3)_3$), mp $127-8^\circ$ (under nitrogen)²⁹; IR (Table 1); 1H NMR (C_6D_6) δ 1.06 (s, 9H), 3.75 (s, 2H) ppm; MS (50 eV) parent ion 512 m/e (0.06 RIC), fragments corresponding to loss of CO ligands; Anal. Calc'd for $C_{15}H_{11}Co$: C, 35.18; H, 2.17; Co, 34.53. Found: C, 35.49; H, 2.37; Co, 34.50.

Preparation of $(CH_3)_3C(CH_2)_2CHO$ (4)³⁰

$MeNH_2$ (100ml) was transferred under vacuum from a lecture bottle to a 250ml Schlenk flask cooled to -196° . The flask containing the frozen amine was then attached via glass tubing to an evacuated, -196° , 250ml 3-necked flask containing $Me_3C(CH_2)_2COOH$ (5.0g, 38.5mmol) and lithium wire (350mg, 50mmol). The amine was allowed to warm to room temperature and to transfer

quantitatively into the reaction vessel containing the acid. A deep blue color was observed on contact of the amine with the lithium wire. The solution was allowed to warm to 0° during which time an argon atmosphere was applied as soon as a positive pressure (from MeNH₂ gas) was noted. The blue solution received a second dose of lithium wire (740mg, 106mmol) and was left stirring at 0° (under a -78° condenser) 4h, at which time no carboxyl stretch was seen in the IR. The solution was then slowly quenched with saturated aqueous NH₄Cl (100ml), transferred to a separatory funnel, and extracted with diethyl ether (2 x 50ml). The organic layer was slowly washed with 10% HCl (1 x 50ml; however the author recommends future use of 5% HCl), 10% NaHCO₃ (2 x 50ml), and H₂O until the aqueous layer tested neutral. The organic layer was dried over MgSO₄ and concentrated on a rotary evaporator to a light yellow liquid, 1.5g (crude yield 34%). Analytical samples of aldehyde 4 were provided by distillation at reduced pressure (bp 47°, 33mm): IR (benzene) 2960 (s), 2868 (w), 2715 (w), 1728 (vs), 1462 (br,w), 1366 (m) cm⁻¹; IR (thin film - care must be taken to record thin film spectra quickly or with precautions to exclude exposure to the atmosphere since neat samples of the aldehyde rapidly picked up water (see Results Section for discussion)) 2958 (vs), 2870 (m,sh), 2715 (w), 1728 (s), 1470 (m), 1408 (m), 1390 (m), 1372 (m) cm⁻¹; ¹H NMR (C₆D₆) δ 0.67 (s, 9H), 1.21 (m, 2H), 1.83 (m, 2H), 9.35 (t, 1H) ppm; MS (15 eV) m/e (RIC, suggested fragment) 114 (0, no parent ion (characteristic of aldehydes, see text)),

99 (1.30, RCHO-{CH₃}), 96 (2.27, RCHO-{H₂O}), 81 (17.41, RCHO-{CH₃}-{H₂O}), 57 (32.30, C₄H₉), 56 (6.44, C₄H₈ or \cdot CH₂CH₂CHO), 55 (3.35, C₄H₇ or \cdot CH₂CH₂ - {H}), 43 (12.44, CH₃CO or \cdot CH₂CHO or C₃H₇), 41 (5.22, CHCO or C₃H₅); Anal Calcd for C₇H₁₄O: C, 73.61; H, 12.38. Found: C, 73.39; H, 12.34.

Preparation of (CH₃)₃C(CH₂)₂OH (5)

3,3-Dimethylbutanol was prepared from 3,3-dimethylbutene according to the literature procedure for hydroboration of olefins³¹ and distilled as a clear, colorless liquid (bp 61°, 19mm): IR (thin film) 3350 (br,s), 2958 (s), 2865 (sh,m), 1478 (br, m), 1366 (m), 1037 (m), 991 (m) cm⁻¹; ¹H NMR (CCl₄) δ 0.93 (s, 9H), 1.46 (t, 2H), 2.52 (s, 1H), 3.59 (t, 2H) ppm. IR and NMR data are in agreement with Aldrich's published spectra of 5.

Preparation of (CH₃)₃C(CH₂)₂OSO₂CH₃ (6)

In a 100ml, nitrogen-purged, ice-cooled, 3-necked flask was placed 3,3-dimethylbutanol (5) (422mg, 4.14mmol), mesyl chloride (593mg, 5.18mmol), and CH₂Cl₂ (12ml). Triethylamine (922mg, 9.11mmol) was added slowly from an addition funnel to the stirring solution over 0.5h. Much white precipitate (NEt₃HCl) was formed over the course of the addition and an additional 20ml CH₂Cl₂ was required to maintain stirring. The ice bath was removed and after 1h at room temperature an IR of the solution contained no hydroxyl absorbance. The solution was filtered,

combined with an equal volume of H₂O, and washed successively with H₂O, 10% HCl, H₂O, 10% NaHCO₃, and finally repeatedly with H₂O until the aqueous layer tested neutral. The organic layer was dried over MgSO₄ and reduced on a rotary evaporator to a light yellow oil, 550mg (yield 74%): IR (thin film) 2960 (s), 2875 (m), 1478 (m), 1350 (vs), 1175 (vs), 972 (s), 950 (vs), 890 (m), 847 (m), 800 (m) cm⁻¹; ¹H NMR (CCl₄) δ 1.0 (s, 9H), 1.67 (t, 2H), 2.88 (s, 3H), 4.18 (t, 2H) ppm. The mesylate was used without further purification in subsequent reactions with NaI and Co(CO)₄⁻.

Preparation of (CH₃)₃C(CH₂)₂I (7)

3,3-Dimethylchlorobutane did not react with NaI (1.4fold excess) in acetone at room temperature. At reflux, the reaction was still sluggish (monitored by gc). The alkyl chloride was then replaced with the mesylate (6) as the alkyl substrate. 3,3-Dimethylmesylbutane (6) (30mg, 0.16mmol) and NaI (38mg, 0.25mmol) were combined in d⁶ acetone (0.5ml) in an NMR tube, heated at 40°, and monitored by NMR (after filtration from NaOSO₂Me). After 24h 75% of the mesylate had been converted to the alkyl iodide, (CH₃)₃C(CH₂)₂I (7) (re:NMR t-butyl chemical shifts of 0.96 and 0.90 ppm for 6 and 7, respectively). Due to this slow rate of substitution, the reaction was repeated on a preparative scale using 2-butanone as solvent, thus allowing a higher reaction temperature. 3,3-Dimethylmesylbutane (6) (5.0g, 28mmol) was placed in 2-butanone (50ml) in a 250ml flask outfitted with a

reflux condensor and N_2 purge. NaI (10g, 67mmol) in 2-butanone (25ml) (the slurry took on a light orange color) was added to the mesylate solution and heated to reflux with stirring. Within 5min, copious amounts of precipitate ($NaOSO_2Me$) had formed and more solvent (125ml) was added to facilitate stirring. The reaction was monitored by tlc (Et_2O :hexane, 1:1) for 4h (during which time the solution assumed a deep orange color). Filtration, followed by removal of solvent on a rotary evaporator, yielded a deep orange oil which was then taken up in Et_2O (50ml). The ether solution was washed sequentially with H_2O , 5% $Na_2S_2O_3$ (the color of the organic layer lightened to a pale yellow), H_2O , 5% $NaHCO_3$, and finally H_2O until the aqueous layer tested neutral. After drying over $MgSO_4$, the organic layer was reduced on a rotary evaporator to a light yellow liquid, 2.54g (crude yield 30%). The alkyl iodide, $(CH_3)_3C(CH_2)_2I$ (7), was purified by distillation at reduced pressure (bp 47° , 8mm): IR (thin film) 2958 (s), 2868 (m), 1467 (m,br), 1392 (w), 1377 (m), 1325(w), 1245 (m), 1215 (w), 1164 (m) cm^{-1} ; 1H NMR (CCl_4) δ 0.9 (s, 9H), 1.85 (m, 2H), 3.03 (m, 2H) ppm. Anal. Calcd for $C_6H_{13}I$: C, 33.98; H, 6.19; I, 59.83. Found: C, 34.24; H, 6.21; I, 59.58. The colorless alkyl iodide was stored over copper wire, free from light, at $20^\circ C$.

Preparation of $Co(CO)_4^-M^+$, M = Na, Li, PPN

Lithium tetracarbonylcobaltate was prepared by treating a solution of $Co_2(CO)_8$ (91mg, 0.27mmol) in THF (2ml) with $HBEt_3Li$ (0.5ml of a 1.0M THF solution, 0.5mmol). IR of the metal

carbonyl bands indicated that reaction was immediate and complete (Table 1)³².

Solutions of sodium tetracarbonylcobaltate were afforded by combining $\text{Co}_2(\text{CO})_8$ (40mg, 0.12mmol) and Na/Hg amalgam (0.65%, 2.0g, 0.5mmol in Na) in THF (1ml) (cf. Table 1 for IR data).

$[\text{Ph}_3\text{PNPPH}_3]^+[\text{Co}(\text{CO})_4]^-$ was prepared by treating the above THF solution of $\text{NaCo}(\text{CO})_4$ with an equivalent of PPN^+Cl^- . Filtration (from NaCl) provided a THF solution of $[\text{PPN}]\text{Co}(\text{CO})_4$ (IR data in Table 1).

Attempted Preparation of $\text{Co}(\text{CO})_4(\text{CH}_2)_2\text{C}(\text{CH}_3)_3$ (8)

Several attempts to synthesize 8 from $\text{Co}(\text{CO})_4^-$ and alkyl electrophiles were not successful. Neither chloro-, iodo-, nor mesyl-3,3-dimethylbutane reacted with $\text{Co}(\text{CO})_4^-$ (sodium, lithium, or PPN salts) in THF at 20°C under a nitrogen atmosphere. Attempts to alkylate the cobalt anion (sodium salt) with the alkyl iodide in benzene at 70°C also did not proceed, at least in part due to the anion's insolubility in benzene. In all the above cases, unreacted starting material was the only observed component of the reaction mixtures.

Preparation and Procedure of Monitored Hydrogenation Reactions

The preparation of the sample for exp 3 of Table 2 is presented as an example of a typical NMR-monitored hydrogenation. A standard, thin-walled tube equipped with a 14/20 ground glass joint was loaded with 1 (5.6mg, 10.9umol) and topped with a stopcock. The tube was then placed on the vacuum line,

evacuated, cooled, and deuterobenzene was transferred in under vacuum. A known (manometrically) amount of TMS (tetramethylsilane internal standard) was then transferred in under vacuum. While immersed in a liquid nitrogen bath, the tube was filled with a known pressure of H_2 and sealed off (with a torch). Alternatively, the NMR tube (outfitted with ground glass joint) could be charged by weighing in 1, internal standard (e.g., ferrocene), and solvent. In this procedure, the solution then had to be thoroughly degassed prior to introduction of hydrogen on the vacuum line.

Chemical shifts for mixtures of starting material and products of hydrogenations in NMR tubes follow.

In cyclohexane- d^{12} (ppm): 1 1.07 (s, 9H), 3.75 (s, 2H); 2 0.92 (s, 9H), 4.72 (q, 2H), 5.65 (q, 1H); 3 0.77 (s, 9H), alkyl region obscured by t-butyl and solvent peaks.

In benzene- d^6 (ppm): 1 1.04 (s, 9H), 3.72 (s, 2H); 2 1.0 (s, 9H), 4.94 (t, 2H), 5.83 (q, 1H); 3 0.88 (s, 9H), alkyl region obscured by other aliphatic hydrogens; 4 0.70 (s, 9H), 9.30 (t, 1H), alkyl region obscured.

The experimental procedure for preparation and execution of hydrogenations on the high-pressure manifold is described in the Results Section.

Data Handling

Data from the NMR-monitored reaction (exp 3, Table 2) were processed and plotted using relative concentration terms for each component (relative to internal standard TMS). The concentrations of gc-monitored reactions were measured against an internal standard (benzene) and then converted to absolute concentrations (product response factors were comparable within experimental error). A least squares linear regression program was used in conjunction with an x,y-plotter to calculate and plot kinetic data.

REFERENCES AND NOTES

1. Fischer-Tropsch synthesis can be briefly described as the process of homologation of Co (and H₂) to hydrocarbons using solid-phase metal catalysts.
2. For a recent review of Fischer-Tropsch Chemistry, see E.L.Muetterties and J.Stein, *Chem. Rev.*, 495 (1979).
3. See, for example,
 - a. G.Palyi, F.Piacenti, and L.Marko, *Inorg. Chim. Acta Rev.*, 4, 109 (1970).
 - b. B.R.Penfold and B.H.Robinson, *Acc. Chem. Res.*, 6, 73 (1973).
 - c. D.Seyferth, *Adv. Organomet. Chem.*, 14, 97 (1976).
 - d. G.Schmid, *Angew. Chem. Int. Ed. Engl.*, 17, 392 (1978).
 - e. W.C.Dent, L.A.Duncanson, R.G.Guy, H.W.B.Reed, and B.L.Shaw, *Proc. Chem. Soc. London*, 169 (1961).
4. D.Seyferth, C.N.Rudie, and M.O.Nestle, *J. Organomet. Chem.*, 178, 227 (1979).
 D.Seyferth, O.N.Rudie, and J.S.Merola, *J. Organomet. Chem.*, 162, 89 (1978).
 D.Seyferth, M.O.Nestle, and C.S.Eschbach, *J. Am. Chem. Soc.*, 98, 6724 (1976).
 D.Seyferth, G.H.Williams, P.L.K.Hung, and J.E.Hallgren, *J. Organomet. Chem.*, 71, 97 (1974).
 D.Seyferth, J.E.Hallgren, and P.L.K.Hung, *J. Organomet. Chem.*, 50, 265 (1973).
5. G.L.Geoffroy and R.A.Epstein, *Inorg. Chem.*, 16, 2795 (1977).
6. R.C.Ryan, C.U.Pittman, and J.P.O'Connor, *J. Am. Chem. Soc.*, 99, 1986 (1977).
 see also E.R.Tucci, *Ind. Eng. Chem. Prod. Res. Devel.*, 7, 32, 125, 227 (1968); *ibid*, 9, 516 (1970).
7. R.Markby, I.Wender, R.Friedel, F.A.Cotton, and H.Sternberg, *J. Am. Chem. Soc.*, 80, 6529 (1958).
8. Co₃(CO)₉CCH₂C(CH₃)₃ (1) has been reported as a dark violet solid, mp 122-123°C, and attributed to unpublished results of W.Hubel et al in "Organic Synthesis via Carbonyls", Vol 1, I.Wender and P.Pino, Eds., Wiley Interscience, New York (1968), p.307.
9. The reaction was unsuccessfully attempted at lower temperatures, with a weaker acid (paratoluenesulfonic acid), and in organic solvent (hexane).

10. D.Seyferth, J.E.Hallgren, and R.J.Spohn, *J. Organomet. Chem.*, **23**, C55 (1970).
R.Ercoli, E.Santambrogio, G.T.Casagrande, *Chim. Ind. (Milan)* **44**, 1344 (1962).
W.T.Dent, L.A.Duncanson, R.G.Guy, H.W.B.Reed, and B.L.Shaw, *Proc. Chem. Soc. London*, 169 (1961).
H.Patin, G.Mignani, M.T.VanHulle, *Tet. Lett.*, **26**, 2441 (1979).
11. "The Chemist's Companion", A.J.Gordon and R.A.Ford, Eds., Wiley Interscience, New York (1972) p.197.
12. "Interpretation of Mass Spectra", Second Ed., F.W.McLafferty, Benjamin (1973), New York, pp.56ff.
13. R.G.Pearson and P.E.Figdore, *J. Am. Chem. Soc.*, **102**, 1541 (1980).
14. "Organic Synthesis via Metal Carbonyls", Vol 1, op.cit., p.378 and refs therein.
15. L.S.Stuhl and R.G.Bergman, unpublished results. LSS used gc and MS as means of analysis of the two products formed in hydrocarbon solvents. This author's use of GCMS, NMR, and gc (comparison with authentic samples) confirmed these assignments.
16. P.Pino, F.Piacenti, M.Bianchi, and R.Lazzaroni, *Chim. Ind. (Milan)*, **50**, 106 (1968).
17. "Organic Synthesis via Metal Carbonyls", op.cit., Vol.2 (1977), pp.48-50 and refs 20 and 25 therein.
18. The rate constant for disappearance of starting material was derived from a plot of $\ln([I]_0/[I]_t)/(p_{H_2})$ vs time and that for appearance of total products from a plot of $\ln([total\ products]_{final}/[total\ products]_t)/(p_{H_2})$ vs time.
19. The rate constants for appearance of total products were supplied by a plot of $\ln([tot\ prods]_{final}/[tot\ prods]_{final}-[tot\ prods]_t)$, and are in units of sec^{-1} . Dividing each k_{obs} by its respective hydrogen pressure yields values of k (in $sec^{-1}atm^{-1}$) normalized to one atmosphere H_2 : 2.51×10^{-5} (at 2.5 atm), 2.14×10^{-5} (at 5.1 atm) and 1.97×10^{-5} (at 6.8 atm).
20. Assuming good agreement between the rates for disappearance of starting material and appearance of total products as was demonstrated in exp 3.

21. Here are several literature sources for the solubility of hydrogen in organic solvents (ref 21d confirms that Henry's Law applies in our pressure ranges):
- R.Battino and H.Clever, *Chem. Rev.*, **66**, 395 (1966).
 - M.W.Cook, D.N.Hanson, and B.J.Alder, *J. Chem. Phys.*, **26**, 748 (1957).
 - J.E.Jolley and J.H.Hildebrand, *J. Am. Chem. Soc.* **80**, 1050 (1958).
 - S.Kruyer and A.P.P.Nobel, *Rec. Trav. Chim.*, **80** 1145 (1961).
22. a. R.A.Epstein, H.W.Withers, and G.L.Geoffroy, *Inorg. Chem.*, **18** 942 (1979).
b. S.Aime, L.Milone, and M.Valle, *Inorg. Chim. Acta*, **18**, 9 (1976).
23. In a separate control experiment (exp 12 of Table 2) a solution of 1 in deuterobenzene was heated under a hydrogen-free atmosphere (argon). No decomposition was noted (by NMR) after 11h at 56°. See also refs 5 and 6 for CO inhibition of $\text{Co}_3(\text{CO})_9\text{CR}$ decomposition.
24. The hydrogenation of 1 in deuterobenzene has been carried out in the presence of an excess of propylene and monitored by NMR (exp 10 of Table 2). The alkyl region of the NMR spectrum indicated formation of at least one new product in addition to the usual three products. Examination of the region from 9 to 10 ppm did not reveal whether more than one aldehyde had been formed (low signal intensities). A control experiment in which 1 was heated with propylene in the absence of hydrogen showed 1 to be stable to propylene under these conditions (exp 11, Table 2).
25. The partitioning of volatile products into the gas phase is not considered a serious problem since most of the starting material's alkyl ligand can be accounted for in the total product concentration of the hydrogenations.
26. Reaction mixtures that have been left under hydrogenation conditions for several days show little change in product distribution apart from decomposition.
27. The solubility of hydrogen in benzene at 60°C and 5 atm is 0.0225 Mol/l^{21d}. The solubility of hydrogen in mesitylene is expected to be somewhat greater than in benzene. Cf. ref 21b and J.H.Hildebrand, *I & EC Fundamentals*, **17**, 365 (1978).

28. For representative syntheses of similar $\text{Co}_3(\text{CO})_9\text{CR}$ compounds, see refs 3, 7, and 10.
29. The literature reports⁸ a mp of $122-3^\circ$ which is similar to the one we observe on performing the melting point in air.
30. A.O.Bedenbaugh, J.D.Bedenbaugh, W.A.Bergin, and J.D.Adkins, *J. Am. Chem. Soc.*, **92**, 5774 (1970).
31. a. H.C.Brown, "Organic Synthesis via Boranes", John Wiley and Sons, New York (1975), pp22-3.
b. H.C.Brown and G.Zweifel, *J. Am. Chem. Soc.*, **82**, 4708 (1960).
32. A flash of red color was observed on adding the borohydride to $\text{Co}_2(\text{CO})_8$ before the solution assumed the characteristic brown color of solutions of $\text{LiCo}(\text{CO})_4$. It is known that $\text{LiCo}(\text{CO})_4$ (white) reacts with $\text{Co}_2(\text{CO})_8$ (orange) to produce $\text{LiCo}_3(\text{CO})_{10}$ (red). Although this reaction is reported to not proceed in THF, it is possible that the fleeting red color observed on addition of HBET_3Li to $\text{Co}_2(\text{CO})_8$ is due to $\text{LiCo}_3(\text{CO})_{10}$ formed from the first-generated $\text{LiCo}(\text{CO})_4$ and residual $\text{Co}_2(\text{CO})_8$. If this be the case, treatment of $\text{Co}_2(\text{CO})_8$ with $1/3$ eq HBET_3Li might provide a one-step synthesis of $\text{LiCo}_3(\text{CO})_{10}$ in THF.
33. G.Fachinetti, *J. Chem. Soc. Chem. Commun.*, 397 (1979).

Chapter III

Propositions

PROPOSITION 1 : The Formation of Tricobalt Nonacarbonyl Methynyl Complexes from Cobalt Carbonyl and Alkynes - A Mechanistic Discussion.

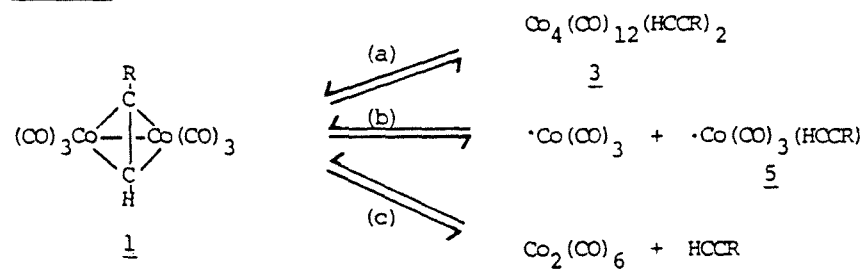
Metal clusters have become a popularly studied class of compounds, particularly since an analogy to metal surface chemistry is often drawn to reactions of their derivatives. Claiming that a multinuclear metal group might display properties similar to an active metallic surface¹, researchers have come up with clusters whose catalytic behavior models important industrial processes, e.g., the Wacker², Oxo³, water-gas shift⁴, and Fischer-Tropsch⁵ processes. One class of these compounds is based on trinuclear methynyl derivatives of Group VIII transition metals: $M_3L_nCR^6$. One of their most interesting features is the carbonyl carbon which is equally shared between several metals, hence mimicking a carbon atom sitting on a metal surface. These trinuclear metal carbynes have arisen from several synthetic preparations⁷ using mono-, di-, or trimetallic starting materials. Formation of a $Co_3(CO)_9CR$ complex from a dinuclear cobalt carbonyl and an unsymmetric alkyne will be the subject of this proposition, with particular emphasis on mechanism and reaction intermediates.

In a typical synthesis of $Co_3(CO)_9CR'$ (2)⁸, $Co_2(CO)_6(HCCR)$ (1) (formed on combining $Co_2(CO)_8$ and HCCR) is heated in an acidic (H_2SO_4) methanol solution to give, on crystallization, a

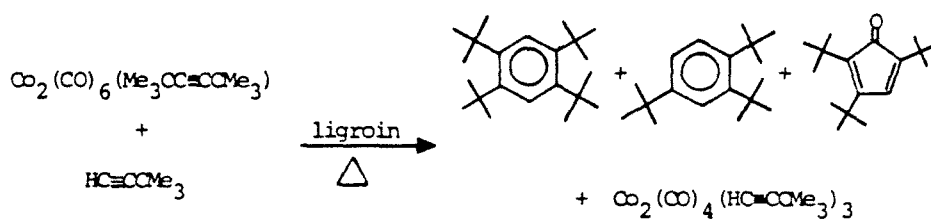
34% yield of **2** ($R'=\text{CH}_2R$). No comment on the whereabouts of the other ~66% of the cobalt starting material is included. Similar yields are reported by other authors⁹, again with no mention of the fate of the rest of the cobalt. Therefore, a study of $\text{Co}_2(\text{CO})_6(\text{HCCR})$ and its reactions would aid in elucidating the formation pathway of its 'derivative', $\text{Co}_3(\text{CO})_9\text{CR}'$ (**2**).

To start, in order to derive a trimetallic cluster from a dimetallic one, some sort of disproportionation must be occurring. Examples of plausible initiation pathways are (Scheme 1) a) combination of 2 $\text{Co}_2(\text{CO})_6(\text{HCCR})$ to form a tetracobalt species which later falls apart to trimetallic **2**; b) an initial fragmentation of **1** to two mononuclear cobalt species, one (or both) of which then combines with a dimeric starting compound to yield trimer; or c) dissociation of the alkynyl ligand and homolysis of the resulting $\text{Co}_2(\text{CO})_6$ group. Pathway (a) is unlikely, based on previous work involving similar cobalt tetramers¹⁰: compounds of the form $\text{Co}_4(\text{CO})_{10}(\text{RCCR}')$ are made by treating $\text{Co}_4(\text{CO})_{12}$ with RCCR' (at 20° or 90°C) and decompose readily to binuclear **1** (on being heated to 70° in the presence of additional alkyne). This decomposition from a tetramer to a dimer does not appear to be reversible since heating **1** does not produce a tetramer. Instead, heating $\text{Co}_2(\text{CO})_6(\text{RCCR}')$ (**1**) leads to organic products derived principally from the alkynyl ligands (Scheme 2)¹¹. Furthermore, heating **1** in the presence of another alkyne results in analagous organic products which have

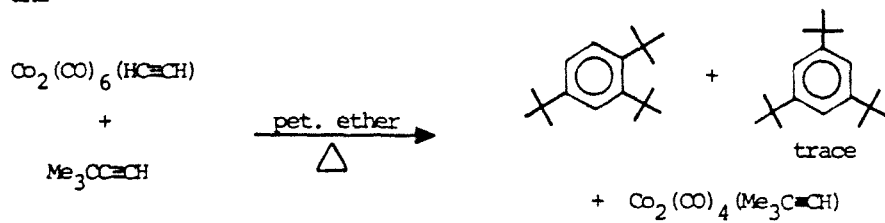
Scheme 1



Scheme 2

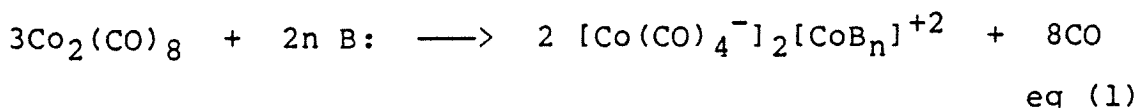


and

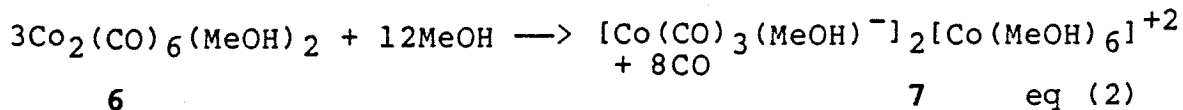


incorporated the new alkyne in addition to the complex's original alkyne. The appearance of products arising from alkyne exchange (Scheme 2) supports the proposed dissociative equilibrium between 1 and free alkyne, path (c) of Scheme 1.

If pathway (c) of Scheme 1 is the first step in conversion of 1 to 2, an unsaturated dimer, $\text{Co}_2(\text{CO})_6$ (6), is being generated under acidic conditions (H_2SO_4) in a ligating solvent (MeOH). Alcohol, as one of a class of 'basic' (oxygen-containing) solvents, has the potential to interact with cobalt carbonyl in a redox reaction^{1,2}, viz



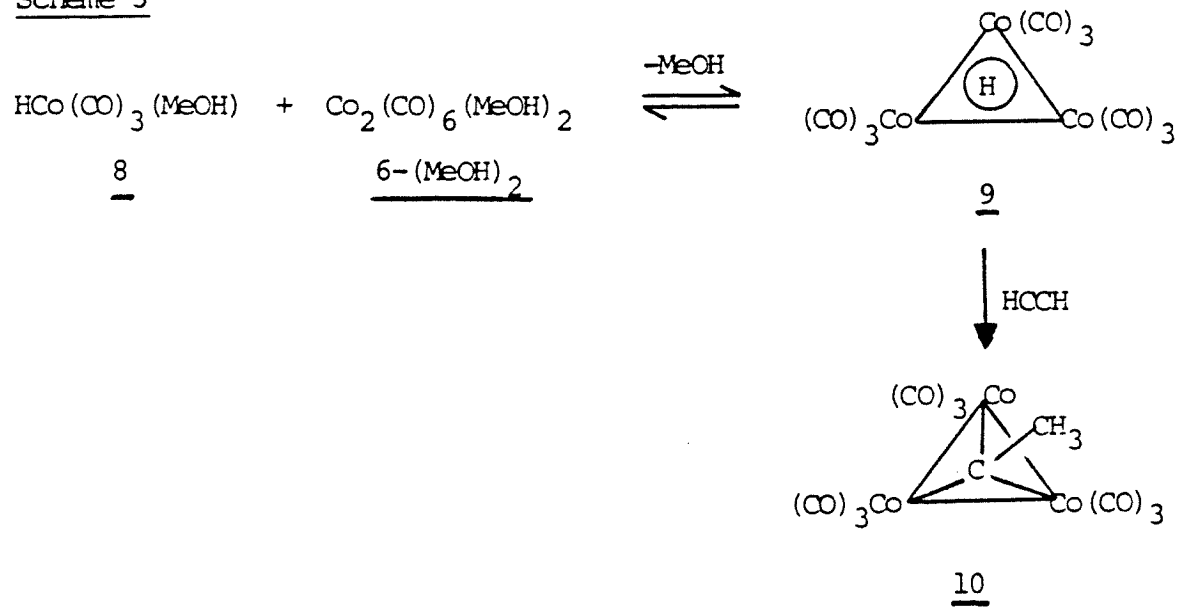
(In fact, the above equation, followed by protonation with strong acid, outlines a popular preparative method for hydridocobalt tetracarbonyl^{1,2a,b}.) Such a redox process could be occurring with 6, ultimately yielding a cobalt carbonyl hydride (8) in the highly acidic reaction medium:

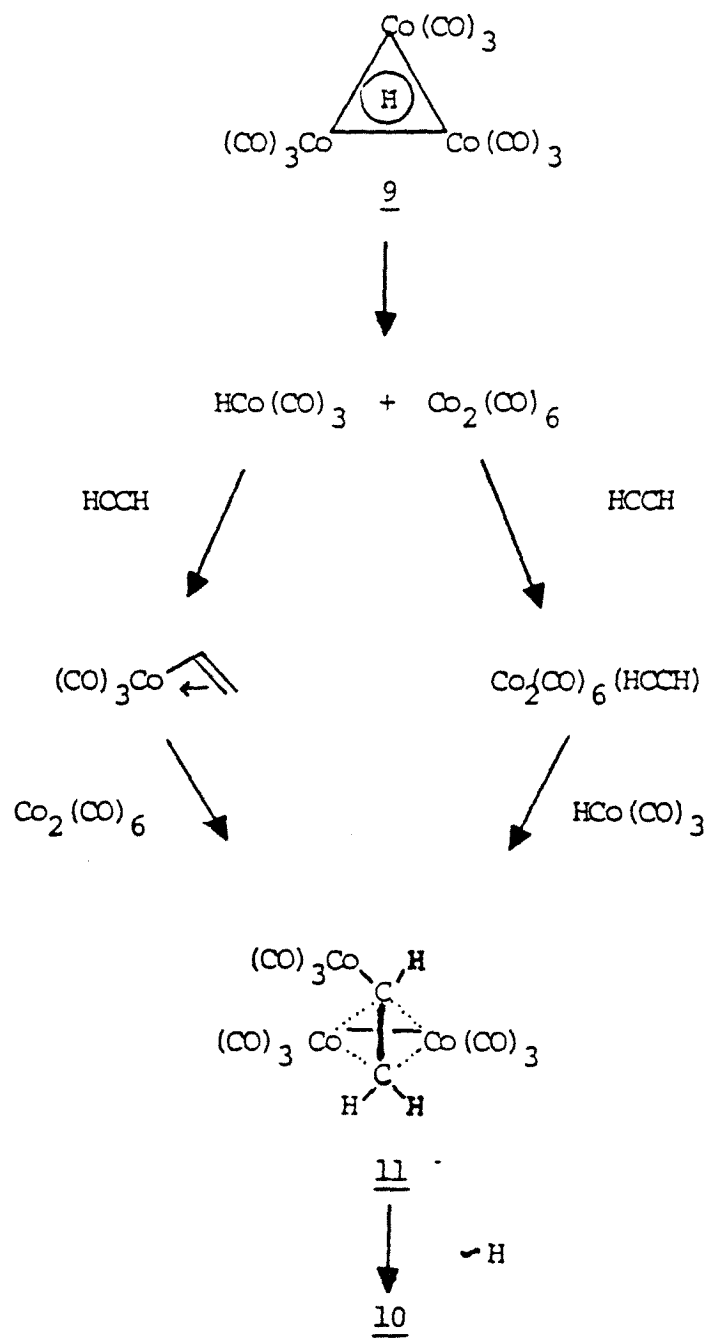


($\text{Co}_2(\text{CO})_6$ is written with its open coordination sites saturated with solvent molecules, MeOH.) Suggesting the presence of cobalt

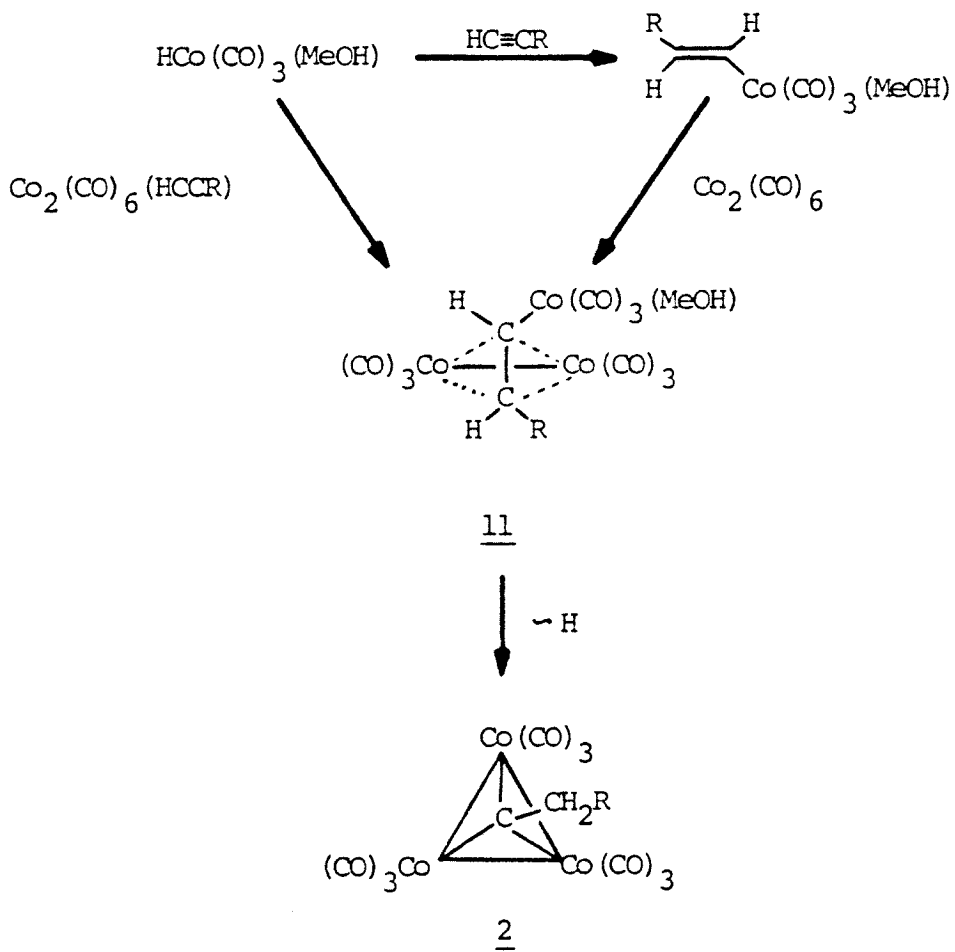
hydrocarbonyl in solution opens up many mechanistic possibilities. The action of hydrodocobalt carbonyl 8 on $\text{Co}_2(\text{CO})_6(\text{MeOH})_2$ might lead to formation of $\text{Co}_3(\text{CO})_9\text{H}$ (9) (Scheme 3). Cobalt cluster 9 has been shown to react with acetylene, yielding an example of title compound 2, $\text{Co}_3(\text{CO})_9\text{CCH}_3$ (10)¹³. The reaction is doubtfully so straightforward as to be a simple bimolecular reaction between 9 and an alkyne. Since $\text{Co}_3(\text{CO})_9\text{H}$ (9) is known¹³ to decompose to $\text{Co}_4(\text{CO})_{12}$ (and $\text{HCo}(\text{CO})_4$ under CO), the possibility presents itself that the observed reaction of $\text{Co}_3(\text{CO})_9\text{H}$ with acetylene to produce $\text{Co}_3(\text{CO})_9\text{CCH}_3$ proceeds through the mono- and/or dinuclear cobalt fragments from decomposition of 9 (Scheme 4). The mechanism in Scheme 4, proposed here to justify Fachinetti's results, perhaps applies to the general class of reactions under study: 1 \longrightarrow 2. Substituting $\text{HCo}(\text{CO})_3(\text{MeOH})$ for $\text{HCo}(\text{CO})_3$ and $\text{Co}_2(\text{CO})_6(\text{HCCR})$ for $\text{Co}_2(\text{CO})_6(\text{HCCH})$ of Scheme 4 provides Scheme 5¹⁴.

The following experiment(s) could be performed to support the mechanism outlined in Scheme 5. $\text{HCo}(\text{CO})_4$ (as prepared in ref 12c) is introduced to a methanol solution of $\text{Co}_2(\text{CO})_6(\text{HCCR})$ (1) (as prepared in refs 8 and 10). The reaction can be monitored by IR or by NMR for appearance of $\text{Co}_3(\text{CO})_9\text{CCH}_2\text{R}$. Reaction temperature will depend on the results of first combining the two reagents at low temperature (anticipating $\text{HCo}(\text{CO})_4$'s instability at ambient temperatures). Raising the reaction temperature and/or inclusion of strong acid (to sustain the cobalt hydride, a

Scheme 3

Scheme 4

Scheme 5



strong acid itself) might be required. Alternatively, a derivative of $\text{HCo}(\text{CO})_4$ might be used as a means of introducing a cobalt hydride to $\text{Co}_2(\text{CO})_6(\text{HCCR})$, e.g., $\text{HCo}(\text{CO})_3(\text{PX}_3)^{15}$. Use of $\text{HCo}(\text{CO})_3(\text{PX}_3)$ would both increase the longevity of the cobalt hydride and more closely model the reaction sequence of Scheme 5. Finally, addition of $\text{Co}_2(\text{CO})_8$ to the reaction mixture might increase yields of **2** as a result of the higher cobalt to alkyne ratio (*vide infra*).

Several concluding remarks are due on the literature's low yields for preparations of compounds of the form $\text{Co}_3(\text{CO})_9\text{CR}'$ (**2**) from $\text{Co}_2(\text{CO})_6(\text{HCCR})$ (**1**) in refluxing acidic methanol. In separate studies on the reactivity of dicobalt hexacarbonyl alkyne adducts¹⁰, the following results have been reported. Heating $\text{Co}_2(\text{CO})_6(\text{HCCMe}_3)$ with two equivalents of HCCMe_3 in petroleum ether (90-100° cut) at reflux for 3h yields two cobalt products, $\text{Co}_2(\text{CO})_4(\text{HCCMe}_3)_3$ and $\text{Co}_2(\text{CO})_6(\text{HCCMe}_3)_4^{16}$, and several organic products, including 1,2,4-tri-*tert*-butyl benzene, a diketone with an empirical formula of $(\text{HCCMe}_3)_3(\text{CO})_2$, and cyclopentadienone¹⁷. Similarly, a $\text{Co}_2(\text{CO})_4(\text{HCCF}_3)_3$ complex was isolated from heating $\text{Co}_2(\text{CO})_6(\text{HCCF}_3)$ to 110° in pentane (sealed steel bomb) for 15h ($\text{Co}_3(\text{CO})_9\text{CCH}_2\text{CF}_3$ was also obtained)¹⁸. Finally, Hubel et al¹⁰ isolate a 15% yield of stilbene on heating $\text{Co}_2(\text{CO})_6(\text{PhCCPh})$ in acidic (H_2SO_4) methanol for 3h. The above three examples, in addition to the plausible loss of a cobalt hydride species from volatilization, suggest pathways for consumption of **1** competitive with the desired formation of **2**. As

mentioned earlier, addition of $\text{Co}_2(\text{CO})_8$ to the acidic medium for rearrangement of 1 to 2 might increase yields of 2 at the expense of $\text{Co}_2(\text{CO})_4(\text{alkyne})_3$, having increased the cobalt to alkyne ratio in the reaction mixture¹⁸.

REFERENCES

1. a. E.L.Muetterties, Bull. Soc. Chim. Belg., **84**, 959 (1975).
b. *ibid*, **85**, 451 (1975).
c. E.L.Muetterties, Science, **196**, 839 (1977).
2. T.H.Whitesides and R.A.Budnick, J. Chem. Soc. Chem. Commun., 87 (1973).
3. R.C.Ryan, C.U.Pittman and J.P.O'Connor, J. Am. Chem. Soc., **99**, 1986 (1977).
4. R.M.Laine, R.G.Rinker, and P.C.Ford, J. Am. Chem. Soc., **99**, 252 (1977).
5. L.Kaplan, U.S.Patent 3,944,588 (1976).
6. a. C.U.Pittman and R.C.Ryan, Chem. Tech., 170 (1978) and refs 37 and 20 therein.
b. E.L.Muetterties and J. Stein, Chem. Rev., **79**, 479 (1979) and refs 32-37 therein.
7. a. G.Palyi, F.Piacenti, and L.Marko, Inorg. Chim. Acta Rev., **4**, 109 (1970) and refs therein.
b. G.Schmid, Angew. Chem. Intl. Ed. Eng., **17**, 392 (1978) and refs therein.
8. R.Markby, I.Wender, R.A.Friedel, F.A.Cotton, and H.W.Sternberg, J. Am. Chem. Soc., **80**, 6529 (1958).
9. Organic Synthesis via Metal Carbonyls, Vol 1, . Wender and P.Pino, Eds., (1968), Interscience, New York, p.307 and refs therein.

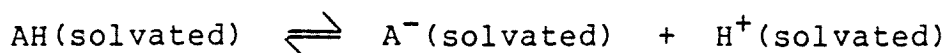
10. U. Krueke and W. Hubel, *Chem. Ber.*, **94**, 2829 (1961).
11. a. C. Hoogzand and W. Hubel, *Tet. Lett.*, **18**, 637 (1961).
b. E. M. Arnett, M. E. Strem, and R. A. Friedel, *Tet. Lett.*, **19**, 658 (1961).
c. The second equation of Scheme 2 is an unpublished experiment of W. Hubel.
12. a. A. J. Chalk and J. F. Harrod, "Catalysis by Cobalt Carbonyls" in *Adv. in Organomet. Chem.* vol 6 (1968), p.138 and refs 64, 66, 88, and 158 therein.
b. H. W. Sternberg, I. Wender, R. A. Friedel, and M. Orchin, *J. Am. Chem. Soc.*, **75**, 2717 (1953).
c. I. Wender, H. W. Sternberg, and M. Orchin, *J. Am. Chem. Soc.*, **74** 1216 (1952).
13. G. Fachinetti, S. Pucci, P. F. Zanazzi, and U. Methong, *Angew. Chem. Int. Ed., Engl.*, **18**, 619 (1979).
14. If $\text{Co}_4(\text{CO})_{12}$ is produced in the decomposition of 1, either by dimerization of two $\text{Co}_2(\text{CO})_6$ fragments or as a $\text{Co}_4(\text{CO})_{12-n}(\text{MeOH})_n$ derivative, it is reasonable to suppose that the conditions generating hydridocobalt carbonyl from the dinuclear cobalt precursor (eq (2)) might also generate it from the tetranuclear cobalt carbonyl.
15. F. Piacenti, M. Bianchi, and E. Beneditti, *Chim. Ind. (Milan)*, **49** 245 (1967).
16. The dicobalt hexacarbonyl tetraalkyne product is unsatisfactorily described as a ketone complex¹⁰.
17. U. Krueke, C. Hoogzand, and W. Hubel, *Chem. Ber.*, **94**, 2817 (1961) and ref 10. Information on the yields of this reaction is very confusing.
18. D. A. Harbourne and F. G. A. Stone, *J. Chem. Soc. (A)*, 1765 (1968). See also ref. 11.

PROPOSITION 2 : Determination of Transition Metal Hydride Acidities via Negative Ion Mass Spectrometry .

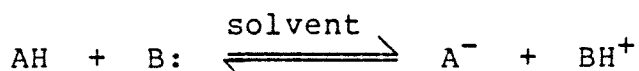
Negative Ion Mass Spectrometry has garnered increased use in the recent past as refinements on technique and instrumentation have improved its utility¹. Concurrently, organometallic compounds are being seen with increased frequency as substrates in (positive ion) mass spectrometry, for purposes of molecular identification as well as in studies of metal-ligand bonding interaction². The combination of these two lines of study, negative ion M.S. and organometallics, has received little attention³. This is surprising since negative ion M.S. has produced molecular ions in some cases with greater success than conventional (positive ion) M.S.⁴, and therefore would appear to be particularly amenable to organometallic systems where parent ions are unattainable (e.g., multinuclear complexes which fragment to yield mononuclear species as the highest positive ion mass detected in the mass spectrum). In the following proposition, several methods are suggested for establishing a relative ordering of neutral metal hydride gas-phase acidities based on ion-pair formation in the negative ion mass spectrum.

Information presently available on the acidity of transition metal hydride complexes is scant. Data from solution equilibrium

studies⁵ as well as gas-phase proton affinities of cationic metal hydrides⁶ have been published. Relative pKa's determined in solution carry the qualification that the ordering is solvent (or solvent-type) specific:



or

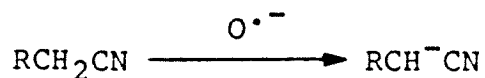


Dielectric constants and dipole moments, among other solvent effects, affect the dissociative equilibrium between a neutral acid and its conjugate anion, thereby rendering pKa's a function of the particular solvent. Gas-phase techniques, as they have been applied to organometallics up to now, analyze the proton affinity of a positively charged metal complex, MH^{+} , generated (for example) in an ICR ionizing chamber. Extrapolation of these data for positively charged species to neutral metal complexes (MH) is questionable. The use of negative ion M.S. should provide acidity data which are both independent of solvent effects and valid for a neutral metal hydride molecule. Two alternative approaches are presented for the determination of relative pKa's of metal hydrides via negative ion M.S.: A) direct observation of the conjugate anions (M^{-}) of the acids under study and B) analysis of metastable transitions from anionic bridging-hydride mixed metal dimers formed in the ionization chamber of a reverse geometry mass spectrometer.

A. The direct observation of anionic conjugate bases of

acids by negative ion M.S. has precedence in organic systems. Aplin et al⁷ have ionized formic, acetic, propionic, butanoic, and *iso*-butanoic acids with 70eV electrons. Their ordering of gas-phase acidities, based on the relative abundances of the carboxylate anions in the negative ion mass spectrum, roughly parallels the ordering of the acids' strengths in aqueous solution ionic dissociations: $\text{HCOOH} \gg \text{CH}_3\text{COOH} > (\text{CH}_3)_2\text{CHCOOH} > \text{CH}_3\text{CH}_2\text{COOH} > \text{CH}_3\text{CH}_2\text{CH}_2\text{COOH}$.

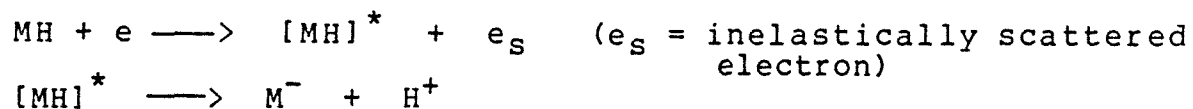
Dawson and Nibbering⁸ use chemical ionization negative ion M.S. (the primary reactant ion is $\text{O}^{\bullet-}$, generated from nitrous oxide) with organic nitriles to derive their conjugate bases:



That the base abstracted a proton exclusively from the **alpha**-position was found from deuterium labelling experiments. Subsequent proton transfer reactions of these nitrile anions with other nitriles, alcohols, diazo compounds, H_2O , and aldehydes yielded an ordering of gas-phase acidities of the organic molecules (too numerous to list here).

The carboxylate and nitrile anions of the above two studies are not necessarily generated in the same manner. Use of a chemically ionizing base ($\text{O}^{\bullet-}$) in the latter study most likely assures that nitrile anions are the products of proton abstraction by $\text{O}^{\bullet-}$. In the absence of an independently generated base, the carboxylate anions of the former study could have

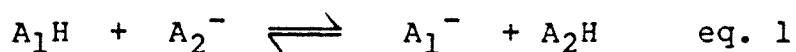
arisen from two mechanisms (at the ionizing potentials used): a) ion pair production, $AB + e^- \longrightarrow A^- + B^+ + e$, or b) dissociative electron capture, $AB + e^- \longrightarrow A^- + B^\bullet$. By increasing the carrier gas pressure, one should be able to determine which of these two mechanisms is primarily operative in carboxylate production since in the rate expressions for mechanisms a and b, enhancing (carrier) gas pressure is first order in the former and second order in the latter^{9,10}. For the purposes of this proposition, it is the abundance of anion produced by mechanism a, ion pair production, which is of interest. Therefore, from the experience of the above researchers, two means for dissociating a metal hydride to its conjugate metal anion and a proton are offered, using similar or updated instrumentation: chemical ionization as in reference 8, or the primary ionization process of ion pair formation as in reference 7. Recording the negative ion M.S. of a series of metal hydrides of interest (vs an internal standard) and comparing relative abundances of the deprotonated M^- signal arising from ion pair formation should give rise to an ordering for the relative ease of deprotonating each metal hydride:



Among the growing number of transition metal hydrides¹¹ there should be no lack of suitable substrates for this study.

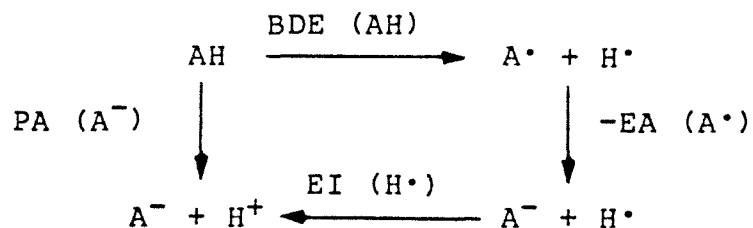
An important consideration left unattended in this treatment is the correlation between the acidity of a ground state metal hydride (MH) and its electronically excited counterpart (MH^{*}). In the above reaction scheme outlining ion pair formation, the charged products are derived from an excited parent molecule, MH^{*}, and possibly also from excited precursors M^{-*} and H^{+*}. Therefore, in establishing a relative order for the acidities of metal hydrides by the above method, the assumption is made that their excited state acidities follow the same order.

Application of the data generated in the above-proposed experiments to a calculation of free energies of deprotonation is made feasible by the pioneering work of Kebarle and Brauman. Kebarle and coworkers¹² have performed an extensive series of gas-phase acidity measurements on organic substrates using pulsed electron beam high ion source pressure mass spectroscopy. To briefly summarize their methods and theory, equilibrium constants were obtained from the proton transfer equilibria



between a standard acid (HCl, A₂H) and the acid under study (A₁H). The anions A₂⁻ and A₁⁻ are generated by deprotonation with F⁻, the fluoride ion having been produced in the electron capture reaction of NF₃ in the ion source (NF₃, A₁H, and A₂H are introduced simultaneously in methane buffer gas to the ion source). The experimentally derived equilibrium constants provide ΔG° for equation 1 from ΔG° = -RTlnK_{eq}. From this ΔG°

(for reaction temperatures of 500-600°K), ΔH° and ΔG° of deprotonation at room temperature are calculated, based on extensive entropic considerations and heat capacity adjustments. The thermodynamic cycle (below) ties together the properties 'controlling' these experiments: bond dissociation energy (BDE), electron affinity (EA), ionization energy (IE), and proton affinity (PA, $PA = \Delta H_{\text{deprot}}$).



Since $\Delta H_{\text{deprot}}^\circ = \text{BDE (A-H)} - \text{EA (A}^\bullet) + \text{IE (H}^\bullet)$, and methods for determining electron affinities are available and reliable¹³, reasonable numbers for M-H bond dissociation energies can be expected (given an IE for H^\bullet of 313.6 kcal/mol) from an analogous application of the above methodology to metal hydride systems.

B. The second proposed technique of using metastable transitions from charged μ -H dimers has no precedent in negative ion M.S. The relative base strengths of substituted amines has been documented in the gas-phase of positive ion M.S.¹⁴: dimers of the form $(\text{RH}_2\text{N-H-NH}_2\text{R}')^+$, created in the ion source (of a chemical ionization positive ion mass spectrometer) in the

secondary reaction of RH_2NH^+ with $\text{R}'\text{H}_2\text{N}$, undergo metastable decomposition to a protonated and a neutral monomer. The resulting protonated amine presumably is the stronger base.

Evidence for proton-bound anionic dimers in negative ion M.S. has been provided in a couple of literature reports. Winkler and Stahl¹⁵ present negative ion metastable spectra of **cis** and **trans**-1,3-cyclohexanediols in which stabilization of the **cis** isomer is provided by hydrogen bonding between the two negatively charged oxygens. In their study of gas-phase (negative ion M.S.) proton transfer equilibria of acids, McMahon and Kebarle¹⁶ detect substantial quantities of AHA^- . Indeed, detection of metastable transitions in negative ion M.S. is well-documented¹⁷, even being detected in an organometallic system¹⁸. That organometallics are amenable to study by negative ion M.S.^{3,18}, together with the above citations of anionic proton-sharing dimers^{15,16}, leads to the postulation of $(\text{M-H-M}')^-$ formation in the chemical ionization negative ion mass spectrometer ionization chamber. The proposed experimental procedure would entail co-ionization of the two different metal hydrides in a reverse geometry mass spectrometer, documenting their metastable transitions from $(\text{M}'\text{-H-M})^-$. A reverse geometry mass spectrometer offers the advantage of detecting daughter ions from a **specific** metastable transition, in this case, specifically those daughter ions from $(\text{M}'\text{-H-M})^-$. Relative abundances of detected metal anions should reflect preferential dissociation of $(\text{M-H-M}')^-$ to $\text{MH} + \text{M}'^-$ or to $\text{M}'\text{H} + \text{M}^-$. The metal complex more

often found protonated could then be designated the weaker acid.

In summary, two approaches in negative ion mass spectroscopy are offered for ordering transition metal hydride complexes according to relative acidities. The first relies on direct observation of the metal hydride's conjugate base while the second uses metastable transitions of the molecular ion. Discussion is extended to include determination of metal complex proton affinities and M-H bond dissociation energies.

REFERENCES

1. For mass spectroscopy reviews which include advances in negative ion M.S., see
 - a. F.W.McLafferty and J.Pinzelik, *Anal. Chem.*, **38**, 350R (1966).
 - b. R.W.Kiser and R.E.Sullivan, *ibid*, **40**, 273R (1968).
 - c. D.C.DeJongh, *ibid*, **42**, 169R (1970).
 - . (every two years *Anal. Chem.* contains a M.S. review)
 - . d. A.L.Burlingame, T.A.Baillie, P.J.Derrick, and O.S.Chizhov, *ibid*, **52**, 214R (1980).

For reviews of NIMS, see also

 - e. K.Jennings, 'Mass Spectrometry', vol 4, *Specialist Periodical Reports*, The Chemical Society, Burlington House, London (1977).
 - f. J.G.Dillard, *Chem. Rev.*, **73**, 589 (1973).
 - g. J.H.Bowie and B.D.Williams, 'Negative Ion Mass Spectroscopy' in *International Reviews of Science, Mass Spectrometry, Physical Chemistry, Series 2*, vol 5, chapter 3, ed. by A.Maccoll, Butterworths, London (1975).
 - h. J.H.Bowie, 'Mass Spectrometry' *op cit*, vol 5 (1979),

- p.279 and refs 393 - 397 therein.
2. T.R.Spalding, 'Mass Spectrometry' *ibid* vol 5 (1979), p.312 and refs therein.
 3. a. M.R.Blake, J.L.Garnett, I.K.Gregor and S.B.Wild, *Org. Mass Spec.*, **13**, 20 (1978).
b. J.L.Garnett, I.K.Gregor, and M.Guilhaus, *ibid*, **13**, 591 (1978).
c. R.N.Compton and J.A.Stockdale, *Internat. J. Mass Spec. Ion Phys.*, **22**, 47 (1976).
d. M.R.Blake, J.L.Garrett, and I.K.Gregor, *J. Organomet. Chem.*, **178**, C37 (1979).
 4. a. J.Rullkotter and K.Budzikiewicz, *Internat. J. Mass Spec. Ion Phys.*, **20**, 269 (1976).
b. J.H.Bowie, *Org. Mass Spec.*, **9**, 304 (1974).
c. J.H.Bowie, *ibid*, **5**, 945 (1971).
 5. H.W.Walker, C.T.Kresge, P.C.Ford, and R.G.Pearson, *J. Am. Chem. Soc.*, **101**, 7428 (1979) and ref 3 therein.
 6. P.B.Armentrout and J.L.Beauchamp, *J. Am. Chem. Soc.*, **102**, 1737 (1980) and refs therein.
 7. R.T.Aplin, H.Budzikiewicz, and C.Djerassi, *J. Am. Chem. Soc.*, **87**, 3180 (1965) and ref 19 therein.
 8. J.H.Dawson and N.M.Nibbering, *Internat. J. Mass Spec. Ion Phys.*, **33**, 3 (1980).
 9. For a brief background on negative ions by electron bombardment, see 'Principles of Mass Spectrometry and Negative Ions', C.E. Melton, Marcel Dekker, New York, 1970, chapter 7.
 10. Enhancing gas assumes a greater order in mechanism b since secondary electrons (electrons produced from the ionization of AB) play an active role in mechanism b and their production is very sensitive to enhancing gas pressure. For more information on this effect, see R.C.Dougherty and C.R. Weisenberger, *J. Am. Chem. Soc.*, **90**, 6570 (1968) and ref 9 p.201.
 11. See, for example, 'Organometallic Mechanisms and Catalysis', J.K.Kochi, Academic Press, New York, 1978, p.292ff and refs therein; and 'Transition Metal Hydrides', R.Bau, Ed., and authors therein, *Adv. in Chemistry Series #167*, American Chemical Society, Washington D.C., 1978.
 12. J.B.Cumming and P.Kebarle, *Can. J. Chem.*, **56**, 1 (1978) and refs 1-9 therein. See also J.E.Bartmess and R.T.McIver in

'Gas Phase Ion Chemistry', vol 12, M.T.Bowers, Ed., Academic Press, New York, 1979, chapter 11.

13. A.H.Zimmerman, K.J.Reed, and J.I.Brauman, J. Am. Chem. Soc., **99**, 7203 (1977) and refs of the same principle author therein. See also B.K.Janousek and J.I.Brauman in 'Gas Phase Ion Chemistry' *op cit*, chapter 10.
14. R.G.Cooks in 'High Performance Mass Spectrometry: Chemical Applications', M.L.Gross, Ed., ACS Symposium Series 70 (1978), p.69 and ref 8 therein.
15. F.J.Winkler and D.Stahl, J. Am. Chem. Soc., **100**, 6779 (1978).
16. T.B.McMahon and P.Kebarle, J. Am. Chem. Soc., **99**, 2222 (1977).
17. a. J.H.Bowie and B.J.Stapleton, Org. Mass. Spec., **12**, 436 (1977).
b. J.H.Bowie and S.G.Hart, Internat. J. Mass. Spec. and Ion Phys., **13**, 319 (1974).
18. R.E.Sullivan and R.W.Kiser, J. Chem. Phys., **49**, 1978 (1968).

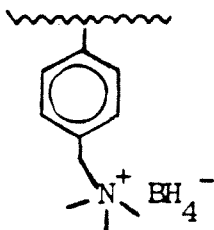
PROPOSITION 3: The Synthesis, Utility, and Advantages of a Polymer-bound, Soluble Reducing Agent: **poly-naphthalide**.

The application of polymer supports to organic synthesis has been the subject of several review articles¹. Affixing organic synthetic reagents to a polymer support assures facile purification of the desired organic substrate: simple filtration removes the bound reagent from the reaction mixture, often leaving behind a one-component system of the desired product. Of use to the organic chemist is a polymer-bound reducing agent, yet only two examples have appeared in the literature², each with considerable drawbacks. Two syntheses of a polymer-bound reducing agent, resino-naphthalide radical anion (sodium or lithium), are proposed. This reagent should offer both ease in the work-up of its reactions and facile regeneration to its reduced state.

Weinshenker and coworkers^{2a} prepared an insoluble polymer-bound *n*-butyl tin dihydride which is active in the reduction of halides to hydrocarbons and in the reduction of aldehydes and ketones to alcohols. An excess of polymeric dihydride reagent (typically three to four equivalents) is required to effect conversion. Attempts to regenerate active tin hydride on the once-used resin with LiAlH_4 failed. The authors attribute this to the affectively irreversible formation of tin oxides, Sn-Sn, Sn-O-Sn, or divalent tin derivatives on the polymer during the

reduction-hydrolysis sequence. The polymer-bound tin hydride, although effective as a reducing agent for one turnover, is limited in practicality by its rapid deactivation.

A second polymer-bound reducing agent in the literature is coordinated borohydride, BH_4^- ^{2b}. Gibson and Bailey have cleverly coordinated BH_4^- to a solid support by stirring an aqueous solution⁴ of NaBH_4 with an anion exchange resin of a bound quaternary ammonium salt. This cation exchange, sodium for tetraalkylammonium, affords an active bound reducing agent:



The insoluble beads reduce benzaldehyde at 65 to 72% of their calculated capacity. The authors mention neither the regenerability of active borohydride sites nor the possibility of solution contamination by leached boron derivatives. The ionic nature of attachment of the boron moiety to the polymer raises the question of exchange at cationic sites on the polymer between anionic borane complexes and free alkoxide (from solvent)⁶. Such an exchange could lead to borane contamination in the solution of reduced organic substrate.

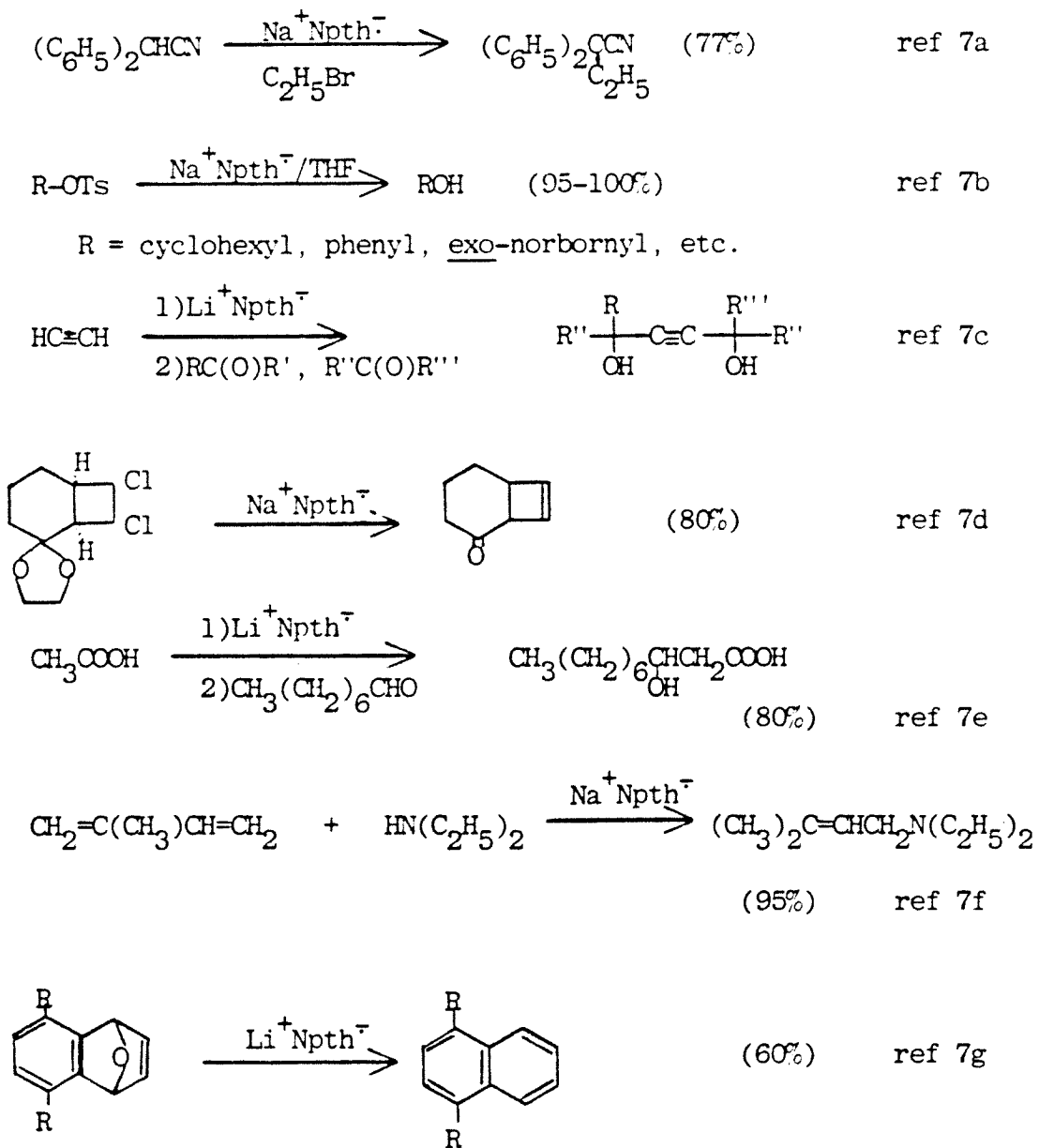
The advantages of a covalently bound sodium (or lithium) naphthalide on a soluble polymer are multiple: 1) Generation and indefinite regeneration of the active reducing agent, sodium (or lithium) naphthalide, is effected by simply stirring a solution of polymer-bound naphthalene over elemental sodium (or lithium)⁸.

Filtration from remaining metal leaves a homogeneous solution of polymeric reducing agent which can then be used *in situ* for the reduction of organic substrates. 2) The traditional problem of naphthalene contamination in reduced organic substrates is obviated by precipitating and filtering the polymer-bound naphthalene from the reaction solution containing the desired organic product. 3) Leaching of naphthalene from the polymer support should not occur since the naphthalene is covalently bound through a carbon-carbon σ bond to the polymer backbone. 4) The soluble naphthalene polymer is amenable to several analytical techniques which insoluble polymers are not qualified for (due to their insolubility) in quantitatively determining its degree of functionalization.

An abbreviated list of reactions for which monomeric sodium or lithium naphthalide is used as a reducing agent is given in Table 1⁷.

Two synthetic routes are feasible for arriving at polymeric naphthalene: functionalization of a preformed commercial polymer with naphthalene moieties or copolymerization of vinyl-naphthalene with another monomer¹¹, both of which will be discussed. Among the methods available for quantitative analysis of resino-naphthalene are UV and esr. The ultraviolet spectra of polystyrene (a comonomer in the proposed synthesis) and polyvinyl-naphthalene exhibit large differences in extinction coefficients at 279 and 320.5 $m\mu$ ⁹. Because of this difference, it is possible to use UV spectroscopy to determine the weight

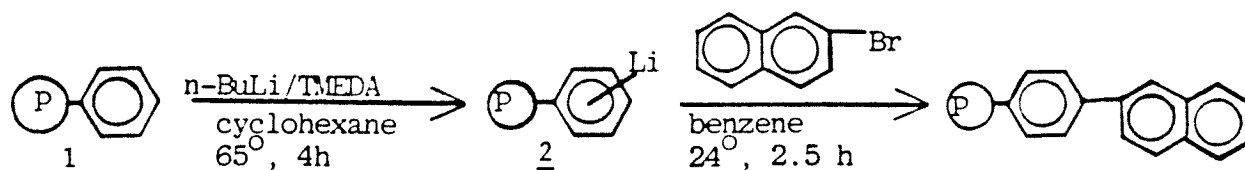
Table I - Reductions with sodium and lithium naphthalide



fraction of each component, styrene and vinyl-naphthalene, in the product polymer¹⁰.

The first proposed synthesis is the less complicated of the two approaches for making poly-naphthalene (Scheme 1).

SCHEME I

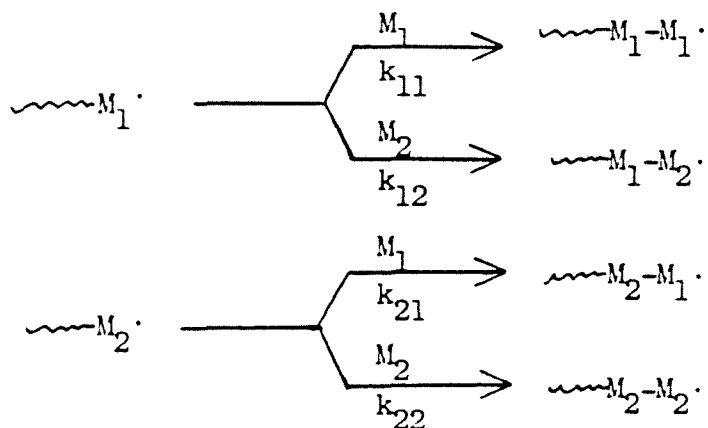


The first step, lithiation of the phenyl rings of polystyrene (1), is well precedented¹². Soluble polystyrene is widely available in a range of polymer chain lengths¹³. Reaction of the phenyllithium polymer 2 with bromonaphthalene¹⁴ should proceed without difficulty^{12c}. Precipitation from the benzene solution with methanol followed by filtration completes the preparation of naphthalene-substituted polystyrene.

The advantage of this route for producing resino-naphthalene is that the details of polymerization technology are left to the suppliers. The drawbacks include limited control over both the extent of functionalization (substitution) and the polar nature of the polymer backbone. For example, 50% substitution of styrene monomers by naphthalene leads to a polymer which is approximately 65% styrene in composition; although not necessarily detrimental, a dominant styrene character will govern the polymer's compatibility with future solvents and substrates¹⁵.

Alternatively, copolymerization of vinyl naphthalene offers greater control in regulating the concentration of naphthalene in the final polymer. In choosing a comonomer, two factors are taken into consideration: polarity and ability to polymerize. First, the hydrophilic/hydrophobic nature of the polymer can be varied according to the composition of the polymer backbone. Incorporation of a nonpolar comonomer such as styrene or 2,3-dimethylbutadiene extends the hydrocarbon nature established by the naphthalene monomer, whereas methyl methacrylate or vinylpyridine comonomers would render a more polar polymeric environment. In anticipation of the wide ranges of functionalities that will be present in organic substrates to be reduced by the naphthalide polymer (cf. Table 1), a styrene or butadiene copolymer avoids the problem of heteroatom involvement arising from the polymer backbone in the reduction process. On the other hand, the solubility of a methyl methacrylate copolymer in polar organic solvents broadens its applicability to systems where more polar solvents are required. Both copolymers are worthy of pursuing.

The second factor, the requirements of a comonomer, is a function of r , e , and Q values. The polymer industry has developed empirical parameters for characterizing the reactivities of monomers toward polymerization¹⁶. Briefly, for a monomer pair M_1 and M_2 , four reaction rate constants are possible (shown for free radical polymerization):



The reactivity ratios, r_1 for M_1 and r_2 for M_2 , are defined as

$$r_1 = k_{11}/k_{12} \quad \text{and} \quad r_2 = k_{21}/k_{22}$$

That is, r is a relative measure of a monomer's preference to react with its own radical or with the other monomer's radical. The Q-e scheme, at best, is an empirical approach at quantifying monomer reactivity. Q_1 describes the resonance effects in monomer and radical M_1 ; e_1 describes the polarity of monomer and radical M_1 . The three parameters are drawn together in the following relation:

$$r_1 = Q_1/Q_2 \exp[-e_1(e_1 - e_2)]$$

(and an analogous expression with the appropriate substitutions for r_2). The practical value these parameters carry is the ability to predict the compatibility of two monomers. Applied to the system at hand, i.e., vinyl naphthalene and a second monomer, the following values for r , e , and Q are provided in the literature^{17,19} (also included below are the parameters of the well-known styrene-divinylbenzene copolymerization for

comparison):

<u>Monomer</u>	<u>r</u>	<u>e</u>	<u>Q</u>
M ₁ = 2-vinylnaphthalene	1.4 +/- 0.1	-0.2	1.35
M ₂ = styrene	0.5 +/- 0.1	-0.8	1.0
M ₁ = 2-vinylnaphthalene	1.0 +/- 0.15	-0.55	1.25
M ₂ = methyl methacrylate	0.4 +/- 0.05	0.4	0.74
M ₁ = styrene	0.65 ¹⁸		
M ₂ = divinylbenzene	0.60 ¹⁸		

note: e and Q are unitless, relative to the arbitrarily chosen styrene reference of e = -0.8 and Q = 1. Values are for 60°C.

The conclusion that 2-vinylnaphthalene should easily copolymerize with either styrene or methyl methacrylate is seen in the favorable reactivity ratios (r) of the two components. That slightly more vinylnaphthalene than styrene will be incorporated in the polymer can also be deduced from these ratios.

Knowing the e and Q values of several monomers which successfully copolymerize with 2-vinylnaphthalene, a list of additional eligible monomers can be drawn up on the basis of similar e and Q values^{20, 21}:

M ₂	e ₂	Q ₂
Styrene	-0.8	1.0
Methyl methacrylate	0.4	0.74
N-phenyl methacrylamide	-0.78	0.85
alpha -Acetoxystyrene	-0.65	0.82
2-Methyl-5-vinylpyridine	-0.58	0.99
4-Vinylpyridine	-0.20	0.82
N,N-Dimethylacrylamide	-0.5	1.08
Dimethyl-4-vinylphenylsilane	-0.04	0.97
CH ₃ (CH ₂) ₄₋₉ methacrylate	-0.32 to -0.14	0.70 to 0.97

These monomers, while having suitable parameters for copolymerization with vinylnaphthalene, must also be considered for their reactivity toward organic substrates that the sodium (or lithium) naphthalide polymer will reduce. As seen from Table 1, esters, ketones, and amines remain intact under reduction conditions. Hence, any of the suggested comonomers are eligible on the basis of inertness. For each pair of comonomers, several trial polymerizations should be performed to determine their reactivity ratios (as outlined in ref 19). If conditions require a polymer consisting totally of carbon and hydrogen, then copolymers of vinylnaphthalene and styrene or butadiene²² fulfill this requirement.

The vinylnaphthalene radical copolymerization should proceed with azobisisobutyronitrile (AIBN, $[(\text{CH}_3)_2(\text{CN})\text{CN}=\text{N}]_2$) as initiator at 60° in benzene.

In summary, a soluble polymer containing naphthalene units is proposed as an advantageous and regenerable reducing agent for synthetic chemistry. Two methods for synthesizing the polymer are proposed: naphthalene functionalization of a pre-existing commercial polymer or copolymerization of 2-vinylnaphthalene. The product naphthalene polymer is converted to the active reducing agent, sodium or lithium naphthalide radical anion, by stirring over elemental metal. The characteristic deep green color of monomeric sodium naphthalide should carry over to the polymeric analogue. Once used, the polymer is quantitatively

removed from reaction mixtures by precipitation, leaving behind a solution of only organic substrate. The shelf life of polymeric naphthalene should be indefinite. Regeneration of the active sodium (or lithium) naphthalide moieties is achieved from a solution of the polymer and sodium (or lithium) metal prior to its use.

REFERENCES

- C.C. Leznoff, *Chem Soc. Rev.*, **3**, 65 (1974).
 - J.I. Crowley and H. Rapoport, *Accts. Chem. Res.*, **9**, 135 (1976).
 - E.C. Blossey and D.C. Neckers, Eds, 'Solid Phase Synthesis', Halsted Press, New York, 1975.
 - C.G. Overberger and K.N. Sannes, *Angew. Chim., Int. Ed. Eng.*, **13**, 159 (1974).
- N.M. Weinshenker, G.A. Crosby, and J.Y. Wong, *J. Org. Chem.*, **40**, 1966 (1975).
 - H.W. Gibson and F.C. Bailey, *JCS Chem. Comm.*, 815 (1977).
- LiAlH_4 is effective in reducing the corresponding homogeneous tin products to active tin hydride, cf. ref 2a and refs 14 and 22 therein.
- It is questionable whether BH_4 was the sole species coordinated to the polymer since NaBH_4 reacts with water to evolve hydrogen.
- H.C. Brown, 'Hydroboration', Benjamin, Inc., New York, 1963,

p.242; H.C.Brown, 'Organic Synthesis via Boranes', Wiley Interscience, New York, 1975, p.260.

6. D.C.Wigfield and R.W.Gowland, Tet. Lett., 3373 (1976).
7. Examples are extracted from Fieser & Fieser, Reagents for Organic Synthesis, vols 1-6, Wiley, New York, 1967- .
 - a. L.Horner and H.Gusten, Ann **652**, 99 (1962).
 - b. W.D.Closson, P.Wriede, and S.Bank, J. Am. Chem. Soc., **88** 1581 (1966).
 - c. S.Watanabe, K. Suga, and T.Suzuki, Chem. Ind., 1489 (1968).
 - d. C.G.Scouten, F.E.Barton, Jr., J.R.Burgess, P.R.Story, and J.F.Gaust, Chem. Comm., 78 (1969).
 - e. S. Watanabe, K.Suga, T.Fujita, and K.Fujiyoshi, Chem. Ind., 1811 (1969).
 - f. T.Fujita, K.Suga, and S.Watanabe, Chem. Ind., 231 (1973).
 - g. S.B.Polovsky and R.W.Franck, J. Org. Chem., **39**, 3010 (1974).
8. This is analagous to the method used for generation of monomeric sodium naphthalide. See, for example, H.E.Zieger, I.Angres, and L.Maresca, J. Am. Chem. Soc., **95**, 8201 (1973).
9. C.Price, B.Halpern, and S.Voong, J. Polymer Sci., **11**, 575 (1953).
10. The process for computing the weight fraction of polystyrene in styrene-vinylnaphthalene copolymer is as follows:

Given: the extinction coefficients of polystyrene (0.13 l/g-cm at 279 μ and 0.03 l/g-cm at 320.5 μ),
 : the extinction coefficients of poly- β -vinylnaphthalene (30.0 l/g-cm at 279 μ and 2.29 l/g-cm at 320.5 μ),
 : the concentration of the copolymer in g/l in the sample cell,
 : sample cell path length,
 : the UV spectrum of the copolymer with the total extinction coefficient (E_{tot}) at 279 μ and 320.5 μ ,

Then the weight fraction of polystyrene (X) is given by:

$$E_{tot}(279\mu) = (0.13)X + (1-X)30.0$$

and again by

$$E_{tot}(320.5\mu) = (0.03)X + (1-X)(2.29).$$

11. A polymer made solely from vinylnaphthalene monomers would lead to such a high density of naphthalene that steric and electronic problems are anticipated in subsequent reductions and oxidations. However, its potential as a conductor is worthy of consideration.

- 12.a. C.H.Brubaker et al., J. Am. Chem. Soc., **97**, 2128 (1975).
 b. N.M.Weinshenker, G.A.Crosby, and J.Y.Wong, J. Org. Chem., **40**, 1966 (1975).
 c. M.R.Farrall and J.M.Frechet, J. Org. Chem., **41**, 3877 (1976).
13. See, for example, the catalogues of BioRad Laboratories, Poly-science Inc., and Aldrich Chemical Corp.
14. 1- and 2-bromonaphthalene are available from Aldrich Chemical Company.
15. N.Takaishi, H.Imai, C.Bertelo, and J.Stille, J. Am. Chem. Soc., **100**, 264 (1978) and refs 11-19 therein.
16. Suggested texts and references:
 a. G.Odian, 'Principles of Polymerization', McGraw Hill Co., New York, 1970.
 b. W.R.Sorenson and T.W.Campbell, 'Preparative Methods of Polymeric Chemistry', Interscience Publishers, New York, 1968.
 c. 'Polymer Handbook', J.Brandrup and E.Immergut, Eds., Interscience Publishers, New York, 1966.
17. See ref 16c, Tables on ppII-270, 358, and 359. See also ref 9.
18. r_1 is the monomer reactivity ratio of styrene relative to vinyl in divinylbenzene, and r_2 is the monomer reactivity ratio of the vinyl group in divinylbenzene relative to styrene.
19. r_1 and r_2 were determined experimentally by analyzing the percent composition of polymers derived from seven different ratios of monomers. Given M_1 = mole fraction of comonomer 1 and M_2 = mole fraction of comonomer 2, then the copolymerization equation (derived on p.367 of ref 16a from equilibrium expressions and steady state assumptions) is:

$$\frac{d[M_1]}{d[M_2]} = \frac{[M_1] (r_1[M_1] + [M_2])}{[M_2] ([M_1] + r_2[M_2])}$$

where $d[M_1]/d[M_2]$ is the ratio of rates at which the two monomers enter the polymer (= copolymer composition).

r_1 and r_2 are calculated by plotting the rearranged copolymerization equation as a straight line with r_1 as the abscissa and r_2 as the ordinate, and obtaining their respective intercepts. Q and e for 2-vinylnaphthalene were derived using previously known Q and e values for styrene and methyl methacrylate and the above-determined r values.

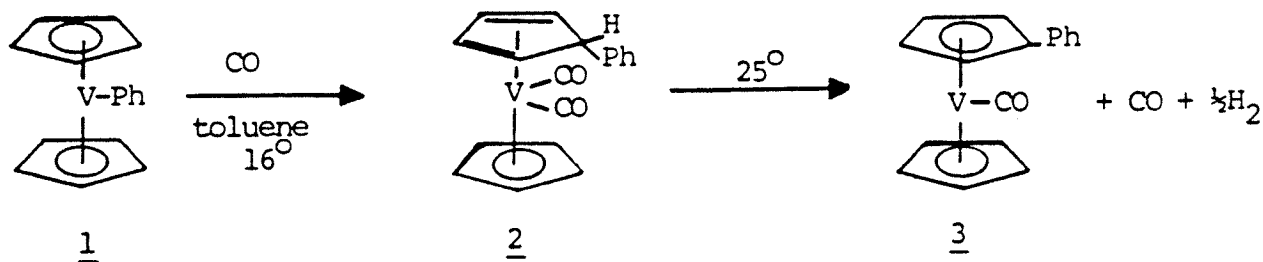
20. See ref 16c, Tables on pp. II-340-362.
21. Q and e values can vary considerably for a single monomer, depending on its comonomer (an inherent deficiency in the Q - e scheme). Not only are steric factors disregarded in this scheme, but assigning the same e value to a monomer and its corresponding radical is inaccurate.
22. A vinyl naphthalene-butadiene copolymer is cited by C.E. Schildknecht in 'Vinyl and Related Polymers', John Wiley and Sons, New York, 1952, p.160, for use in tire manufacture (PB 11,193 and PB 16,714).

PROPOSITION 4 : Migrations of Alkyl Ligands to Cyclopentadienyl Ligands in Organometallic Complexes - A Literature Overview, Mechanistic Possibilities, and Substantiating Experiments.

Alkyl ligands in some organometallic complexes have been known to 'migrate' from the metal to a second ligand in the complex: $R-M-L \longrightarrow M-L-R$. One of the most frequently noted of these rearrangements is migration of an alkyl group to a metal-bound CO^1 , creating an acyl ligand (also referred to as CO 'insertion' into a metal-alkyl bond): $RM(CO) \longrightarrow M(COR)$. Less widely observed, yet now backed by numerous examples², is the migration of an alkyl ligand to a cyclopentadienyl (Cp) ligand: $RM(C_5H_5) \longrightarrow M(C_5H_4R)$. This too can be viewed as a net insertion of the cyclopentadienyl carbon into a metal alkyl bond. However, in most cited cases, in addition to an alkyl group's having 'moved' from metal to ring, the net transformation also involves loss of a hydrogen from the cyclopentadienyl ring. To date, a proposed intermediate for the alkyl migration, $M(C_5H_5R)$, has been observed only twice^{2e,g}. This proposal focuses on mechanisms and supporting experiments for the migration of an alkyl to the cyclopentadienyl ring in organometallic compounds.

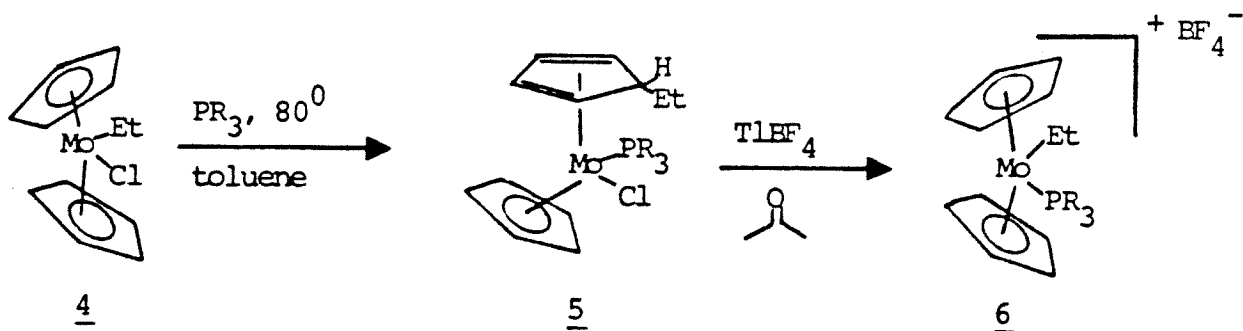
In some CpMR systems, migration of an alkyl group to the cyclopentadienyl ring has been observed to require assistance from external ligands. Fachinetti^{2e} and coworkers treated $Cp_2V(C_6H_5)$ with CO to yield a vanadocene analogue which contained

a phenyl-substituted Cp:

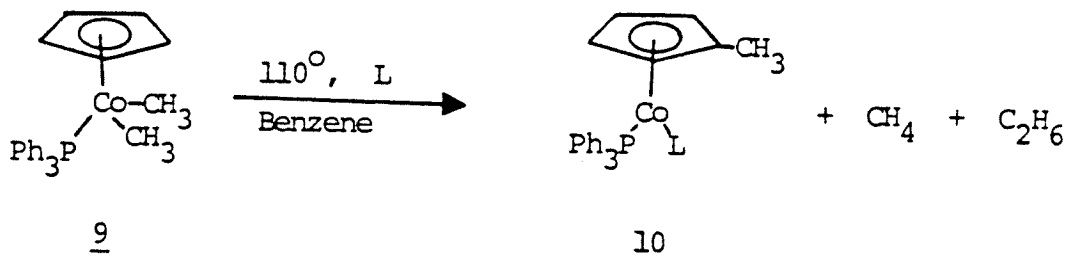


The assignment of the **endo** position for the phenyl group on the cyclopentadiene was on the basis of an **exo**-cyclopentadienyl C-H band³ in the IR spectrum of **2** (for the cyclopentadienyl hydrogen geminal to the phenyl). Compound **2** rapidly evolved CO (1 eq) and H₂ (1/2 eq) at room temperature to yield **3**.

Another ligand-assisted alkyl-to-Cp migration was reported by Benfield and Green²⁹. It too produces an isolable intermediate **5** in which the Cp ligand has five hydrogen atoms in addition to the newly acquired alkyl:

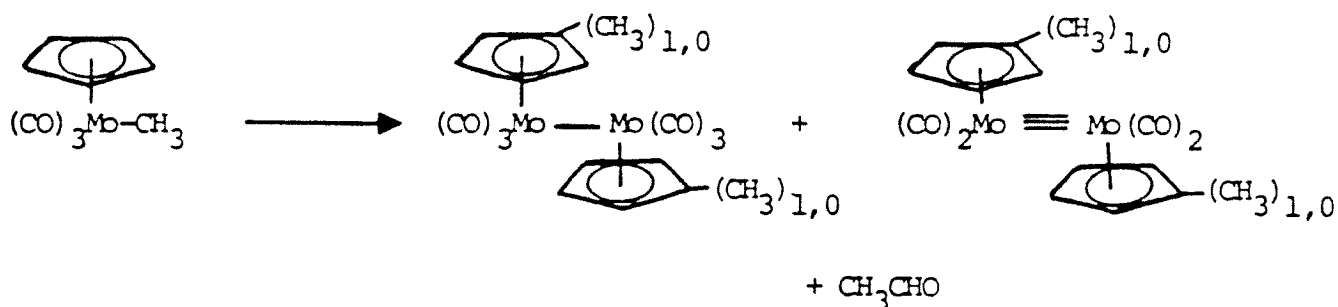


A unique feature of Benfield and Green's system is that the migration was observed to be 'reversible'; treatment of **5** with



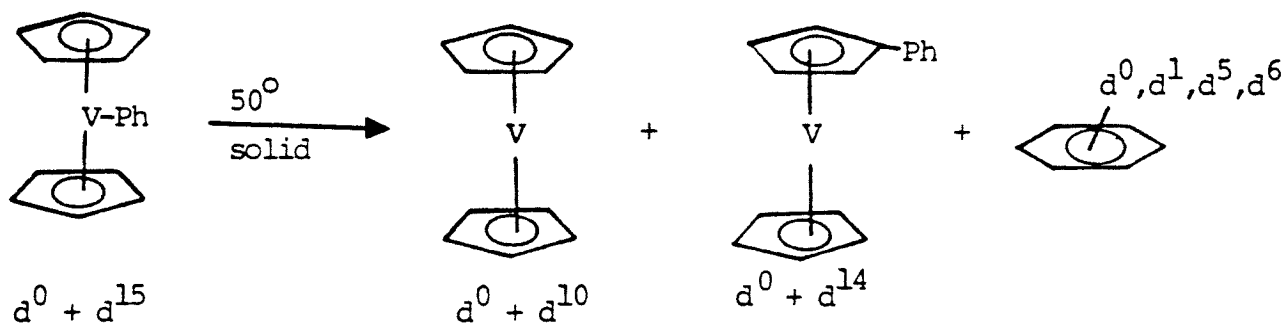
Methane produced in this way from d^{21} -9 (perdeuterated methyl and PPh₃ groups) in deuterated solvent was mostly CD₃H, implicating the C₅H₅ ligand as the source of methane's fourth hydrogen.

A second example of ring substitution from our labs^{2h} arose from a mild solution thermolysis:



Thermolyses in which either the methyl or the Cp were labelled with deuterium indicated that the aldehydic hydrogen was being provided at least in part by the Cp ring.

Finally, Boekel and coworkers^{2d}, through use of isotopic labelling, present informative results from an alkyl vanadocene system:



(no reported yields)

From the location of deuterium in the products, it can be postulated that alkyl migration is intramolecular, whereas benzene formation can occur intermolecularly.

The existence of one unifying mechanism for the above seven systems is unlikely. In proposing experiments to test suggested mechanisms, consistent results from one system to the next are not expected, owing to the wide range of metals and ligands involved. In fact, differing results from the various systems might be due to the relative predominances of kinetic and thermodynamic effects. That is, lack of consistency in results from one system to the next might be a case of a common mechanism masked by different K_{eq} 's and rate constants. With these reservations, it is still deemed worthwhile to probe any number of these systems for mechanistic information on alkyl migration.

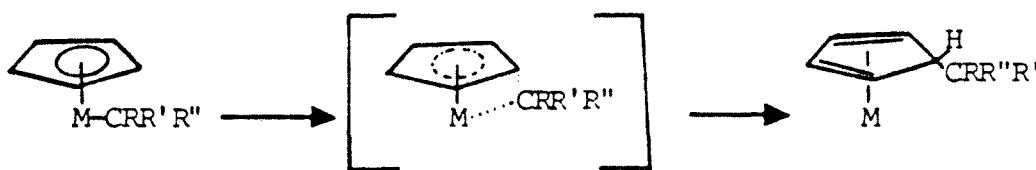
The net transformation that occurs in moving an alkyl to Cp can be viewed as a reductive elimination from the metal:

$RM^n(C_5H_5) \longrightarrow M^{n-2}(C_5H_5R)$. Four (at least) major alternative mechanisms are seen for moving an alkyl to the Cp ring:

A) concerted intramolecular migration; B) homolysis to a radical pair ($M\cdot + R\cdot$) followed by cage attack by $R\cdot$ on Cp (cage disproportionation); C) homolysis to a radical pair ($M\cdot + R\cdot$),

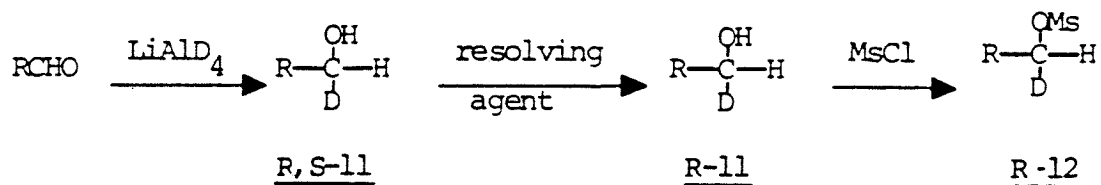
cage escape, and subsequent free radical attack by $R\cdot$ on a Cp ligand; and D) a bimolecular mechanism in which two metal centers are involved in the transition state for alkyl transfer. Of these four alternatives, no single pathway is expected to predominate; a combination of two or more probably determine final product distributions.

Proposed pathway (A), concerted intramolecular migration, should occur with inversion of stereochemistry at the migrating carbon, viz



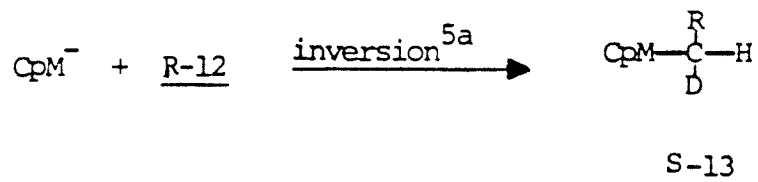
For total inversion to have occurred, two assumptions about the migrating process can be made: that migration proceeded endo (as two researchers have observed^{2e,g}) and that no ring exchange or racemization of the tetrahedral carbon took place. In order to test for stereospecificity in the migration, the metal starting complex, $CpMC^*RR'R''$, would have to be synthesized from an optically active alkyl precursor in a stereochemically 'faithful' reaction. The following reaction schemes are suggested.

Synthesis of the alkylating agent:

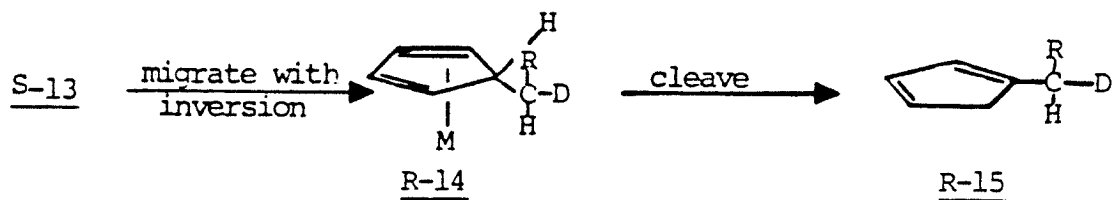


R = CH₃, CMe₃, or Ph

Synthesis of the starting metal complex:



The stereoselectivity of the migration could be checked by cleavage of the Cp ligand from the metal complex:



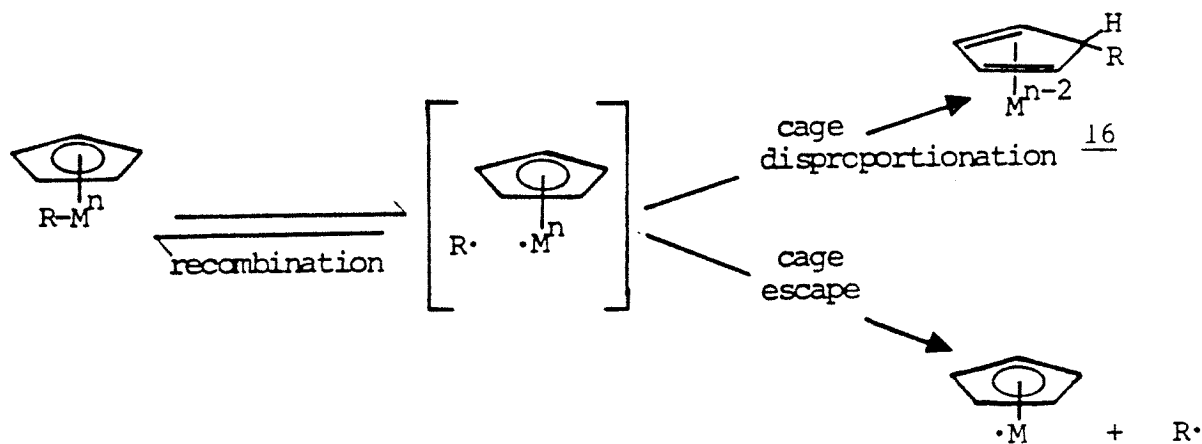
R-15 could be compared with an independently synthesized model:



Stereochemical purity in the cleaved Cp ligand would serve as strong evidence for a concerted alkyl migration⁶. While these

syntheses appear straightforward on paper, syntheses of optically active substrates and their subsequent stereospecific reactions are often complicated and 'challenging', especially in organometallic systems⁵.

The next two mechanistic possibilities (B & C) both arise from metal-carbon bond homolysis and will be treated together. There has been much interesting discussion and experimental evidence recently on homolysis of transition metal-alkyl bonds⁷. The convincing evidence of Halpern et al.^{7a} for homolysis of metal-alkyl bonds to produce alkyl and metal-centered radicals facilitates proposing that the first step in alkyl migration might be homolysis to a radical pair, $M^{\cdot} + R^{\cdot}$. This pair can either remain within a cage or escape to two free radicals. Should they take the former path, two (at least) reactions can ensue: recombination to form the original molecule or attack by the alkyl radical on another part of the metal complex (disproportionation), e.g., attack on the Cp ligand to yield a new alkyl-substituted cyclopentadiene on the metal:



The same product 16 could result from attack by free radical R \cdot on an unsubstituted Cp⁸; however, such an attack would probably proceed *exo* for steric reasons^{3c}. Whether alkyl substitution is occurring via free radicals or cage recombination is easily probed by a crossover experiment^{2d}: tagging both the alkyl and Cp ligands of the metal complex (with ²H, ³H, ¹³C, or ¹⁴C) and allowing it to react in the presence of its unlabeled analogue. This crossover reaction is valid only if starting material ligands are not labile and do not exchange^{2a}. Mass spectral analysis of the products should reveal if the two labeled ligands have remained confined to the same molecule, i.e., that the migration has proceeded intramolecularly.

If instead scrambling of labels has occurred, intermolecular interaction can be assumed, having possibly proceeded via mechanism (C) or (D): free radical attack or a dimetallic intermediate (or transition state). These two alternatives should be experimentally distinguishable. If the scrambling has resulted from free radical attack, it is likely that other products of free radicals will be observed: R-R, M-M, R-H, etc. An effective way to test for free radicals is by addition of a radical trap or initiator to the reaction medium. Nitrosodurene is an effective scavenger⁹ in this way of both metal and alkyl radicals, and the resulting aminyloxides are characterized by ESR^{9b}. The effect of radical chain initiators, e.g., azoisobutyronitrile (AIBN), on reaction rates and product yields

can also support the involvement of free radicals in the studied reactions. In fact, it is possible^{3d} that primary reaction products can themselves homolyze, producing radicals which then catalyze the reactions suspected of proceeding via radical mechanisms (autocatalysis). Therefore, the product metal dimers which often result in the above-cited alkyl migrations might also serve as radical initiators in reactions being tested for radical mechanisms.

Variation of the alkyl ligand can aid in establishing the presence of radicals. For example, R itself can contain a moiety which is capable of reacting in an intramolecular fashion with the radical generated on the **alpha**-carbon, by cyclizing or ring-opening. Several examples of such R ligands are 1-hexenyl¹⁸, allyloxyethyl¹⁹, or methylcyclopropylcarbonyl²⁰. Otherwise, variation of the alkyl ligand can also serve to stabilize (or destabilize) the incipient R \cdot , this stabilization being reflected in reaction rates and product yields. For example, a benzyl radical's being ~ 35 kcal mole⁻¹ more stable than a phenyl radical¹⁰ might result in faster reaction rates or more products from radical precursors from a MCH₂Ph complex than from a MPh complex under similar conditions. In experiments of this kind, however, caution must be taken to differentiate between thermodynamic (e.g., radical stability) and kinetic (e.g., reaction rate) control. Lack of response in changing the nature of the alkyl ligand does not necessarily imply that the reaction does not involve radicals; rather, it most likely indicates that

the rate-limiting step does not involve radicals.

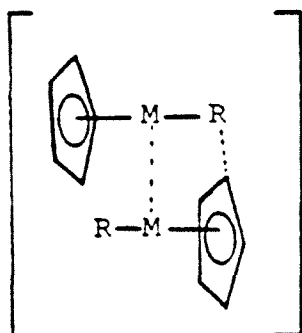
Thermolysis carried out in an ESR probe would provide convincing evidence for the presence of radical species¹¹. Using either literature values for g^{9b} , $12c$, or ones derived from independently generated standards of the organic^{12c} and metal-centered^{9b} radicals, quantitative information on the relative predominance of radical species in the studied reaction could also be provided by ESR.

Another spectrometric method of determining radicals is NMR-monitored CIDNP (Chemically Induced Dynamic Nuclear Polarization)¹¹. CIDNP offers the advantage (over esr) that radical cage escape processes can be differentiated from radical cage combination. Although CIDNP of organometallics is relatively new and the number of literature examples are few¹³, in principle it is capable of providing useful information on degradative pathways for metal complexes. Briefly, CIDNP is observed as enhanced absorptions or emissions (or a combination of the two) in the NMR spectrum of products arising from reactions which involve a radical pair. These spectral features arise from the dependence of the electronic spin state on the nuclear spin states of the coupled nuclei in the radical pair. The method can be used to distinguish: singlet from triplet radical pairs (μ), cage combination from cage escape products (E), the radical pair's relative g -values (Δg), and the sign of the electron-nuclear coupling constant (a). For the purpose

of probing the mechanism by which an alkyl ligand moves to the Cp ligand, ^{13}C or ^1H CIDNP of the migrating alkyl is hoped to provide a distinction between cage combination and free radical attack (mechanisms B and C). Given Kaptein's formula¹⁵ for CIDNP net effects, $\Gamma_n = \mu E \Delta g a$, a prediction for the NMR spectrum of the alkyl ligand can be made. For the thermally induced homolysis, μ (singlet/triplet) can be assigned a negative sign (singlet precursor)^{13b}; the electron-nuclear coupling constant parameter, a , will be negative for a carbon centered radical and positive for the proton attached to the carbon radical¹⁶; and the difference in g values between the metal-centered and alkyl radicals, $g_{\text{alkyl}} - g_{\text{metal}}$, can be postulated as negative, based on previous literature reports^{13b, 17}. Whether net enhancement or net emission will be observed depends then on E , the symbol for cage escape/cage combination. According to Kaptein's formula and the sign assignments made above, $\Gamma_n = \mu E \Delta g a = (-)(+)(-)(-) = (-)$, the proton NMR of the migrating alkyl should show either net emission if substitution is occurring via cage combination or conversely net absorption should the path involve free radical $\text{R}\cdot$. The ^{13}C NMR should show the opposite effect (opposite sign in parameter a). Naturally, lack of any CIDNP effect could imply the absence of a radical mechanism.

Finally, mechanism (D) (a binuclear transition state for alkyl transfer) could be tested against a concerted unimolecular mechanism (A) by multiple dilution experiments (in addition to evidence from crossover experiments presented earlier). Running

the experiment under high dilution should disfavor the formation of binuclear species (for entropic reasons), reflected in reaction rates or in a redistribution of products arising from competing pathways. Such a transition state,



might account for anomalously low barriers^{13b} or high selectivity^{2d} for M-R bond dissociation observed in other systems.

In summary, an overview of literature reports of alkyl migration to cyclopentadienyl ligands in organometallic complexes has been presented. Proposed are mechanistic possibilities and experiments designed to distinguish between them. The mechanisms include concerted, radical, and bimolecular pathways. The methods include isotopic labelling, substituent effects, radical detection (ESR and CIDNP), and dilution effects.

REFERENCES

1. For a review of CO insertion in organometallic complexes, see F. Calderazzo, *Angew. Chem. Int. Ed. Engl.*, **16**, 299 (1977).
2.
 - a. E.R.Evitt, Ph.D. Thesis, California Institute of Technology, Pasadena, CA, 1980.
 - b. H.Werner and W.Hoffman, *Angew. Chem. Int. Ed. Engl.*, **17**, 464 (1978).
 - c. H.Werner and W.Hoffman, *ibid*, **16**, 794 (1977).
 - d. C.P.Boekel, A.Jelsma, J.H.Teuben, and H.S.de Liefde Meijer, *J. Organomet. Chem.*, **136**, 211 (1977).
 - e. G.Fachinetti, S.DelNeso, and C.Floriani, *J. Chem. Soc. Dalton*, 203 (1976).
 - f. C.U.Pittman and R.F.Fellis, *J. Organomet. Chem.*, **72**, 399 (1974).
 - g. F.W.Benfield and M.L.H.Green, *J. Chem. Soc. Dalton*, 1324 (1974).
 - h. A.N.Nesmeyanov, L.G.Makarova, N.A.Ustynyuk, and L.V.Bogatyreva, *J. Organomet. Chem.*, **46**, 105 (1972).
 - i. A.N.Nesmeyanov, Y.A.Chapovski, B.F.Lokchin, A.V.Kisin, and L.G.Makarova, *Dokl. Akad. Nauk., SSSR*, **171** 637 (1969).
 - j. J.A.McCleverty and G.Wilkinson, *J. Chem. Soc.*, 4096 (1963).
 - k. J.M.Huggins, Ph.D. Thesis, California Institute of Technology, Pasadena, CA, 1981.
3. **Exo**-cyclopentadienyl C-H IR bands are cited frequently in the papers of ref 2. For literature sources, see
 - a. D.A.White, *Organomet. Chem. Rev.*, **A3**, 497 (1968).
 - b. D.H.Bird and M.R.Churchill, *Chem. Comm.*, 777 (1967).
 - c. P.M.Treichel and R.L.Shubkin, *Inorg. Chem.*, **6**, 1328 (1967).
 - d. T.H.Whitesides and J. Shelly, *J. Organomet. Chem.*, **92**, 215 (1975).
 - e. R.F.Borch, M.D.Bernstein, and H.D.Durst, *J. Am. Chem.Soc.*, **93**, 2897 (1971).
 - f. R.B.King, M.B.Bisnette, and A.Fronzaglia, *J. Organomet. Chem.*, **4**, 256 (1965).

For **endo**-cyclopentadienyl C-H IR bands, see ref 3c and:

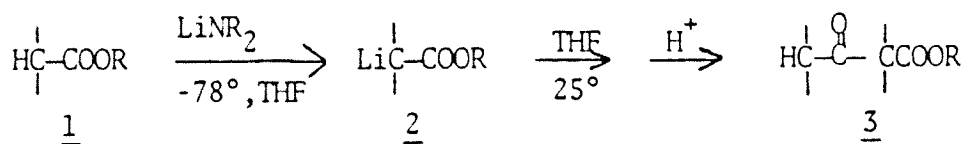
 - g. A.Davison, M.L.H.Green, and G.Wilkinson, *J. Chem. Soc.*, 3172 (1961).
 - h. M.R.Churchill and R.Mason, *Proc. Roy. Soc. (London)*, **A273** (1961).
 - i. M.L.H.Green, L.Pratt, and G.Wilkinson, *J. Chem. Soc.*, 3753 (1959).
4. When extra PPh_3 was added to the reaction, the yield of methane increased and that of ethane decreased^{2a}.

5. a. R.G. Pearson and P.E. Figdore, *J. Am. Chem. Soc.*, **102**, 1541 (1980).
 b. D. Milstein and J.K. Stille, *J. Am. Chem. Soc.*, **101**, 4981 (1979).
 c. P.L. Bock, D.J. Boschetto, J.R. Rasmussen, J.P. Demers, and G.M. Whitesides, *ibid*, **96**, 2814 (1974).
 d. P.L. Bock and G.M. Whitesides, *ibid*, **96**, 2826 (1974).
6. Metal-alkyl bond homolysis followed by nearly instantaneous (i.e., before R[•] can tumble) attack by R[•] on the **endo** face of the Cp ring could also result in inversion at the asymmetric carbon. The experiments designed to test for radicals (*vide infra*) should be able to differentiate between these two possibilities.
7. a. J. Halpern, *Pure Appl. Chem.*, **51**, 2171 (1979) and refs therein
 b. J.K. Kochi, *ibid*, **52**, 571 (1980) and refs therein.
 c. J.S. Bradley, D.E. Conner, D. Dolphin, J.A. Labinger, and J.A. Osborn, *J. Am. Chem. Soc.*, **94**, 4043 (1972).
 d. A.V. Kramer, J.A. Labinger, J.S. Bradley, and J.A. Osborn, *ibid*, **96**, 7145 (1974).
 e. D.J. Cardin, M.F. Lappert, and P.W. Lednor, *J. Chem. Soc. Chem. Comm.*, 350 (1973).
 f. N.G. Hargreaves, R.J. Puddephatt, L.H. Sutcliffe, and P.J. Thompson, *ibid*, 861 (1973).
 g. P.J. Krusic, P.J. Fagan, and J. SanFilippo, *J. Am. Chem. Soc.*, **99**, 250 (1977).
8. Later CIDNP experiments proposed to test for cage radicals should distinguish between these two options.
9. a. The necessary controls must be run to determine that the nitroxyl radical itself does not induce reaction.
 b. A. Hudson, M.F. Lappert, P. Lednor, and B. Nicholson, *JCS Chem. Comm.*, 966 (1974).
 c. see also L.M. Lawrence and G.M. Whitesides, *J. Am. Chem. Soc.*, **102**, 2493 (1980) and ref 10 therein.
10. $H_f^\circ (\text{Ph}^\bullet) = 80.8 \text{ kcal/Mol}$
 $H_f^\circ (\bullet\text{CH}_2\text{Ph}) = 44.6 \text{ kcal/Mol}$
 D.M. Golden and S.W. Benson, *Chem. Rev.*, **69**, 125 (1969).
11. For examples of thermally generated metal radicals, see refs 3d, 9b, 7a and relevant refs therein, and
 a. R.D. Adams, D.E. Collins, and F.A. Cotton, *J. Am. Chem. Soc.*, **96**, 749 (1974).
 b. H.D. Murdock, E.A. Lucken, *Helv. Chim. Acta.*, **47**, 1517 (1964).
 c. W. Hieber and W. Freyer, *Chem. Ber.*, **92**, 1765 (1959); *ibid*, **93**, 462 (1960).
 d. T. Madach and H. Wahrenkamp, *Z.f. Naturforschung*, **33b** 1301, (1978).

- e. J.P.Fawcett, A.J.Poe, and M.V.Twigg, *J. Organomet. Chem.*, **51**, C17 (1973).
12. The reader is referred to the following extensive reviews for more information on CIDNP:
- 'Chemically Induced Magnetic Polarization', L.T.Muus, P.W.Atkins, K.A.McLauchlin, and J.B.Pedersen, Eds., D.Reidel Publ. Co., Boston, 1977.
 - G.L.Closs, *Adv. in Mag. Resonance*, **7**, 157 (1974).
 - R.Kaptein, *Adv. in Free Radical Chemistry*, **5**, 319 (1975).
 - A.R.Lepley and G.L.Closs, 'Chemically Induced Magnetic Polarization', John Wiley, New York, 1973.
13. a. B.J.Shaart, H.W.Bodewitz, C.Blomberg, and J.Bickelhaupt, *J. Am. Chem. Soc.*, **98**, 3712 (1976).
b. R.L.Sweany and J. Halpern, *ibid*, **99**, 8335 (1977).
c. A.V.Kramer and J.A.Osborn, *ibid*, **96**, 7832 (1974).
d. P.W.VanLeeuwen, R.Kaptein, R.Huis, and C.F.Roobeck, *J. Organomet. Chem.*, **104**, C44 (1976).
14. Theoretically, CIDNP should be observed in the NMR spectrum of the metal atom as well. With the appropriate technology (i.e., a tunable NMR probe), this method could be extended to the NMR of metals, given an appreciable natural abundance of NMR-detectable isotopes and an appropriately long nuclear spin-lattice relaxation time.
15. R.Kaptein, *J. Chem. Soc. D*, 732 (1971).
16. T.H.Lowry and K.S.Richarson, 'Mechanism and Theory in Organic Chemistry', Harper and Row, New York, 1976, p.465.
17. a. H.Fischer in 'Free Radicals', J.K.Kochi, Ed., Wiley, New York, 1973, vol 2, p.453.
b. H.R.Ward, *ibid*, vol 1, chapter 8.
c. see also ref 9b and ref 3 therein.
18. D.Lal, D.Griller, S.Husband, and K.U.Ingold, *J. Am. Chem. Soc.*, **96**, 6355 (1974).
19. A.L.J.Beckwith, I.Blair, and G.Phillipon, *ibid*, **96**, 1613 (1974).
20. R.J.Kinney, W.D.Jones, and R.G.Bergman, *ibid*, **100**, 635 (1978).

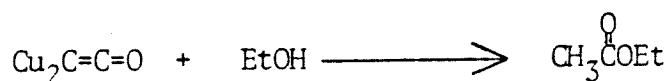
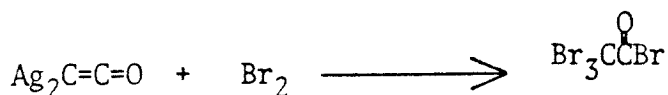
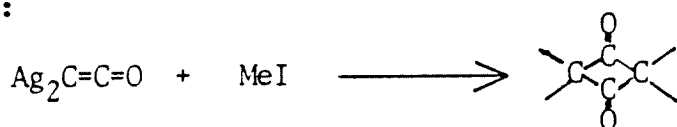
PROPOSITION 5 : β -Keto Esters from Ester Enolates: Mechanism and Supporting Experiments.

Ester enolates **2** differ markedly from ketone or aldehyde enolates in their tendency to self condense¹, ultimately yielding β -keto esters **3**:

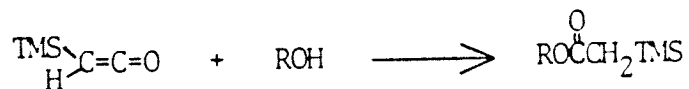


The mechanism of formation of **3** has been difficult to elucidate owing to the fleeting nature of reaction intermediates. In this proposal, a mechanism involving a ketene intermediate is presented, together with experiments designed to observe and trap the ketene.

Several interesting examples of ketene intermediates are given below. The reaction of silver and copper ketenides with electrophiles² presumably proceeds through a ketene intermediate in which the attacking electrophile has replaced the two metal atoms (e.g., $\text{Br}_2\text{C}=\text{C}=\text{O}$ for the case where the electrophile is Br_2):

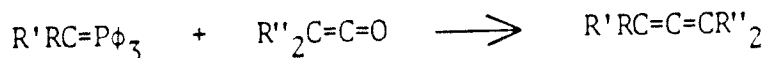


The trimethylsilyl derivative of a ketene, Me_3SiCHCO (4), has served as a reactive yet reasonably stable intermediate in the acylation of alcohols³:



A mechanism involving nucleophilic attack on the central ketenic carbon, followed by protonation at the alpha position, is supported by the catalytic effect of added BF_3 etherate.

Allenes have been afforded from the combination of triphenylphosphonium ylids and ketene^{4,5}:



$\text{R} = \text{H}, \text{Me}, \phi$

$\text{R}' = \text{Me}, \text{COOEt}, \text{COMe}, \text{CO}\phi$

$\text{R}'' = \text{H}, \phi$

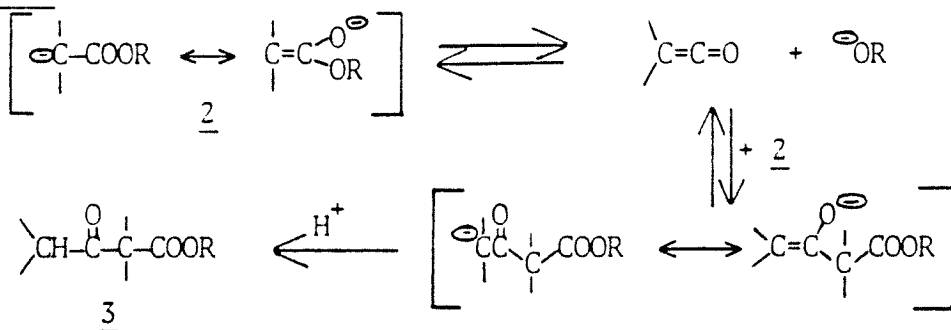
Isolation of a stable intermediate 5 (below) as a crystalline solid in this Wittig reaction confirmed the mechanism of nucleophilic attack on the central carbon atom of the ketene by the electronegative carbon of the Wittig reagent, aided by electronic interaction between the resulting phosphorous and oxygen:



Ester enolates are generated⁶ by addition of base (e.g., lithium amide) to a THF solution of the ester maintained at -78° .

The ester enolate thus formed is indefinitely stable at -78° . Warming to room temperature, followed by quenching with acid⁷, produces condensation product 3. A possible reprotonation of the enolate by HNR_2 to give ester which then condenses with a molecule of enolate to give the observed product 3 cannot account for all of 3 since solutions of enolate which have been separated from amine^{7b} also yield some condensation product 3. An alternative mechanism for the formation of condensation product 3 from the ester enolate 2 is given in Scheme 1.

Scheme I

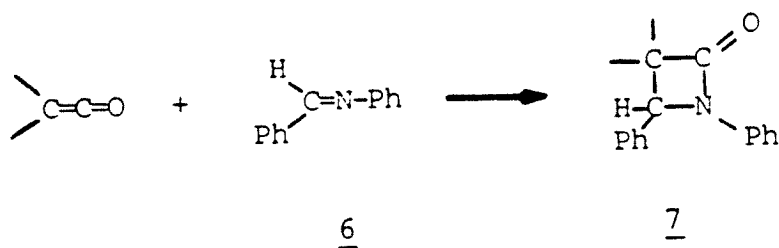


Support for the proposed ketene intermediate should result from the following experiments.

Low temperature IR spectra taken during the conversion of 2 to 3 should contain bands corresponding to the ketene^{8,9} at $\sim 2100 \text{ cm}^{-1}$. The reaction should be performed by slowly warming a solution of 2 in a low temperature IR cell from -78° to room temperature (as in the literature preparation^{6,7} of 3), and monitoring for disappearance of the enolate bands of 2, appearance of ketene bands (*vide supra*), and finally appearance of product 3's β -keto ester bands (on addition of acid). A

similar experiment could be carried out in a variable temperature NMR probe as well, monitoring the ^{13}C spectrum for chemical shifts accompanying the transitions from enolate 2 to ketene to β -dicarbonyl 3.

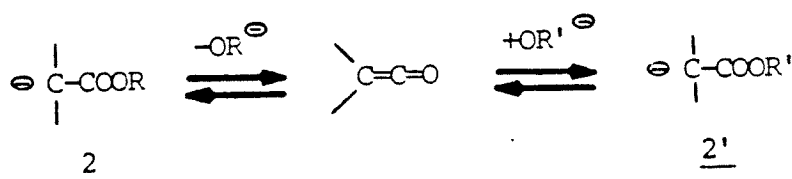
Additional evidence for a ketene intermediate can be obtained by chemical trapping. Addition of an imine acceptor 6 (e.g., benzyl aniline) to solutions containing ketene should result⁸ in formation of the [2 + 2] adduct, 7 (the stereochemistry of a similar addition has been found to be a function of the order of addition of the reactants^{8b}):



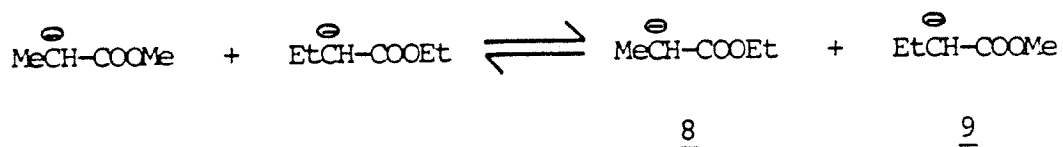
The reaction could be performed under the same conditions as the previously described reaction, i.e., slowly warming a solution of 2 and 6 from -78° to room temperature in an IR cell or NMR probe. In this way, ketene would be generated in the presence of the imine acceptor 6, and the appearance of adduct 7 could be monitored spectrometrically. The identification of 7 should be completed by its isolation from the reaction mixture and thorough characterization. Ample information on compounds of its general type is available in the β -lactam literature.

Another means for probing ketene formation involves reversal of the equilibrium which led to its formation. Addition of an

alkoxide to a solution suspected of containing ketene should result in production of enolate ester 2':



The new enolate ester 2' could be detected by above-described means. This proposed initial equilibrium between enolate 2 and ketene could also be 'observed' by performing a crossover experiment between two different enolates:



Detection of 8 and 9 would support the initial reversible equilibrium in ketene formation from enolate 2 (Scheme 1).

In summary, a mechanism involving ketene formation is presented to account for the formation of B-keto esters from ester enolates. The proposed experiments to support this mechanism include variable temperature spectroscopy, chemical trapping, and substituent scrambling studies.

REFERENCES

1. D.F.Sullivan, R.P.Woodbury, and M.W.Rathke, *J. Org. Chem.*, **42**, 2039 (1977).
2. a.E.T.Blues, D.Bryce-Smith, H.Hirsch, and M.J.Simons, *Chem. Comm.*, 688 (1970).
b.E.T.Blues, D.Bryce-Smith, B.Kettlewell, and M.Roy, *J. Chem. Soc. Chem. Commun.*, 921 (1973).
3. R.A.Ruden, *J. Org. Chem.*, **39**, 3607 (1974).
4. Z.Hamlet and W.D.Barker, *Synthesis*, **2**, 543 (1970).
5. G.Wittig and A.Haag, *Chem. Ber.*, **96**, 1535 (1963).
6. M.W.Rathke and A.Lindert, *J. Am. Chem. Soc.*, **93**, 2318 (1971).
7. a.L.Lochmann and D.Lim, *J. Organomet. Chem.*, **50**, 9 (1973).
b.M.W.Rathke and D.F.Sullivan, *J. Am. Chem. Soc.*, **95**, 3050 (1973).
8. a.V.Georgian, S.K.Boyer, and B.Edwards, *J. Org. Chem.*, **45**, 1686 (1980).
b.V.Georgian, S.K.Boyer, and B.Edwards, *Heterocycles*, 1003 (1977).
9. a.L.G.Drayton and H.W.Thompson, *J. Chem. Soc.*, 1416 (1948).
b.L.L.Shchukovskaya, A.Koltsov, A.Lazarev, and R.Palchick, *Dokl. Akad. Nauk., SSSR*, **179**, 892 (1968).